Aalborg Universitet

AALBORG UNIVERSITY
DENMARK

Multiple Antenna Techniques for Frequency Domain Equalization-based Wireless Systems

Marchetti, Nicola

Publication date:
2007

Document Version
Publisher's PDF, also known as Version of record

Citation for published version (APA):
Marchetti, N. (2007). *Multiple Antenna Techniques for Frequency Domain Equalization-based Wireless Systems*. Institut for Elektroniske Systemer, Aalborg Universitet.

Aalborg University, Center for TeleInFrastruktur (CTIF)

Multiple Antenna Techniques for Frequency Domain Equalization-based Wireless Systems

by

Nicola Marchetti, M.Sc.

Dissertation

Presented to the International Doctoral School of Technology and Science

Aalborg University

in Partial Fulfillment of the Requirements for the Degree of

Doctor of Philosophy

Aalborg University

Defended on September 6, 2007

Supervisors:
Prof. Ramjee Prasad
Assist. Prof. Ernestina Cianca

Dedicated to my parents Pierina and Elvino,

to all the people that believed in me,

to all the people that spent their lives looking for the Truth, no matter where it was hidden

Abstract

This Thesis work gives original contributions to the application of multi-antenna techniques to Frequency Domain Equalization (FDE)-based systems, in particular to Single Carrier - Frequency Domain Equalization (SCFDE) systems, which are emerging as an attractive alternative/complement to Orthogonal Frequency Division Multiplexing (OFDM) in future wireless systems.

The main focus of the Thesis is the proper application of multi-antenna techniques to SCFDE. In particular, in spite of the many similarities between OFDM and SCFDE systems, multi-antenna techniques operating in the space and frequency domains (either diversity-only, hybrid diversity-multiplexing and advanced Linear Dispersion Codes (LDC)), which represent an attractive solution for OFDM systems in specific propagation scenarios (i.e., highly time variable channels), cannot be easily (i.e., without increasing the transceiver complexity) extended to SCFDE systems. In fact, in SCFDE systems there is no direct access to subcarriers at the transmitter, unless Fast Fourier Transform (FFT) and Inverse Fast Fourier Transform (IFFT) operations are performed, thus greatly increasing the transceiver complexity. The present work overcomes this issue proposing new low-complexity pre-processing techniques (complexity comparable with the one of space-time techniques).

Especially interesting it is the extension to SCFDE systems of LDC in the frequency domain: the Thesis presents a method to build the linear space-time dispersion matrices to be used at the transmitter, as a function of the desired dispersion matrices in the space and frequency domains. Performance comparisons prove their suitability in a wide range of propagation scenarios (level of frequency and time diversity of the channel). Moreover,

coding across antennas and subcarriers, instead of across antennas and symbol periods can help in reducing the latency due to the processing time at the receiver: in case of space-time techniques, the receiver has to wait for more than one symbol period before processing.

The Thesis also addresses the trade-off between diversity and multiplexing gain, for both OFDM and SCFDE systems. More specifically, two Joint Diversity and Multiplexing (JDM) schemes, namely Spatial Multiplexing (SM)-Orthogonal Space-Frequency Block Code (OSFBC) and SM-Quasi-orthogonal Space-Frequency Block Code (QSFBC), have been proposed and investigated for both OFDM and SCFDE systems. Linear and non-linear receivers based on well-known Zero Forcing (ZF), Minimum Mean Square Error (MMSE) and Ordered Successive Interference Cancellation (OSIC) techniques are derived and analyzed. The systems are compared in terms of Frame Error Rate (FER) and spectral efficiency in realistic wireless channel scenario, such as spatial correlation at both ends of the transmission link and presence of Line of Sight (LOS). Performance comparisons show that the proposed schemes are more robust than original spatial multiplexing schemes (such as Vertical - Bell Labs LAyered Space-Time Architecture (VBLAST)) to the channel spatial correlation. Performance results have outlined differences between OFDM and SCFDE in the application of Space-Frequency (SF) techniques and in the trade-off diversity-multiplexing.

Dansk Resumé

Denne PhD afhandling giver et selvstændigt bidrag til anvendelsen af multi-antenna teknikker til Frequency Domain Equalization (FDE) baserede systemer og specielt til Single Carrier - Frequency Domain Equalization (SCFDE) systemer, der har vist sig som et attraktivt alternativ til Orthogonal Frequency Division Multiplexing (OFDM) i fremtidige trådløse systemer. Afhandlingen fokuserer hovedsageligt på den mest hensigtsmæssige applikation af multi-antenna teknikker til SCFDE. På trods af de mange ligheder mellem OFDM og SCFDE systemer, kan især multi-antenna teknikker, der opererer i rum- og frekvensdomænet (enten diversity-only, hybrid diversity-multiplexing and advanced Linear Dispersion Codes (LDC)), og som repræsenterer attraktive løsninger for OFDM systemer i specifikke udbredelsesscenarier (f.eks. med meget tidsvarierende kanaler), ikke let (dvs. uden at indskrænke modtager/sender kompleksiteten) udvikles til SCFDE systemer. I SCFDE systemer er der faktisk ikke direkte adgang til senderens subcarriers, medmindre der udføres Fast Fourier Transform (FFT) og Inverse Fast Fourier Transform (IFFT), hvilket forhøjer senderens/modtagerens kompleksitet. Det foreliggende arbejde løser dette problem ved at foreslå nye forbehandlingsteknikker med lav kompleksitet (dvs. kompleksitet der er sammenlignelig med space-time teknikker). Særlig interessant er forlængelsen af LDC til SCFDE systemer i frekvensområdet. Afhandlingen præsenterer en metode til opbygning af de lineære space-time fordelingsmatricer, der benyttes af senderen som en funktion af den ønskede fordelingsmatrice i rum- og frekvensområdet. Ydelsessammenligningen viser

deres egnethed i en bred vifte af udbredelsesscenarier (størrelsen af kanalens frequency og time diversity). Ydermere, kan ventetiden for modtagerens behandlingstid reduceres ved at kode på tværs af antenner og subcarriers i stedet for på tværs af antenner og symbolperioder. Ved brug af space-time teknikker, skal modtageren vente i mere end én symbolperiode før behandlingen. Afhandlingen omhandler også afvejningen mellem diversity og multiplexing gain for både OFDM og SCFDE systemer. Helt konkret er to Joint Diversity and Multiplexing (JDM) opbygninger, nemlig Spatial Multiplexing (SM)-Orthogonal Space-Frequency Block Code (OSFBC) og SM-Quasi-orthogonal Space-Frequency Block Code (QSFBC), foreslået og undersøgt med sigte på OFDM og SCFDE systemer. Lineære og ikke-lineære modtagere baseret på de velkendte Zero Forcing (ZF), Minimum Mean Square Error (MMSE) og Ordered Successive Interference Cancellation (OSIC) teknikker bliver afledt og analyseret. Systemerne sammenlignes med hensyn til Frame Error Rate (FER) og spektral effektivitet i et realistisk trådløst kanal scenarie vedrørende rumlig sammenhæng i begge ender af transmissionsforbindelsen samt forekomsten af Line of Sight (LOS). Sammenligninger viser, at de foreslåede opbygninger er mere robuste end originale rumlige multiplexing konstruktioner (f.eks. Vertical - Bell Labs LAyered Space-Time Architecture (VBLAST) vedrørende kanalens rumlige funktioner. Ydelsesresultaterne har vist forskellene mellem OFDM og SCFDE i applikationen for Space-Frequency (SF) teknikker og i vurderingen af diversity-multiplexing.

Acknowledgments

On Friday 30th April 2004 I took a plane from Venice and this adventure started. It was the first time I was catching a plane. After that, I faced many other novelties and sometimes it was tough not to get lost. But finally I made it. This achievement is the fruit of hard work but not only. Many people contributed to this achievement. I would like to thank those people now.

Thanks to my family who gave me the strength and the motivation to overcome the difficulties and who made me confident about myself. Thanks to my mother Pierina and my father Elvino, thanks to my grandmothers Angela and Teresa, to my siblings Laura and Gianluca, to my uncle Vittorio and my aunts Licia and Rosanna, to my uncle Don Lorenzo, and all my relatives.

Thanks to my small village, San Pietro Polesine, and to my country, Italy, who will always have a special place in my heart, no matter where I will be.

Thanks to my Supervisors, Prof. Ramjee Prasad and Dr. Ernestina Cianca, for all the technical and moral support they gave me. Thanks because they believed in me, and made me feel I could make it. A part of this Ph.D. is also of them.

Thanks to Dr. Frank H.P. Fitzek who brought me here and introduced me to the professional academic world in such a prestigious and international environment.

A special thank to my friend and colleague Imadur who taught me a lot, not only from the technical point of view.

Thanks to my friends: Malaga, Mik, Margot, Davide, Gi@c, Nik, Sens, Galaka, Kleanthis, Gian Paolo, Joao, Marta, Sylwia, Ewelina, Simone, Francesco, Corrado, Mauro,

Suvra, Basak, Hanane, Albena, and all the special people I met since I came to Denmark.

Thanks to the city of Aalborg where I felt home, even though the real one was two thousands kilometers far away.

Thanks to God, a Friend which at a certain point I lost but finally I met again. A.M.D.G.

NICOLA MARCHETTI

Aalborg University

September 6, 2007

Contents

List of Figures

List of Tables

Part I

Introduction

Chapter 1

Introduction

1.1 General Framework

Current 3G systems based on the Wideband Code Division Multiple Access (WCDMA) and cdma2000 radio-access technologies are gaining momentum in the mobile-communication market. Over several years to come new enhancements and improvements will be gradually introduced for the 3G systems, as part of the *3G evolution*. In parallel to this work on the 3G evolution there is also an increasing activity on defining a new radio-access technology, often referred to as 4G, intended to be part of a future radio-communication network with expected introduction in the 2013-2015 time span. In January 2004 the European WINNER project was launched with a clear focus on defining a future ubiquitous radio-access technology [1]. Extensive work on future radio-access technologies is also carried out in other parts of the world [2] [3].

A key requirement on a new radio-access technology is the provision of significantly enhanced services by means of higher data rates, lower latency, etc., at a substantially reduced cost, compared to current mobile-communication systems and their direct evolution. As an example, within the WINNER project, data rates in the order of 100 Mbps for wide-

1

area coverage and up to 1 Gbps for local-area coverage are set as targets. At the same time, the delay/latency of the radio-access network should be limited to a few milliseconds.

The services that are expected to dominate the future radio-access systems are likely to evolve from the services we see in the fixed networks already today, i.e. best effort and rate-adaptive Transmission Control Protocol (TCP)-based services. In current 3G systems, services are typically divided into different Quality of Service (QoS) classes. However in order to support TCP data rates in the range 100-1000 Mbps, the requirements on delay and packet-loss rates must be kept so stringent that for future radio-access systems it is meaningless to set different requirements for real-time, quasi real-time, and non real-time services.

Currently, it is not clear what spectrum a future radio-access technology is to be operated in. It is anticipated that new spectrum will be allocated for a future radio-access technology, e.g. in the 4-5 GHz band. However, it is highly desirable that a new radio-access technology should also be deployable in other frequency bands, including existing 2G and 3G spectrum. Thus, a new radio-access technology should support a high degree of spectrum flexibility including, among other things, flexibility in terms of frequency-band-of-operation, size of available spectrum, and duplex arrangement.

Based on the requirements discussed above it is possible to give some suggestions about a future radio-access system:

- the Downlink (DL) transmission is OFDM-based with support for fast link adaptation and time- and frequency-domain scheduling;

- the Uplink (UL) modulation is Single Carrier (SC)-based and with different pre-filtering operations it is possible to operate in both a pure OFDM mode and a pure SC mode;

- advanced antennas are integrated in the system design by means of LDC [4].

IEEE 802.16 has considered the following multiple access schemes: Multi-Carrier (MC)-based (Orthogonal Frequency Division Multiple Access (OFDMA)) and SC-based (Time Division Multiple Access (TDMA)). Some recent studies have clearly shown that the basic issue is not OFDM (OFDMA) vs. SC (TDMA) but rather FDE vs. Time Domain Equalization (TDE). FDE has several advantages over TDE in high mobility propagation environments (usually with long tail channel impulse responses). We can also have a SC transmission with FDE so more generally, the chosen approach should be FDE-based, keeping an eye on other possibilities.

For channels with severe delay spread, FDE is computationally simpler than corresponding TDE for the same reason OFDM [5] is simpler: because equalization is performed on a block of data at a time, and the operations on this block involve an efficient FFT operation and a simple channel inversion operation. Sari *et al.* [6] [7] pointed out that when combined with FFT processing and the use of a cyclic prefix, a SC system with FDE (SCFDE) has essentially the same performance and low complexity as an OFDM system. It should also be noticed that a frequency domain receiver processing SC modulated data shares a number of common signal processing functions with an OFDM receiver. In fact, as it is pointed out in Chapter 2, SCFDE and OFDM modems can easily be configured to coexist, and significant advantages may be obtained through such coexistence.

In next generation radio access, a very important role will be played by advanced multiple antennas systems. The transmitter will have one or more antennas and will use an algorithm consisting of four parts [8]:

- *multi-user channel-dependent scheduling over several cells*, which schedules the User Terminal (UT)s connected to an Access-Point (AP) in a coordinated way, taking their average/instantaneous channel properties and quality into account;

- *stream multiplexing with per-stream rate control* (similar to Selective Per-Antenna Rate Control (S-PARC) [9]), which is used when the transmitter has more than one antenna

and when multiplexing is more desirable than diversity;

- Transmit Diversity (TD) using LDC [4]. Transmit diversity requires that the transmitter has more than one antenna and is used when more diversity is needed, at the expense of possibly sacrificing some multiplexing gain. Each data stream can then be spread in space and time to obtain the desired amount of diversity and multiplexing;

- *higher order of sectorization* (implemented using e.g. fixed multi-beam), which is used when the transmitter has more than one antenna and when directivity is more desirable than diversity or multiplexing.

1.2   Thesis Motivation

Since as mentioned above, for both DL and UL the candidates for future systems are FDE-based, i.e. OFDM for DL and SCFDE for UL, and the multiple antenna techniques will be a key component of next generation wireless systems, the study of Multiple Input Multiple Output (MIMO) for FDE systems is very important.

        While a lot of work has been done on the application of multiple antenna techniques to OFDM, there are much less studies for SCFDE case. The extension of MIMO techniques to SCFDE is straightforward in some cases, but it is complex for some schemes such as the ones involving coding in frequency domain. In future wireless systems, the application of diversity techniques where coding is done across antennas and subcarriers instead of antennas and time, is important for two main reasons:

- SF schemes can fulfill the requirement of low latency, as Space-Time (ST) schemes processing might not be suitable, since the receiver has to wait for more than one symbol period before processing the received stream. This extra-delay can be reduced when the coding is done across subcarriers. In this thesis the only latency considered is the one possibly due to ST coding; this delay is in relation with other processing

delays (imposed by interleaving, channel coding, channel estimation etc.) whose study is not an objective of the present work, and are left for further investigations;

- SF schemes can work efficiently over high mobility environments, where ST schemes might fail (since they have to assume the channel constant over several symbol periods).

Therefore, one of the main objectives of this Thesis is the efficient introduction of space-frequency diversity techniques for SCFDE systems. Furthermore, the requirement to have air interfaces able to work in different propagation environments makes important the possibility to use techniques that are able to get the best the trade-off diversity-multiplexing. Again, no much work has been done in investigating this trade-off in SCFDE systems and, in spite of the similarities between OFDM and SCFDE systems, different approaches might be needed for the design of those MIMO techniques. Therefore, in the Thesis some schemes combining diversity and multiplexing gain have been proposed and studied for both OFDM and SCFDE systems, outlining the different behavior in different propagation environments.

1.3 Original Contributions

Several original contributions have been studied and are presented in this Thesis:

- the combination of SM [10] and Space-Frequency Block Code (SFBC) [11] for OFDM (Section 3.3.1.1) has been proposed;

- the combination of SM and QSFBC for OFDM (Section 3.3.1.2) has been introduced. QSFBC is the Quasi-Orthogonal Design (QOD) code of [12] applied to space and frequency, instead of space and time (as done in [12]);

- the OFDM-SFBC technique has been extended to SCFDE (Section 4.2);

- the combination of SM and SFBC and the combination of SM and Space-Time Block Code (STBC) [13] for SCFDE have been studied (Section 4.3);

Table 1.1: Next generation wireless systems requirements and studied multi-antenna schemes

Requirement	Scheme
high mobility	SF-based
high rate	SM
high reliability	Space Diversity (SD)
rate-reliability trade-off	JDM, LDC
low latency	SF-based

- QSFBC has been extended to SCFDE (Section 4.3);

- SF (ST)-LDC have been extended to SCFDE (Chapter 5).

The studied schemes work differently for different scenarios, and pursue different aims, as summarized in Table 1.1.

1.4 Thesis Outline

The present Thesis is organized as follows: the research field background is presented in Chapter 2; the contribution on OFDM multiplexing and diversity joint scheme can be found in Chapter 3; Chapter 4 is dedicated to the study of SCFDE-MIMO schemes; Chapter 5 studies the application of LDC to SCFDE systems; finally, conclusions and future perspectives are outlined in Chapter 6.

Part II

Background

Chapter 2

Multi-Antenna Schemes in FDE-based Radio Air Interfaces

2.1 Introduction

In the present Chapter, firstly the considered air interfaces, i.e. OFDM and SCFDE, are introduced, compared and their possible coexistence in a real system is discussed. Afterwards, the State-of-the-Art of multiple antenna techniques in OFDM and SCFDE is presented. In particular, the trade-off between spatial multiplexing gain and spatial diversity gain is discussed. The latter topic in further developed in next Chapters of this Thesis.

2.2 Radio Air Interfaces

2.2.1 OFDM

OFDM is a special case of multicarrier transmission, where a single data stream is transmitted over a number of lower-rate subcarriers. It is worth mentioning that OFDM can be seen as either a modulation technique or a multiplexing technique. One of the main reasons

to use OFDM is to increase robustness against frequency-selective fading or narrowband interference. In a single-carrier system, a single fade or interferer can cause the entire link to fail, but in a multicarrier system, only a small percentage of the subcarriers will be affected. Error Correction Coding (ECC) can then be used to correct for the few erroneous subcarriers [5].

The word "orthogonal" indicates that there is a precise mathematical relationship between the frequencies of the carriers in the system. In a normal Frequency-Division Multiplexing (FDM) system, many carriers are spaced apart in such a way that the signals can be received using conventional filters and demodulators. In such receivers, guard bands are introduced in the frequency domain between the different carriers, which results in a lowering of spectrum efficiency.

It is possible, however, to arrange the carriers in an OFDM signal so that the sidebands of the individual carriers overlap and the signals are still received without adjacent carrier interference. To do this the carriers must be mathematically orthogonal. The receiver acts as a bank of demodulators, translating each carrier down to dc, with the resulting signal integrated over a symbol period to recover the raw data. If the other carriers all beat down the frequencies that, in the time domain, have a whole number of cycles in the symbol period T, then the integration process results in zero contribution from all these other carriers. Thus, the carriers are linearly independent (i.e., orthogonal) if the carrier spacing is a multiple of $1/T$ [5].

OFDM transmits multiple modulated subcarriers in parallel. Each occupies only a very narrow bandwidth. Since only the amplitude and phase of each subcarrier are affected by the channel, compensation of frequency selective fading is done by compensating, for each subchannel, amplitude and phase. OFDM signal processing is carried out relatively simply by using one IFFT at the transmitter and one FFT at the receiver.

Coding is required for OFDM systems, since in the presence of multipath, uncoded

OFDM as it is, is not usable as certain subcarriers are subjected to frequency fades. In fact the information carried by subcarriers which are heavily affected by fading can only be reconstructed at the receiver by powerful channel coding methods, which however reduce the bandwidth efficiency [14].

The OFDM transmission scheme has the following key advantages:

- OFDM is an efficient way to deal with multipath; for a given delay spread, the implementation complexity is significantly lower than that of a single-carrier system with a time-domain equalizer;

- in relatively slow time-varying channels, it is possible to significantly enhance capacity by adapting the data rate per subcarrier according to the Signal to Noise Ratio (SNR) of that particular subcarrier;

- OFDM is robust against narrowband interference because such interference affects only a small percentage of the subcarriers;

- OFDM makes single-frequency networks possible, which is especially attractive for broadcasting applications.

On the other hand, OFDM has also some drawbacks with respect to SC modulation:

- OFDM is more sensitive to frequency offset and phase noise;

- OFDM has a relatively large Peak to Average Power Ratio (PAPR), which tends to reduce the power efficiency of the Radio Frequency (RF) amplifier.

2.2.2 SCFDE

Adaptive equalizion in the time domain to compensate for Inter-Symbol Interference (ISI) [15] in SC systems was pioneered in voiceband telephone modems and has been applied in many other digital communications systems. Its main components are one or more transversal
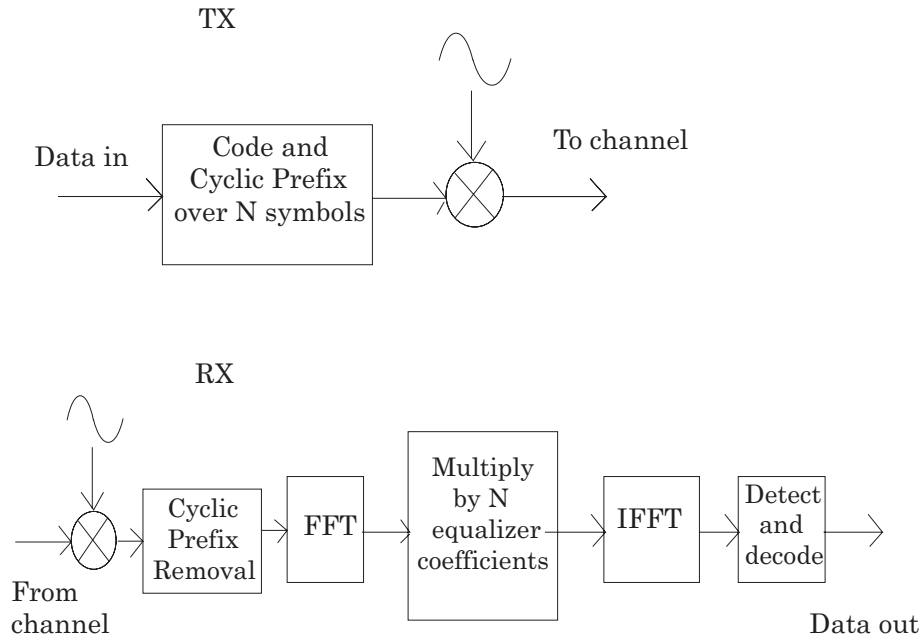
Figure 2.1: SCFDE with linear FDE

filters for which the number of adaptive tap coefficients is on the order of the number of data symbols spanned by the multipath. For tens of Megasymbols per second and more than about 30-50 symbols ISI, the complexity and required digital processing speed become exorbitant, and this TDE approach becomes unattractive [16]. Therefore, for channels with severe delay spread, equalizazion in the frequency domain might be more convenient since the receiver complexity can be kept low.

Figure 2.1 shows conventional linear equalization, using a transversal filter with N tap coefficients, but with filtering done in the frequency domain. The block length N is usually chosen in the range of 64–2048 for both OFDM and SC-FDE systems.

A Cyclic Prefix (CP) is appended to each block of N symbols, exactly as in OFDM. As an additional function, the CP can be combined with a training sequence for equalizer adaptation. An IFFT returns the equalized signal to the time domain prior to the detec-

tion of data symbols. Adaptation of the FDE's transfer function can be done with Least Mean Square (LMS), Recursive Least Squares (RLS), or Least Squares (LS) minimization techniques, analogously to adaptation of time domain equalizers [17] [18].

2.2.3   Analogies and Differences between OFDM and SCFDE

There is a strong analogy between OFDM and SCFDE. With a frequency-domain equalizer at the receiver, single-carrier systems can handle the same type of channel impulse responses as OFDM systems. In both cases, time/frequency and frequency/time transformations are made. The difference is that in OFDM systems, both channel equalization and receiver decisions are performed in the frequency domain, whereas in SCFDE systems the receiver decisions are made in the time domain, although channel equalization is performed in the frequency domain.

From a purely channel equalization capability standpoint, both systems are equivalent, assuming they use the same FFT block length. They have, however, an essential difference: *since the receiver decisions in uncoded OFDM are independently made on different carriers, those corresponding to carriers located in a region with a deep amplitude depression will be unreliable.* This problem does not exist for SCFDE, in fact *once the channel is equalized in the frequency domain, the signal is transformed back to the time domain, and the receiver decisions are based on the signal energy transmitted over the entire channel bandwidth.* In other words, the SNR value that dictates performance (assuming that residual ISI is negligible) corresponds to the average SNR of the channel. In fact, as noted in [7], the effect of the deep nulls in the channel frequency response is spread out over all symbols by the IFFT operation. Consequently, the performance degradation due to a deep notch in the signal spectrum remains small with respect to that suffered by OFDM.

The foregoing analysis indicates that with FDE, SC transmission is substantially superior to OFDM signaling. Without channel coding, OFDM is in fact not usable on

fading channels, as deep notches in the transmitted signal spectrum lead to an irreducible Bit Error Rate (BER). In order to work satisfactorily, *OFDM requires ECC with frequency-domain interleaving so as to scatter the signal samples falling in a spectral notch.* In this case, the interleaver uniformly distributes the low-SNR samples over the channel bandwidth. *In contrast, SCFDE can work without ECC.*

The main hardware difference between OFDM and SCFDE is that for SCFDE the transmitter's IFFT block is moved to the receiver. The complexities are the same. *Both OFDM and SCFDE can be enhanced by* adaptive modulation and *space diversity* [19].

The use of SC modulation and FDE by processing the FFT of the received signal has several attractive features:

- SC modulation has reduced PAPR requirements with respect to OFDM, thereby allowing the use of less costly power amplifiers;

- its performance with FDE is similar to that of OFDM, even for very long channel delay spread;

- frequency domain receiver processing has a similar complexity reduction advantage with respect to that of OFDM: complexity is proportional to *log* of multipath spread;

- coding, while desirable, is not necessary for combating frequency selectivity, while it is needed in nonadaptive OFDM;

- SC modulation is a well-proven technology in many existing wireless and wireline applications, and its RF system linearity requirements are well known.

Comparable SCFDE and OFDM systems would have the same block length and CP lengths. The CP at the beginning of each block (Figure 2.2), used in both SCFDE and OFDM systems, has two main functions:

- it prevents contamination of a block by ISI from the previous block;
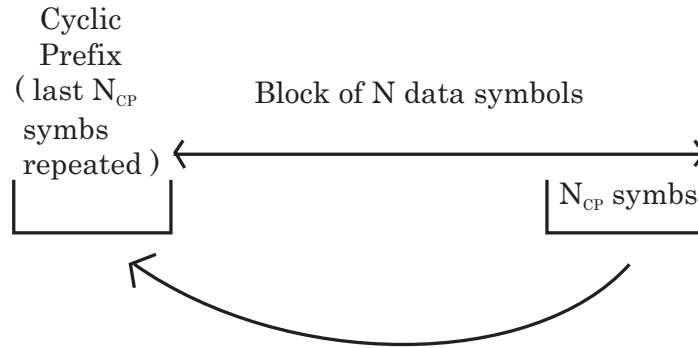
Figure 2.2: Block Processing in FDE

- it makes the received block appear to be periodic of period N, which is essential to the proper functioning of the FFT operation.

If the first and the last N_{CP} symbols are identical unique word sequences of training symbols, the overhead fraction is $\frac{2N_{CP}}{N+2N_{CP}}$.

2.2.4 Interoperability of SCFDE and OFDM

Figure 2.3 shows block diagrams for OFDM and SC systems with linear FDE. It is evident that the two types of systems differ mainly in the placement of the IFFT operation: in OFDM it is placed at the transmitter to multiplex the data into parallel subcarriers; in SC it is placed at the receiver to convert FDE signals back into time domain symbols. The signal processing complexities of these two systems are essentially the same for equal FFT block lengths [16]. A dual-mode system, in which a software radio modem can be reconfigured to handle either SC or OFDM signals, could be implemented by switching the IFFT block between the transmitter and receiver at each end of the link, as suggested in Figure 2.4. *There may actually be an advantage in operating a dual mode system, wherein the base station uses an OFDM transmitter and an SC receiver, and the subscriber modem uses an SC transmitter and an OFDM receiver*, as illustrated in Figure 2.5. This arrangement - OFDM in the downlink and SC in the uplink - has two potential advantages [16]:
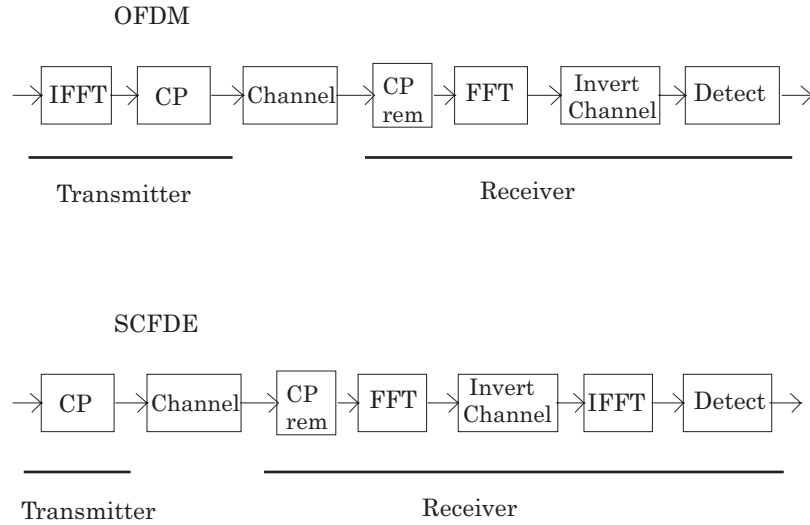
OFDM

Figure 2.3: OFDM and SCFDE signal processing similarities and differences
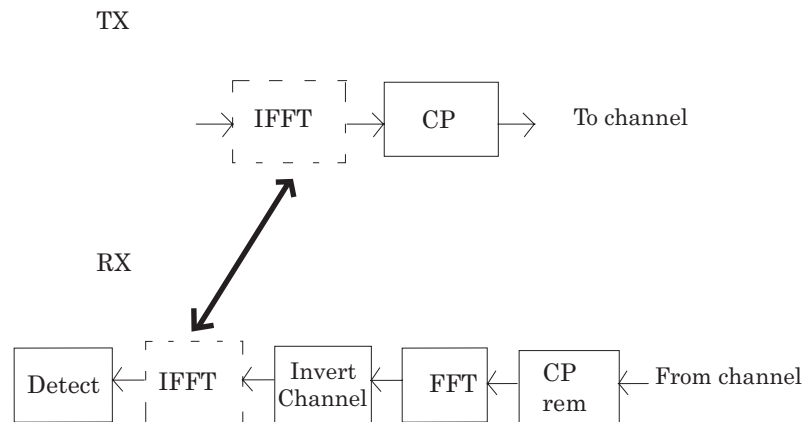
Figure 2.4: Potential interoperability of SCFDE and OFDM: a "convertible" modem

```
→ IFFT → CP → Channel → CP rem → FFT → Invert Channel → Detect →
```

Downlink OFDM transmitter   Downlink OFDM receiver
        at hub   at subscriber

```
← Detect ← IFFT ← Invert Channel ← FFT ← CP rem ← Channel ← CP ←
```

Uplink SC receiver   Uplink SC
      at hub   transmitter
                                        at subscriber
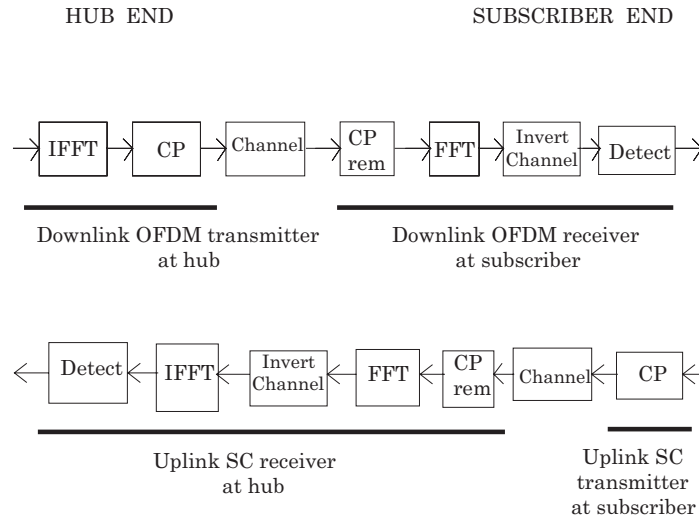
Figure 2.5: Coexistence of SCFDE and OFDM: uplink/downlink asymmetry

- concentrating most of the signal processing complexity at the hub or base station. The hub has two IFFTs and one FFT, while the subscriber has just one FFT;

- the subscriber transmitter is SC, and thus inherently more efficient in terms of power consumption due to the reduced power backoff requirements of the SC mode. This may reduce the cost of a subscriber's power amplifier.

2.3   Multi-Antenna Techniques: State-of-the-Art

Multiple antennas can be used at both ends of a wireless transmission system to exploit the spatial dimension either to get diversity gain via SD techniques or to get multiplexing gain via SM techniques, or a combination of them. SD schemes provide higher SNR at the receiver, whereas SM schemes provide higher rate.

Traditionally, multiple antennas have been used to better exploit the diversity due to the multipath phenomena. Each pair of transmit and receive antennas provides a signal path from the transmitter to the receiver. By sending signals that carry the same information through different paths, multiple independently faded replicas of the data symbol

can be obtained at the receiver end; hence, more reliable reception is achieved. For example, in a slow Rayleigh-fading environment with one transmit and N_R receive antennas, the transmitted signal is passed through N_R different paths. It is well known that if the fading is independent across antenna pairs, a maximal diversity gain (advantage) of N_R can be achieved: the average error probability can be made to decay like $1/\rho^{N_R}$ at high SNR ρ, in contrast to the ρ^{-1} for the single-antenna fading channel [20]. The underlying idea is averaging over multiple path gains (fading coefficients) to increase the reliability. In a system with N_T transmit and N_R receive antennas, assuming the path gains between individual antenna pairs are independent and ideally identically distributed (i.i.d.) Rayleigh faded, the maximal diversity gain is $N_T N_R$, which is the total number of fading gains that one can average over.

Transmit SD schemes have multiple antennas at the transmitter, and may have only one or more than one receive antennas, whereas SM schemes must have multiple antennas at both sides. The SD schemes do not require any channel information at the transmitter, thus, they can be implemented at fairly low system complexity and signaling overhead.

Transmit and receive diversity are means to combat fading. A different line of thought suggests that in a MIMO channel, fading can in fact be beneficial, through increasing the degrees of freedom available for communication [21], [22]. Essentially, if the path gains between individual transmit-receive antenna pairs fade independently, the channel matrix is well conditioned with high probability, in which case multiple parallel spatial channels are created. Therefore, in rich scattering environment, the independent spatial channels can be exploited to send multiple signals at the same time and frequency, resulting in higher spectral efficiency. By transmitting independent information streams in parallel through the spatial channels, the data rate can be increased. This effect is also called spatial multiplexing [23], and is particularly important for the high-SNR regime where the system is degrees-of-freedom limited (as opposed to power limited). Foschini [21] has shown that in

the high-SNR regime, the capacity of a channel with N_T transmit antennas, N_R receive antennas, and i.i.d. Rayleigh-faded gains between each antenna pair, is given by:

$$\mathcal{C}(\rho) = min(N_T, N_R)log\ \rho + O(1) \tag{2.1}$$

where ρ is the SNR. The number of degrees of freedom is thus the minimum of N_T and N_R. In recent years, several schemes have been proposed to exploit the spatial multiplexing phenomenon (for example, Bell labs LAyered Space Time (BLAST) [21]).

SM schemes can be either Channel State Information (CSI) assisted or non-CSI based, i.e. so called blind SM schemes. Typical CSI assisted systems are Singular Value Decomposition (SVD) based SM, eigen-mode MIMO etc. These schemes provide higher system capacity, but require a feedback path, thus they are more complex and difficult to implement.

Blind SM schemes can have different kinds of receivers:

1. Linear ZF or MMSE: simple receiver, but poor performance [24];

2. Non-linear Maximum Likelihood (ML): optimal and most complex receiver [25][26];

3. Non-linear OSIC with ZF or MMSE nulling: sub-optimal receiver [10].

The need for high data-rate in wireless communication systems has as a consequence the increase in the attention for MIMO techniques. A problem in high data rate wireless communications is the ISI of the signal caused by multipath propagation. This is particularly challenging when high data rates are requested because of the short duration of the information symbols: to solve this problem equalization is needed. Traditionally this equalization is performed in time domain (TDE), but increasing data rates lead to huge increase in complexity. The alternative approach of FDE guarantees the complexity minimization of the multi-dimensional equalization process required in a wideband MIMO system. As

mentioned above, FDE is used in two recent years approaches to counteract ISI: OFDM and SCFDE.

2.3.1   Multi-Antenna in OFDM

Most of the available MIMO techniques are effective in frequency flat scenarios [27][28]. All these narrowband algorithms can be implemented on OFDM sub-carrier level, because OFDM converts a wideband frequency selective channel into a number of narrowband sub-carriers. In other words, OFDM turns a frequency-selective MIMO fading channel into a set of parallel frequency-flat MIMO fading channels. So, in wideband scenarios, OFDM can be combined with MIMO systems, for both diversity and multiplexing purposes [29]. In frequency selective environments, amalgamation of SM and OFDM techniques can be a potential source of high spectral efficiency at reasonable complexity. MIMO-OFDM drastically simplifies equalization in frequency-selective environments.

Let us assume an OFDM-MIMO system with N_T transmit antennas, N_R receive antennas and N subcarriers. The input-output relation for the MIMO system for the kth tone, $k = 1, \ldots, N$ may be expressed as:

$$\mathbf{Y}_k = \sqrt{\frac{P_T}{N_T}} \mathbf{H}_k \mathbf{s}_k + \mathbf{N}_k \tag{2.2}$$

where $\mathbf{Y}_k$ and $\mathbf{N}_k$ are $N_R \times 1$ vectors, $\mathbf{H}_k$ is a $N_R \times N_T$ matrix, $\mathbf{s}_k$ is a $N_T \times 1$ vector, and P_T is the total transmit power. The matrix $\mathbf{H}_k$ is the frequency response of the matrix channel corresponding to the kth tone.

From Equation (2.2) we can see that, just as in Single Input Single Output (SISO) channels, OFDM-MIMO decomposes the otherwise frequency selective channel of bandwidth B into N orthogonal flat fading MIMO channels, each with bandwidth B/N (see Figure 2.6) [25]. MIMO signaling treats each OFDM tone as an independent narrowband frequency flat channel. We must take care to ensure that the modulation and demodula-
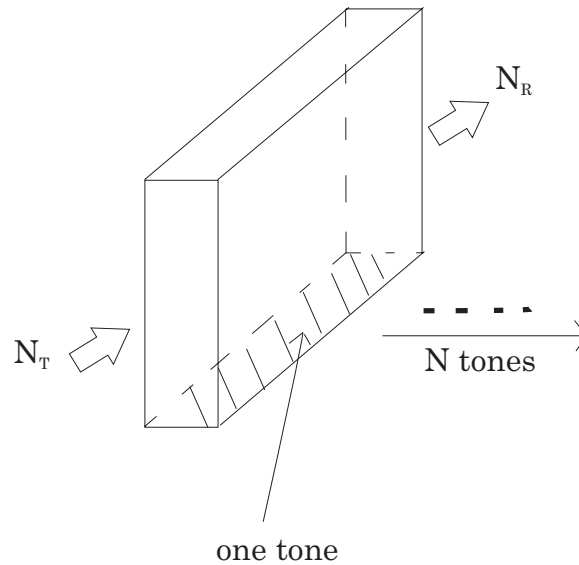
Figure 2.6: Schematic of MIMO-OFDM. Each OFDM tone admits N_T inputs and N_R outputs

tion parameters (carrier, phasing, FFT/IFFT, prefixes, etc.) are completely synchronized across all the transmit and receive antennas. With this precaution, every OFDM tone can be treated as a MIMO channel, and the tone index can be treated as a time index in the already existing ST techniques.

Multiple antennas systems for OFDM based 4G systems can be broadly classified into three categories:

- Diversity combining, which is employed to mitigate fading and increase link reliability;

- Spatial multiplexing, which is used to increase data rate;

- Smart array processing, such as Beamforming (BF), which aims at increasing receiving power and rejecting unwanted interference.

2.3.1.1 Space Diversity

TD-OFDM system model is shown in Figure 2.7. ST diversity schemes map directly to
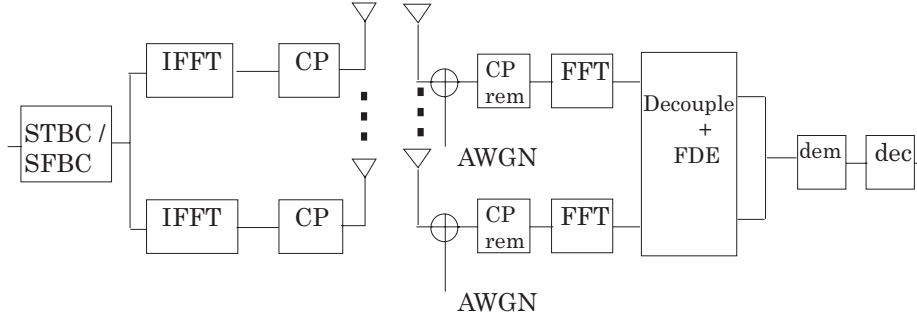
Figure 2.7: Transmit Diversity for OFDM

OFDM by applying these coding techniques on a per tone basis across OFDM symbols in time exactly as in SC modulation. However, this requires that channel remains constant over T OFDM symbol periods. Since the duration of an OFDM symbol $\frac{N+N_{CP}}{f_s}$ is usually large, this may be impractical (f_s is the sampling frequency).

For example, assuming a set of WiMAX parameters [30], i.e. $N = 128$, $N_{CP} = 16$, $f_s = 1.429$ Msps, the OFDM symbol duration is $T_s = \frac{N+N_{CP}}{f_s} = \frac{128+16}{1.429e6} = 100.77 \; \mu s$. At the speed of $v = 150$ Kmph= 41.66 m/s, the maximum Doppler shift $f_m = \frac{v}{c} f_c = \frac{41.66}{3e8} 3.5e9 = 486$ Hz, where c is the speed of light and f_c is the carrier frequency. Therefore, the coherence time [31] is $T_c = \frac{9}{16\pi f_m} = 368 \; \mu s$. To verify the Alamouti's assumption of channel constance over two symbols periods, we have to compare $2T_s$ with the coherence time T_c: since it is only $2T_s < T_c$ and not $2T_s << T_c$, it is risky to take for granted this assumption.

The possibility to access the frequency-domain in OFDM systems suggests to code also in space and frequency, not only in space and time: diversity techniques designed for SC modulation over flat fading channels are easily extended to OFDM modulation with the time index for SC modulation replaced by the tone index in OFDM. As an example, let us consider the Alamouti scheme, which extracts full spatial diversity in absence of channel knowledge at the transmitter with $N_T = 2$. The implementation of the Alamouti scheme requires that the channel remains constant over two consecutive symbol periods. Alamouti scheme applied in space and frequency domains is an example of SFBC schemes. In SFBC
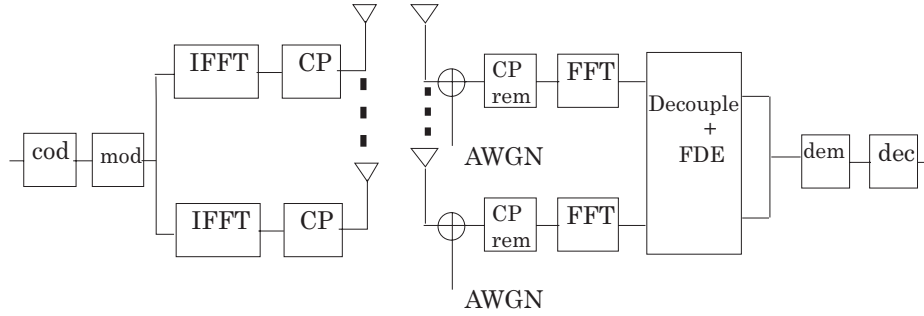
Figure 2.8: Spatial Multiplexing for OFDM

schemes, the requirement of the channel being constant over consecutive symbols becomes a requirement over consecutive tones, i.e. $\mathbf{H}_k = \mathbf{H}_{k+1}$. The receiver detects the transmitted symbols from the signal received on the two tones using the Alamouti detection technique. The use of consecutive tones is not strictly necessary, any pair of tones can be used as long as the associated channels are equal. The technique can be generalized to extract spatial diversity over a larger number of antennas by using the ST techniques developed for SC modulation: in that case we need a block size $T \geq N_T$ and the channel must be identical over the T tones.

2.3.1.2 Spatial Multiplexing

SM-OFDM system model is shown in Figure 2.8. Analogously to SM for MIMO systems with SC modulation, the objective of SM in conjunction with MIMO-OFDM is to achieve the spatial rate $R = N_T$ by transmitting parallel streams [26]. Thus, NN_T scalar data symbols are transmitted over one OFDM symbol, with N_T symbols being transmitted over each subcarrier. Thus SM in MIMO-OFDM system reduces to SM over each tone. The receiver architecture for SM is identical to that for SC modulation. As in SC case we require that $N_R \geq N_T$ in order to support the symbol streams reliably.

2.3.1.3   Beam-Forming

In a BF system, the weights to be multiplied with the signals have to be carefully chosen. From antenna theory, an array with N_T antenna elements has different excitation currents according to the direction of the waves arriving or departing from each element of the array. Considering linear phase progression, the weights have a phase that increases the same amount from one element to the next. Usually, BF is treated in literature as a method for increasing array gain when receiving signals from a specific direction. Direction of Arrival (DoA) is the angle of the wave arriving to the antenna.

Since it is more feasible to have multiple antennas at the Base Station (BS) than at the Mobile Station (MS), it makes sense to place the beamformer at the BS i.e. at the transmitter side in case of DL [32]. This will bring additional complications if it is assumed that there is complete channel knowledge at the receiver, but not at the transmitter. In order to solve this problem, the DL-BF technique can extract the weights to be used in DL from the weights calculated in UL. This method can be used in Time Division Duplex (TDD) systems without losing performance. However, in Frequency Division Duplex (FDD) systems, as a consequence of the frequency dependent steering array response and uncorrelated fading, the UL weight reuse in DL degrades system's performance, since the frequency for UL is different from the one used in DL. A block diagram showing the implementation of DL-BF in an OFDM transmitter is presented in Figure 2.9.

2.3.2   Multi-Antenna in SCFDE

Several works have recently investigated the combination of MIMO schemes and SCFDE modulation, from different points of view: equalizer [33] [34] and receiver design [35], interaction with Trellis Coded Modulation (TCM) and interleaving [36], investigation in multi-user scenario [37].

The key architectural difference between a MIMO-OFDM system and a MIMO-
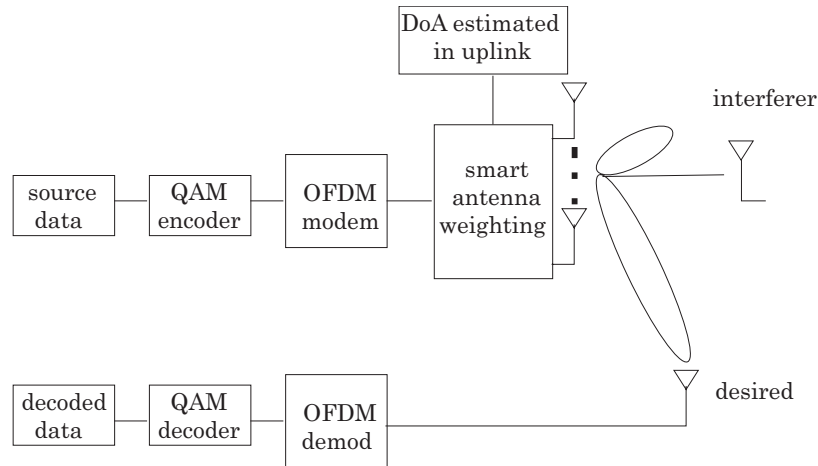
Figure 2.9: OFDM System with Beamforming
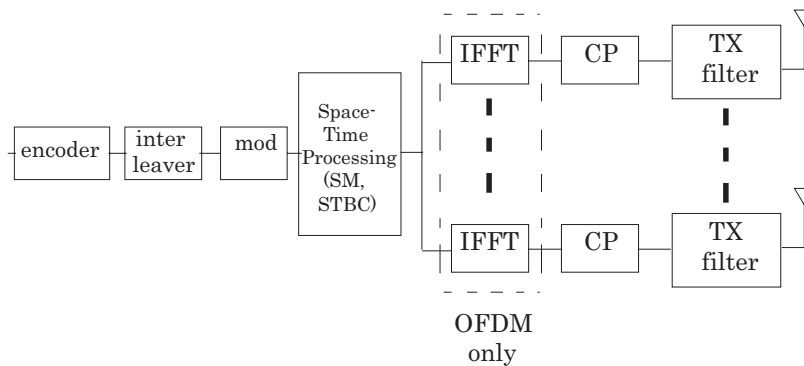
Figure 2.10: OFDM/SCFDE MIMO Transmitter

SCFDE system, namely the order in which the IFFT operation is executed, as outlined in Figure 2.10 and Figure 2.11. Other differences between the SCFDE and OFDM architectures include the implementation of the Viterbi decoder and the design of transmit and receive filters [38].

2.3.2.1   Space Diversity

STBC-SCFDE system model is shown in Figure 2.12. By following the encoding rule [13]:
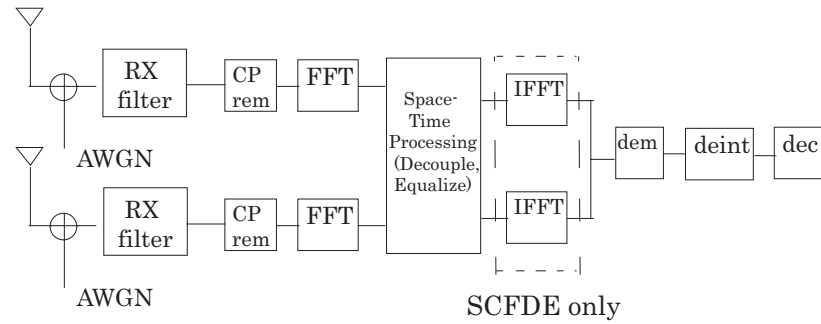
Figure 2.11: OFDM/SCFDE MIMO Receiver
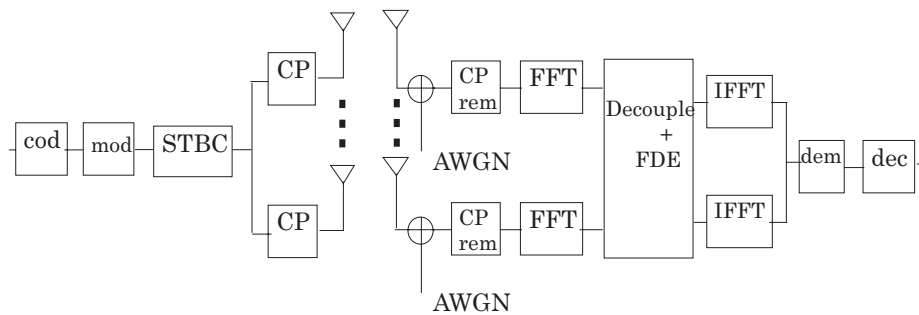
Figure 2.12: STBC for SCFDE

$$\mathbf{x}_1(t) = [x_{1,0}, x_{1,1}, \ldots, x_{1,N-1}]^T \tag{2.3}$$

$$\mathbf{x}_2(t) = [x_{2,0}, x_{2,1}, \ldots, x_{2,N-1}]^T \tag{2.4}$$

$$\mathbf{x}_1(t+T) = \left[-x_{2,0}^*, -x_{2,N-1}^*, \ldots, -x_{2,1}^*\right]^T \tag{2.5}$$

$$\mathbf{x}_2(t+T) = \left[x_{1,0}^*, x_{1,N-1}^*, \ldots, x_{1,1}^*\right]^T \tag{2.6}$$

and because of the FFT properties, we obtain in the frequency domain the same Alamouti structure than for OFDM. The equalized symbol vector has the expression:

$$\begin{bmatrix} \widehat{\mathbf{X}}_1 \\ \widehat{\mathbf{X}}_2 \end{bmatrix} = \begin{bmatrix} \mathbf{W} & \mathbf{0} \\ \mathbf{0} & \mathbf{W} \end{bmatrix} \begin{bmatrix} \widetilde{\mathbf{X}}_1 \\ \widetilde{\mathbf{X}}_2 \end{bmatrix} \tag{2.7}$$

where $\widetilde{\mathbf{X}}_1$ and $\widetilde{\mathbf{X}}_2$ are the symbol vectors after Maximal Ratio Combining (MRC) and in the case of MMSE equalizer we have:

$$\mathbf{W}(i,i) = \frac{\sqrt{N_T/P_T}}{|\mathbf{\Lambda}_1(i,i)|^2 + |\mathbf{\Lambda}_2(i,i)|^2 + \frac{N_T}{\rho}} \tag{2.8}$$

where $\mathbf{\Lambda}_i$, $i = 1, 2$ are $N \times N$ diagonal matrices whose $(l,l)^{th}$ entries are equal to the lth FFT coefficients of the Channel Impulse Response (CIR)s $\mathbf{h}_i$, $i = 1, 2$, and $\rho = P_T/\sigma^2$, with P_T total power of the transmitted signal, and σ^2 variance of the complex Gaussian noise process at one receive antenna. We then go back to the time domain by applying the IFFT:

$$\begin{bmatrix} \widehat{\mathbf{x}}_1 \\ \widehat{\mathbf{x}}_2 \end{bmatrix} = \begin{bmatrix} \mathbf{Q}^H & \mathbf{0} \\ \mathbf{0} & \mathbf{Q}^H \end{bmatrix} \begin{bmatrix} \widehat{\mathbf{X}}_1 \\ \widehat{\mathbf{X}}_2 \end{bmatrix} \tag{2.9}$$

where $\mathbf{Q}$ is the orthonormal $N \times N$ FFT matrix, i.e. $\mathbf{Q}(k,l) = \frac{1}{\sqrt{N}}e^{-j\frac{2\pi}{N}(k-1)(l-1)}$, $1 \leq k, l \leq N$.
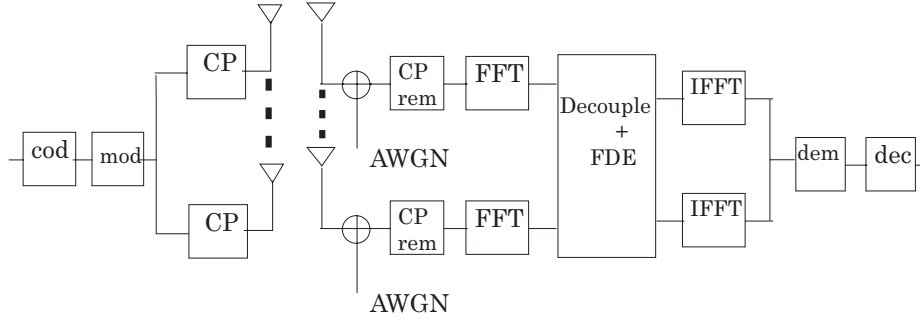
Figure 2.13: Spatial Multiplexing for SCFDE

2.3.2.2   Spatial Multiplexing

SM-SCFDE system model is shown in Figure 2.13. The SCFDE-SM equalized vectors are:

$$\left[\begin{array}{c} \widehat{\mathbf{X}}_1 \\ \widehat{\mathbf{X}}_2 \end{array} \right] = \mathbf{W} \left[\begin{array}{c} \mathbf{Y}_1 \\ \mathbf{Y}_2 \end{array} \right] \tag{2.10}$$

where $\mathbf{Y}_1$ and $\mathbf{Y}_2$ are the vectors received at the two receive antennas and $\mathbf{W}$ is the equalizer which for MMSE is:

$$\mathbf{W} = \sqrt{\frac{N_T}{P_T}} \mathbf{\Lambda}^H \left(\mathbf{\Lambda}\mathbf{\Lambda}^H + \frac{N_T}{\rho}\mathbf{I}_{2N} \right)^{-1} \tag{2.11}$$

where:

$$\mathbf{\Lambda} = \left[\begin{array}{cc} \mathbf{\Lambda}_{1,1} & \mathbf{\Lambda}_{1,2} \\ \mathbf{\Lambda}_{2,1} & \mathbf{\Lambda}_{2,2} \end{array} \right] \tag{2.12}$$

is the MIMO channel matrix with $\mathbf{\Lambda}_{i,j}$ diagonal matrix containing the frequency responses of the N subcarriers between j^{th} transmit and i^{th} receive antenna and ρ is defined as before. At this point there is the IFFT block, as in Equation (2.9).

Aalborg University, Center for TeleInFrastruktur (CTIF)

2.4   Trade-off between Spatial Multiplexing and Spatial Diversity

A MIMO system can provide several types of gains. In this Thesis, the focus is on diversity gain and spatial multiplexing gain. There are schemes which switch between these two modes, depending on the instantaneous channel condition [39]. However, maximizing one type of gain may not necessarily maximize the other. In fact, each of the two design goals addresses only one aspect of the problem. This makes it difficult to compare the performance between diversity-based and multiplexing-based schemes.

In [20] a different viewpoint is put forth, i.e. given a MIMO channel, both gains can be simultaneously obtained, but there is fundamental tradeoff between how much of each type of gain any coding scheme can extract: higher spatial multiplexing gain comes at the price of sacrificing diversity. The focus of [20] is on high-SNR regime. A scheme is said to have a spatial multiplexing gain r and a diversity advantage d if the rate of the scheme scales like $rlog\ \rho$ and the average error probability decays like $1/\rho^d$, where ρ is the SNR. Clearly, r cannot exceed the total number of degrees of freedom $min(N_T, N_R)$ provided by the channel, and d(r) (the diversity gain which the trade-off curve associates to the multiplexing gain r) cannot exceed the maximal diversity gain $N_T N_R$ of the channel. The tradeoff curve bridges between these two extremes, as can be seen in Figure 2.14.

The specific study-cases that will address the multiplexing-diversity trade-off issue in this Thesis are JDM schemes, in Chapter 3 and Section 4.3, and LDC in Chapter 5. The trade-off studies are triggered based on the fact that none of the schemes mentioned above can become an absolute choice for best system performance in all scenarios. To be more precise, a user located very close to access point can better exploit the multiplexing benefits, while a user at farther location may benefit more by using diversity schemes: to explore what is in between is one of the main research goals of this Thesis. Moreover, in
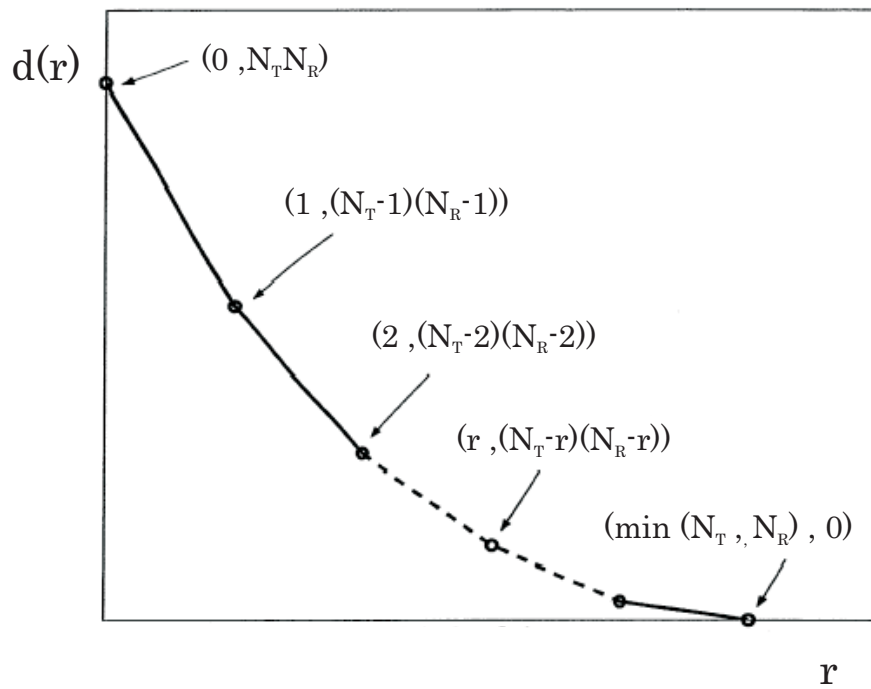
Figure 2.14: Diversity-Multiplexing Trade-off

some scenarios it might be more convenient to apply the coding in the frequency instead of time domain and the extension of space-frequency techniques to SCFDE systems, which is not straightforward, is also addressed in this Thesis.

Part III

Enhancements

Chapter 3

Combining Diversity and Multiplexing in OFDM

3.1   Introduction

A balance goal of fading mitigation and high data rate suggests the investigation of practical designs that can provide both spatial diversity and spatial multiplexing gains. Such designs should be compared with diversity-only and multiplexing-only designs.

The presence of multipath propagation and hence the availability of frequency-diversity generally allows to increase the spatial signaling rate, i.e. to use the multiple antennas to multiplex independent data streams rather than to provide spatial diversity. It is therefore desirable to allocate the channel's degrees of freedom in space and frequency in a flexible way to multiplexing and diversity transmission modes [40].

In a cellular wireless system, the OFDM-STBC [41] and OFDM-SFBC [11] can be used to increase the resultant SNR at the receiver, thus increasing the coverage area: these schemes are good for users at locations farther from the BS. On the other hand, only users located near to the BS can get the rate advantages of SM techniques, which work efficiently

only at high SNRs [39] [42]. Some effort has been already spent in finding techniques to achieve both multiplexing and diversity benefits. MIMO switching schemes, such as [39], are well studied and examined. In switching schemes, either SM or SD schemes are optimally chosen based on some specific selection criterion, so that optimum benefits from both type of schemes can be obtained in the system. This kind of combination is implemented as a time division technique. In recent years, combining SM and SD schemes in the same scheme has gained a lot of interest, because in this case both diversity and multiplexing benefits are available at the same time.

In the present Chapter, a new scheme combining SM and SFBC in OFDM is introduced, trying to achieve both multiplexing and diversity gains, while keeping the latency low.

3.2   JDM Schemes

Schemes that combine SM and SD are hereafter referred as JDM. Let us denote with: P the number of SM branches, Δ the number of transmit antennas per SM branch, $N_T = P\Delta$ the total number of transmit antennas. We can combine SM and SD, such as SFBC, in one structure in the following ways:

1. P, N_R = arbitrary, Δ =2, Alamouti scheme at every SM branch, thus, $2P \times N_R$ Spatially-Multiplexed Orthogonal Space-Frequency Block Coding (SM-OSFBC) systems.

2. P, N_R = arbitrary, $\Delta > 2$, Orthogonal partial rate SFBC scheme at every SM branch, thus, $P\Delta \times N_R$ SM-OSFBC systems. These schemes lose SM benefits because of partial rate SFBC, so they are not considered in this work;

3. P, N_R = arbitrary, $\Delta > 2$, Quasi-orthogonal full rate SFBC scheme at every SM branch, thus, $P\Delta \times N_R$ Spatially-Multiplexed Quasi-orthogonal Space-Frequency Block

Coding (SM-QSFBC) systems.

When coding across space and time is envisioned, we can have Spatially-Multiplexed Orthogonal Space-Time Block Coding (SM-OSTBC) or Spatially-Multiplexed Quasi-orthogonal Space-Time Block Coding (SM-QSTBC) systems.

Recently there are some approaches of incorporating the VBLAST technique with some well known Space-Time Coding (STC) techniques. One such work is described in [43], where a combination of SD and SM for MIMO-OFDM system is proposed. Arguably, the performance of such a JDM system would be better than SD only or SM only schemes. In [43], the SM-OFDM system uses two independent STC for two sets of transmit antennas. Thus, an original 2×2 SM-OFDM system is now extended to 4×2 STC aided SM-OFDM system. At the receiver, the independent STCs are decoded first using pre-whitening, followed by maximum likelihood detection. Again, this increases the receiver complexity quite a lot, though the system performance get much better.

In later work, Alamouti's STBC is combined with SM for OFDM system in [44], and a linear receiver is designed for such a combination. The proposed hybrid SM-STBC design is found to be a good design choice, when compared with SM-only or diversity-only STBC designs. There are many diversity-only strategies that are applicable to OFDM. A "full-diversity full-rate" diversity-only strategy for the case of two transmit antennas ($N_T = 2$) is the Alamouti STBC [45]. A "full-rate diversity" scheme is here defined as a diversity scheme providing rate 1, as in the case of Alamouti, which transmits 2 symbols each 2 time periods (of course, a full-rate diversity scheme is not a full rate scheme generally speaking, since e.g. compared to a 2×2 SM scheme, Alamouti is half-rate). For the general case of $N_T > 2$, however, if a diversity-only design is adopted, only $\frac{1}{2}$-rate full-diversity STBCs exist. Meanwhile, quasi-orthogonal partial-diversity full-rate STBCs are proposed in [12]. An interesting question to which [44] tries to answer is whether the transmit diversity exploited by a full-diversity $N_T = 4$ STBC provides a meaningful gain over the $N_T = 2$ STBC or a

partial-diversity STBC, especially in presence of frequency diversity in coded OFDM.

For a SM-OSTBC scheme similar to the one studied in this Chapter, a non-linear receiver is mentioned in [46]. The main concentration of [46] is on switching between MIMO techniques, i.e. between SD only, SM only and SM-OSTBC schemes. Choosing antenna pairs in SM-OSTBC scheme based on correlation criterion is studied in [47]. Adaptive Modulation and Coding (AMC) applied to SM-OSTBC is studied in [48]. Detection schemes for SM-OSTBC system are analyzed in [49], where linear ZF and QR decomposition based receivers are discussed.

3.3   Proposed Space-Frequency JDM Schemes for OFDM

Following the upper-mentioned trends, we have combined SFBC with SM for OFDM (let us call this scheme OFDM SF-JDM scheme). In SFBC, the coding is done across the subcarriers inside one OFDM symbol duration, while STBC applies the coding across a number of OFDM symbols equal to number of transmit antennas. Therefore an inherent processing delay is unavoidable in STBC [50] and the absence of this delay is one of the advantages of SFBC. A linear receiver for SM-OSFBC system with ZF and MMSE criterion has been analyzed: this linear receiver is very similar to the receiver structure for SM-OSTBC scheme in [44]. The OSIC receiver with ZF and MMSE criterion has been derived, and its FER performance is compared with the linear receiver via simulations. For SM-QSFBC scheme, OSIC receiver with ZF and MMSE is derived, analyzed and simulated. To the best of our knowledge, SM-QSFBC scheme has not been studied and analyzed before this work. It is worth noting here that the OSIC approach taken in this work is similar to original BLAST algorithm in [10]. With the understanding of different receiver structures, the impact of spatial correlation has been investigated. The considered causes for correlation are the insufficient interelement distance at both sides of transmission, and the presence of LOS component in wireless channel.
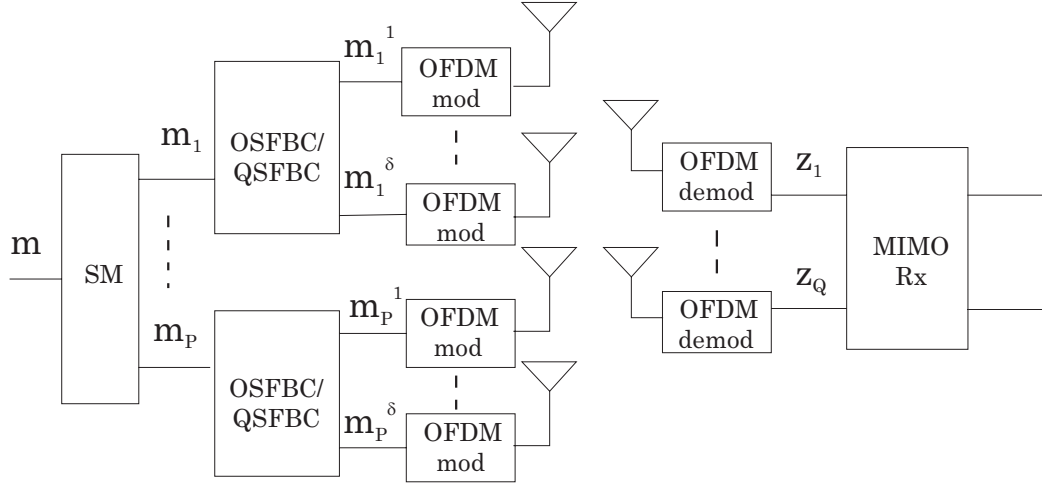
Figure 3.1: Simplified System Model for SM-OSFBC/SM-QSFBC Transmission Scheme

3.3.1   System Model

3.3.1.1   SM-OSFBC Transmission Scheme

In this Section, the transmission structure of the JDM scheme based on combining SM and OSFBC will be explained. A linear two-stages receiver is proposed, which is an extension of the LS receiver in [44], where the linear reception technique is used for SM-OSTBC system based on ZF and MMSE criteria, on sub-carrier by sub-carrier basis. Then a non-linear Successive Interference Cancellation (SIC) receiver is derived, where the detection is based on both ZF and MMSE nulling.

Transmitter

The number of available transmit SM branches and receive antennas are denoted as P, and N_R, respectively. N is the number of sub-carriers in the system. p, q and k are the indices for transmit SM branch, receive antenna and sub-carrier group, respectively. For every p^{th} SM branch, an orthogonal block coding across the sub-carriers is implemented.

Figure 3.1 depicts the basic transceiver architecture. Firstly source bits are Forward Error Correction (FEC) coded. The coded bits stream is baseband modulated using an

appropriate constellation, such as Binary Phase Shift Keying (BPSK), Quadrature Ampli-
tude Modulation (QAM) etc. These baseband modulated symbols are denoted as $\mathbf{m}$. The
sequence of $\mathbf{m}$ is demultiplexed into $\mathbf{m}_1, \ldots, \mathbf{m}_P$ vectors. $\mathbf{m}_p$ is transmitted via p^{th} spatial
channel and can be written as $\mathbf{m}_p = \begin{bmatrix} m_{p,1} & m_{p,2} & \ldots & m_{p,N-1} & m_{p,N} \end{bmatrix}^T$.

For every p^{th} SM branch, a block coding across the sub-carriers is implemented, thus
SFBC is included in the system. For p^{th} SM branch, we have Δ_p number of antennas where
SFBC can be implemented. When $\Delta_p = \Delta$, $\forall p$, then there are $N_T = \Delta \cdot P$ number of
transmit antennas at the transmission side. If well-known Alamouti coding [45] is used
across the sub-carriers, then $\Delta = 2$.

For p^{th} SM branch, $\mathbf{m}_p$ is coded into two vectors $\mathbf{m}_p^{(\delta)}$, with $\delta = 1, 2$. Thus, the
output of the SFBC encoder block of the pth SM branch will be:

$$\mathbf{m}_p^{(1)} = \begin{bmatrix} m_{p,1} & -m_{p,2}^* & \ldots & m_{p,N-1} & -m_{p,N}^* \end{bmatrix}^T \tag{3.1}$$

$$\mathbf{m}_p^{(2)} = \begin{bmatrix} m_{p,2} & m_{p,1}^* & \ldots & m_{p,N} & m_{p,N-1}^* \end{bmatrix}^T \tag{3.2}$$

Let us define:

$$\mathbf{m}_{p,o} = \begin{bmatrix} m_{p,1} & m_{p,3} & \ldots & m_{p,N-3} & m_{p,N-1} \end{bmatrix}^T \tag{3.3}$$

$$\mathbf{m}_{p,e} = \begin{bmatrix} m_{p,2} & m_{p,4} & \ldots & m_{p,N-2} & m_{p,N} \end{bmatrix}^T \tag{3.4}$$

Using these equations, it can be written that:

$$\mathbf{m}_{p,o}^{(1)} = \mathbf{m}_{p,o}; \qquad \mathbf{m}_{p,e}^{(1)} = -\mathbf{m}_{p,e}^* \tag{3.5}$$

$$\mathbf{m}_{p,o}^{(2)} = \mathbf{m}_{p,e}; \qquad \mathbf{m}_{p,e}^{(2)} = \mathbf{m}_{p,o}^* \tag{3.6}$$

After SM and SFBC operations, IFFT modulation is performed and CP is added

before transmission via the respective transmit antenna. Transmitted time domain samples, $\mathbf{x}_p^{(\delta)}$, can be related to $\mathbf{m}_p^{(\delta)}$ as $\mathbf{x}_p^{(\delta)} = \mathcal{F}^H\{\mathbf{m}_p^{(\delta)}\}$, where $\mathcal{F}^H$ is the IFFT matrix.

Two-Stage Linear Receiver

In [51], a two stage interference cancellation receiver scheme for STBC is presented. This receiver treats one of the branches as the interfering source for the other one. This receiver is used to derive a linear reception technique for SM-OSTBC system in [44]. In this work, a similar receiver structure for our SM-OSFBC system is adopted.

After DFT demodulation, the frequency-domain sub-carrier signal can be expressed as:

$$\mathbf{z}_q = \sum_{\delta=1}^{2}\sum_{p=1}^{P} \mathbf{h}_{q,p}^{(\delta)} \odot \mathbf{m}_p^{(\delta)} + \mathbf{n}_q \tag{3.7}$$

where $\mathbf{h}_{q,p}^{(\delta)}$ denotes the Channel Transfer Function (CTF) vector of the wireless channel between q^{th} receive antenna and δ^{th} SFBC antenna of pth SM branch, $\mathbf{n}_q$ is the frequency-domain sample of the received noise at q^{th} received branch, and $\odot$ means element-wise multiplication.

We can divide $\mathbf{z}_q$ in odd and even components $\forall q, \ q = 1, 2$. Using Equations (3.3)-(3.4), it can be expressed:

$$
\begin{aligned}
\mathbf{z}_{q,o} &= \ \mathbf{h}_{q,1,o}^{(1)} \odot \mathbf{m}_{1,o} + \mathbf{h}_{q,1,o}^{(2)} \odot \mathbf{m}_{1,e} + \ldots + \ldots \\
&\quad \mathbf{h}_{q,P,o}^{(1)} \odot \mathbf{m}_{P,o} + \mathbf{h}_{q,P,o}^{(2)} \odot \mathbf{m}_{P,e} + \mathbf{n}_{q,o}
\end{aligned}
\tag{3.8}
$$

$$
\begin{aligned}
\mathbf{z}_{q,e} &= \ -\mathbf{h}_{q,1,e}^{(1)} \odot \mathbf{m}_{1,e}^* + \mathbf{h}_{q,1,e}^{(2)} \odot \mathbf{m}_{1,o}^* + \ldots - \ldots \\
&\quad \mathbf{h}_{q,P,e}^{(1)} \odot \mathbf{m}_{P,e}^* + \mathbf{h}_{q,P,e}^{(2)} \odot \mathbf{m}_{P,o}^* + \mathbf{n}_{q,e}
\end{aligned}
\tag{3.9}
$$

For sake of simplicity, $P = 2$ and $N_R = 2$. It is straightforward to extend this analysis to higher number of transmit and receive antennas. Let us introduce the $N_R \times 1$ column vectors, $\mathbf{h}_{p,o}^{(\delta)}, \mathbf{h}_{p,e}^{(\delta)}, \mathbf{z}_o, \mathbf{z}_e$, whose q^{th} components are respectively, the odd and even elements of

$$
\mathbf{z}_k = \begin{bmatrix} z_{1,o} \\ z_{2,o} \\ z_{1,e}^* \\ z_{2,e}^* \end{bmatrix} = \begin{bmatrix} h_{11,o}^{(1)} & h_{11,o}^{(2)} & h_{12,o}^{(1)} & h_{12,o}^{(2)} \\ h_{21,o}^{(1)} & h_{21,o}^{(2)} & h_{22,o}^{(1)} & h_{22,o}^{(2)} \\ h_{11,e}^{(2)*} & -h_{11,e}^{(1)*} & h_{12,e}^{(2)*} & -h_{12,e}^{(1)*} \\ h_{21,e}^{(2)*} & -h_{21,e}^{(1)*} & h_{22,e}^{(2)*} & -h_{22,e}^{(1)*} \end{bmatrix} \begin{bmatrix} m_{1,o} \\ m_{1,e} \\ m_{2,o} \\ m_{2,e} \end{bmatrix} + \begin{bmatrix} n_{1,o} \\ n_{2,o} \\ n_{1,e}^* \\ n_{2,e}^* \end{bmatrix}
$$

$$
= \begin{bmatrix} \mathbf{z}_o \\ \mathbf{z}_e^* \end{bmatrix}_k = \begin{bmatrix} \mathbf{h}_{1,o}^{(1)} & \mathbf{h}_{1,o}^{(2)} & \mathbf{h}_{2,o}^{(1)} & \mathbf{h}_{2,o}^{(2)} \\ \mathbf{h}_{1,e}^{(2)*} & -\mathbf{h}_{1,e}^{(1)*} & \mathbf{h}_{2,e}^{(2)*} & -\mathbf{h}_{2,e}^{(1)*} \end{bmatrix}_k \begin{bmatrix} m_{1,o} \\ m_{1,e} \\ m_{2,o} \\ m_{2,e} \end{bmatrix}_k + \begin{bmatrix} \mathbf{n}_o \\ \mathbf{n}_e^* \end{bmatrix}_k \quad (3.10)
$$

CTF between δ^{th} transmit antenna of the pth SM branch and q^{th} receive antenna, and the odd and even elements of received frequency domain signal at q^{th} receive antenna. Furthermore, we define the $N_R \times 1$ column vectors, $\mathbf{n}_o, \mathbf{n}_e$, whose q^{th} components are respectively, the odd and even elements of frequency-domain noise at q^{th} receive antenna.

Using these notations above, (3.8) and (3.9) can be rewritten as (3.10), where a subcarrier notation has been used, and it is understood that such a system model is intended $\forall k \in [1, \ldots, \frac{N}{2}]$.

Coherence bandwidth and subcarriers spacing are denoted as B_c and Δf, respectively. We define severely frequency-selective scenario when coherence bandwidth is smaller than a pair of subcarriers bandwidth, i.e. $B_c < 2\Delta f$. In this case, a concept called companion matrix is used.

Given a matrix $\mathbf{A}$:

$$
\mathbf{A} = \begin{bmatrix} \mathbf{a}_{11} & \mathbf{a}_{12} \\ \mathbf{a}_{21} & \mathbf{a}_{22} \end{bmatrix} \quad (3.11)
$$

the companion matrix $\widetilde{\mathbf{A}}$ is defined as:

$$
\widetilde{\mathbf{A}} = \begin{bmatrix} -\mathbf{a}_{22}^T & \mathbf{a}_{12}^T \\ \mathbf{a}_{21}^T & -\mathbf{a}_{11}^T \end{bmatrix} \quad (3.12)
$$

The matrix pair formed by $\mathbf{A}$ and $\widetilde{\mathbf{A}}$ identifies a so called orthogonal pair. $\mathbf{a}_{ij}, \forall i, j,$

are column vectors of size $m \times 1$, thus $\mathbf{A}$ and $\widetilde{\mathbf{A}}$ are matrices of sizes $2m \times 2$ and $2 \times 2m$ respectively.

Let us omit from now on the subcarrier index k. Equation (3.10) can be represented as:

$$\mathbf{z} = \mathbf{Hm} + \mathbf{n} = \left[\ \mathbf{H}_i \,|\, \mathbf{H}_j \ \right] \mathbf{m} + \mathbf{n} \tag{3.13}$$

with:

$$\mathbf{H}_i = \begin{bmatrix} \mathbf{h}_{1,o}^{(1)} & \mathbf{h}_{1,o}^{(2)} \\ \mathbf{h}_{1,e}^{(2)*} & -\mathbf{h}_{1,e}^{(1)*} \end{bmatrix} \ , \ \mathbf{H}_j = \begin{bmatrix} \mathbf{h}_{2,o}^{(1)} & \mathbf{h}_{2,o}^{(2)} \\ \mathbf{h}_{2,e}^{(2)*} & -\mathbf{h}_{2,e}^{(1)*} \end{bmatrix} \tag{3.14}$$

We denote the companion matrices of $\mathbf{H}_i$ and $\mathbf{H}_j$ as $\widetilde{\mathbf{H}}_i$ and $\widetilde{\mathbf{H}}_j$, respectively. We define a new matrix, $\widetilde{\mathbf{H}} = \left[\ \widetilde{\mathbf{H}}_i^T \ \ \widetilde{\mathbf{H}}_j^T \ \right]^T$, with:

$$\widetilde{\mathbf{H}}_i = \begin{bmatrix} \mathbf{h}_{1,e}^{(1)H} & \mathbf{h}_{1,o}^{(2)T} \\ \mathbf{h}_{1,e}^{(2)H} & -\mathbf{h}_{1,o}^{(1)T} \end{bmatrix} \ , \ \widetilde{\mathbf{H}}_j = \begin{bmatrix} \mathbf{h}_{2,e}^{(1)H} & \mathbf{h}_{2,o}^{(2)T} \\ \mathbf{h}_{2,e}^{(2)H} & -\mathbf{h}_{2,o}^{(1)T} \end{bmatrix} \tag{3.15}$$

At the beginning of the receiver, the received signal $\mathbf{z}$ is filtered with $\widetilde{\mathbf{H}}$ as it is shown in (3.16):

$$\begin{aligned} \mathbf{z}' = \widetilde{\mathbf{H}}\mathbf{z} = \widetilde{\mathbf{H}}\left(\mathbf{Hm} + \mathbf{n}\right) \ &= \ \widetilde{\mathbf{H}}\mathbf{Hm} + \widetilde{\mathbf{H}}\mathbf{n} \\ &= \ \begin{bmatrix} \widetilde{\mathbf{H}}_i \\ \widetilde{\mathbf{H}}_j \end{bmatrix} \left[\ \mathbf{H}_i \,|\, \mathbf{H}_j \ \right] \mathbf{m} + \widetilde{\mathbf{H}}\mathbf{n} \end{aligned} \tag{3.16}$$

The part $\widetilde{\mathbf{H}}\mathbf{H}$ can be extended as in Equation (3.17) where $\alpha_1' = \mathbf{h}_{1,e}^{(1)H}\mathbf{h}_{1,o}^{(1)} + \mathbf{h}_{1,o}^{(2)T}\mathbf{h}_{1,e}^{(2)*}$ and $\alpha_2' = \mathbf{h}_{2,e}^{(1)H}\mathbf{h}_{2,o}^{(1)} + \mathbf{h}_{2,o}^{(2)T}\mathbf{h}_{2,e}^{(2)*}$. $\mathbf{G}_{12}$ and $-\mathbf{G}_{21}$ form an orthogonal pair.

$$
\widetilde{\mathbf{H}}\mathbf{H} = \begin{bmatrix} \alpha_1' \mathbf{I}_2 & \mathbf{G}_{12} \\ \mathbf{G}_{21} & \alpha_2' \mathbf{I}_2 \end{bmatrix} \tag{3.17}
$$

$$
\mathbf{G}_{12} = \begin{bmatrix} \mathbf{h}_{1,e}^{(1)H}\mathbf{h}_{2,o}^{(1)} + \mathbf{h}_{1,o}^{(2)T}\mathbf{h}_{2,e}^{(2)*} & \mathbf{h}_{1,e}^{(1)H}\mathbf{h}_{2,o}^{(2)} - \mathbf{h}_{1,o}^{(2)T}\mathbf{h}_{2,e}^{(1)*} \\ \mathbf{h}_{1,e}^{(2)H}\mathbf{h}_{2,o}^{(1)} - \mathbf{h}_{1,o}^{(1)T}\mathbf{h}_{2,e}^{(2)*} & \mathbf{h}_{1,e}^{(2)H}\mathbf{h}_{2,o}^{(2)} + \mathbf{h}_{1,o}^{(1)T}\mathbf{h}_{2,e}^{(1)*} \end{bmatrix}
$$

$$
\mathbf{G}_{21} = \begin{bmatrix} \mathbf{h}_{2,e}^{(1)H}\mathbf{h}_{1,o}^{(1)} + \mathbf{h}_{2,o}^{(2)T}\mathbf{h}_{1,e}^{(2)*} & \mathbf{h}_{2,e}^{(1)H}\mathbf{h}_{1,o}^{(2)} - \mathbf{h}_{2,o}^{(2)T}\mathbf{h}_{1,e}^{(1)*} \\ \mathbf{h}_{2,e}^{(2)H}\mathbf{h}_{1,o}^{(1)} - \mathbf{h}_{2,o}^{(1)T}\mathbf{h}_{1,e}^{(2)*} & \mathbf{h}_{2,e}^{(2)H}\mathbf{h}_{1,o}^{(2)} + \mathbf{h}_{2,o}^{(1)T}\mathbf{h}_{1,e}^{(1)*} \end{bmatrix}
$$

Equation (3.16) can be written as:

$$
\mathbf{z}' = \begin{bmatrix} \alpha_1' \mathbf{I}_2 & \mathbf{G}_{12} \\ \mathbf{G}_{21} & \alpha_2' \mathbf{I}_2 \end{bmatrix} \mathbf{m} + \widetilde{\mathbf{H}}\mathbf{n} \tag{3.18}
$$

The LS receiver is modelled by the matrix:

$$
\mathbf{W} = \frac{1}{\gamma} \begin{bmatrix} \alpha_2' \mathbf{I}_2 & -\mathbf{G}_{12} \\ -\mathbf{G}_{21} & \alpha_1' \mathbf{I}_2 \end{bmatrix} \tag{3.19}
$$

where $\gamma = \alpha_1'\alpha_2' - [\mathbf{G}_{12}(1,1)\mathbf{G}_{12}(2,2) - \mathbf{G}_{12}(1,2)\mathbf{G}_{12}(2,1)]$. Thus, the estimated symbol vector can be written as:

$$
\widehat{\mathbf{m}} = \mathbf{W}\mathbf{z}' = \mathbf{m} + \mathbf{W}\widetilde{\mathbf{H}}\mathbf{n} \tag{3.20}
$$

Under the hypothesis of moderately frequency-selective scenario $(B_c > 2\Delta f)$ it can be assumed that $\mathbf{h}_{p,o}^{(\delta)} = \mathbf{h}_{p,e}^{(\delta)} = \mathbf{h}_{p,oe}^{(\delta)}$. Therefore, Equation (3.10) can be written as:

$$
\mathbf{z} = \begin{bmatrix} \mathbf{z}_o \\ \mathbf{z}_e^* \end{bmatrix} = \begin{bmatrix} \mathbf{H}_1 \,|\, \mathbf{H}_2 \end{bmatrix} \mathbf{m} + \mathbf{n} \tag{3.21}
$$

where:

$$\mathbf{H}_1 = \begin{bmatrix} \mathbf{h}_{1,oe}^{(1)} & \mathbf{h}_{1,oe}^{(2)} \\ \mathbf{h}_{1,oe}^{(2)*} & -\mathbf{h}_{1,oe}^{(1)*} \end{bmatrix} \ , \ \mathbf{H}_2 = \begin{bmatrix} \mathbf{h}_{2,oe}^{(1)} & \mathbf{h}_{2,oe}^{(2)} \\ \mathbf{h}_{2,oe}^{(2)*} & -\mathbf{h}_{2,oe}^{(1)*} \end{bmatrix} \tag{3.22}$$

are two orthogonal matrices, such that:

$$\mathbf{H}_1^H \mathbf{H}_1 = \left(|\mathbf{h}_{1,oe}^{(1)}|^2 + |\mathbf{h}_{1,oe}^{(2)}|^2 \right) \mathbf{I}_2 = \alpha_1 \mathbf{I}_2 \tag{3.23}$$

$$\mathbf{H}_2^H \mathbf{H}_2 = \left(|\mathbf{h}_{2,oe}^{(1)}|^2 + |\mathbf{h}_{2,oe}^{(2)}|^2 \right) \mathbf{I}_2 = \alpha_2 \mathbf{I}_2 \tag{3.24}$$

where $\alpha_1 = |\mathbf{h}_{1,oe}^{(1)}|^2 + |\mathbf{h}_{1,oe}^{(2)}|^2$, $\alpha_2 = |\mathbf{h}_{2,oe}^{(1)}|^2 + |\mathbf{h}_{2,oe}^{(2)}|^2$ and $\mathbf{I}_2$ is the 2×2 identity matrix. Similarly,

$$\mathbf{H}_1^H \mathbf{H}_2 \left(\mathbf{H}_1^H \mathbf{H}_2 \right)^H = \mathbf{H}_1^H \mathbf{H}_2 \mathbf{H}_2^H \mathbf{H}_1 = (a+b)\mathbf{I}_2 \tag{3.25}$$

where $a = |\mathbf{h}_{1,oe}^{(1)H} \mathbf{h}_{2,oe}^{(1)} + \mathbf{h}_{1,oe}^{(2)T} \mathbf{h}_{2,oe}^{(2)*}|^2$ and $b = |\mathbf{h}_{1,oe}^{(1)H} \mathbf{h}_{2,oe}^{(2)} - \mathbf{h}_{1,oe}^{(2)T} \mathbf{h}_{2,oe}^{(1)*}|^2$.

Now we can write the estimated symbol vector by using the LS estimator, i.e. by multiplying the received symbol vector with the Moore-Penrose pseudo-inverse matrix for $\mathbf{H}$,

$$\begin{aligned} \widehat{\mathbf{m}} &= \left(\mathbf{H}^H \mathbf{H} \right)^{-1} \mathbf{H}^H \mathbf{z} \\ &= \frac{1}{\alpha_1 \alpha_2 - (a+b)} \begin{bmatrix} \mathbf{H}_2^H \mathbf{H}_2 & -\mathbf{H}_1^H \mathbf{H}_2 \\ -\mathbf{H}_2^H \mathbf{H}_1 & \mathbf{H}_1^H \mathbf{H}_1 \end{bmatrix} \begin{bmatrix} \mathbf{H}_1^H \\ \mathbf{H}_2^H \end{bmatrix} \mathbf{z} \end{aligned} \tag{3.26}$$

Using the above definitions, we can express the Equation (3.26) as follows:

$$\widehat{\mathbf{m}} = \frac{1}{\alpha_1 \alpha_2 - (a+b)} \begin{bmatrix} \alpha_2 \mathbf{I}_2 & -\mathbf{H}_1^H \mathbf{H}_2 \\ -\mathbf{H}_2^H \mathbf{H}_1 & \alpha_1 \mathbf{I}_2 \end{bmatrix} \begin{bmatrix} \mathbf{H}_1^H \\ \mathbf{H}_2^H \end{bmatrix} \mathbf{z} \tag{3.27}$$

The MMSE receiver can be implemented in the same simple way. Defining ρ_n as the average SNR at each of the receive antennas, and the new constants $\beta_1 = \alpha_1 + \frac{P\Delta}{\rho_n}$,
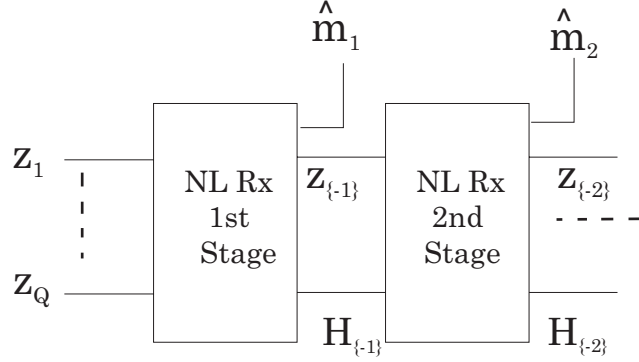
Figure 3.2: Simplified data flow for OSIC receiver

$\beta_2 = \alpha_2 + \frac{P\Delta}{\rho_n}$ then we can rewrite (3.27) as:

$$\widehat{\mathbf{m}} = \frac{1}{\beta_1\beta_2 - (a+b)} \begin{bmatrix} \beta_2\mathbf{I}_2 & -\mathbf{H}_1^H\mathbf{H}_2 \\ -\mathbf{H}_2^H\mathbf{H}_1 & \beta_1\mathbf{I}_2 \end{bmatrix} \begin{bmatrix} \mathbf{H}_1^H \\ \mathbf{H}_2^H \end{bmatrix} \mathbf{z} \qquad (3.28)$$

OSIC-based Non-Linear Receiver

The basic transceiver architecture has been shown in Figure 3.1. In the case of OSIC-based non-linear receiver, the detection part is shown in Figure 3.2. The key idea of the non-linear receiver is to decode the symbol streams successively and extract them away layer by layer. At the beginning of each stage, the stream with the highest SNR is chosen using ZF or MMSE detection for peeling. Once one particular layer is decoded, then the effect of the detected layer is subtracted from the received signal. From the remaining signal, the next branch in terms of SNR strength is chosen. This is continued until the last layer is decoded. This kind of non-linear detection is called OSIC [25],[10]. OSIC is performed on subcarrier by subcarrier basis. On each subcarrier, the detection scheme appears to be very similar to VBLAST detection, as derived in [10]. OSIC improves the detection quality compared to detection without ordering and is shown to be optimal for SIC approach [25].

The assumptions for this algorithm are the absence of errors propagation, the knowledge of the channel at the receiver, and ideal inter-stream interference cancellation, i.e. no residual of the interferent stream will be left after the cancellation operation.

We consider $P = 2$, $\Delta = 2$ and $N_R = 2$. Considering the frequency domain, it can be written:

$$\mathbf{z}_k = \mathbf{H}_k \mathbf{m}_k + \mathbf{n}_k \tag{3.29}$$

where:

$$\mathbf{H}_k = \begin{bmatrix} h_{11,o}^{(1)} & h_{11,o}^{(2)} & h_{12,o}^{(1)} & h_{12,o}^{(2)} \\ h_{11,e}^{(2)*} & -h_{11,e}^{(1)*} & h_{12,e}^{(2)*} & -h_{12,e}^{(1)*} \\ h_{21,o}^{(1)} & h_{21,o}^{(2)} & h_{22,o}^{(1)} & h_{22,o}^{(2)} \\ h_{21,e}^{(2)*} & -h_{21,e}^{(1)*} & h_{22,e}^{(2)*} & -h_{22,e}^{(1)*} \end{bmatrix}_k \tag{3.30}$$

and $\mathbf{z}_k = \left[z_{1,o}\,,\, z_{1,e}^*\,,\, z_{2,o}\,,\, z_{2,e}^* \right]_k^T$; $\mathbf{m}_k = \left[m_{1,o}\,,\, m_{1,e}, m_{2,o}\,,\, m_{2,e} \right]_k^T$; $\mathbf{n}_k = \left[n_{1,o}\,,\, n_{1,e}^*\,,\, n_{2,o}\,,\, n_{2,e}^* \right]_k^T$ with $k \in [1, \ldots, \frac{N}{2}]$.

The OSIC receiver consists of two steps: nulling and cancellation. While implementing the nulling operation, we consider two options, ZF and MMSE. For ZF, we calculate the Moore-Penrose pseudo-inverse of the CTF:

$$\begin{aligned} \mathbf{G}_k &= [\mathbf{g}_1\ \mathbf{g}_2\ \mathbf{g}_3\ \mathbf{g}_4]_k = \sqrt{\frac{\Delta P}{P_T}} \left\{ \mathbf{H}_k^H \mathbf{H}_k \right\}^{-1} \mathbf{H}_k^H \\ &= \sqrt{\frac{4}{P_T}} \left\{ \mathbf{H}_k^H \mathbf{H}_k \right\}^{-1} \mathbf{H}_k^H \end{aligned} \tag{3.31}$$

where P_T is the total transmit power from all transmit antennas, while for the MMSE we consider a kind of pseudo-inverse that considers also the noise term:

$$\mathbf{G}_k = \sqrt{\frac{4}{P_T}} \left\{ \mathbf{H}_k^H \mathbf{H}_k + \frac{4\sigma^2}{P_T} \mathbf{I}_4 \right\}^{-1} \mathbf{H}_k^H \tag{3.32}$$

where $[\mathbf{g}_i]_k$ is the ith column of $\mathbf{G}_k$, σ^2 is the noise variance at each receive antenna and $\mathbf{I}_4$ is the 4×4 identity matrix. For sake of simplicity, for both ZF and MMSE we have assumed $\Delta = 2$ and $P = 2$. At this stage, we calculate the metric:

$$l = arg \; \min_l \{d_1, d_2\} \tag{3.33}$$

where $d_1 = \mathbf{c}(1) + \mathbf{c}(3)$, $d_2 = \mathbf{c}(2) + \mathbf{c}(4)$. For ZF the vector, $\mathbf{c} = [\mathbf{c}(1) \; \mathbf{c}(2) \; \mathbf{c}(3) \; \mathbf{c}(4)] = diag\left(\{\mathbf{H}_k^H \mathbf{H}_k\}^{-1}\right)$ and for MMSE the vector, $\mathbf{c} = [\mathbf{c}(1) \; \mathbf{c}(2) \; \mathbf{c}(3) \; \mathbf{c}(4)] = diag\left(\{\mathbf{H}_k^H \mathbf{H}_k + \frac{4\sigma^2}{P_T} \mathbf{I}_4\}^{-1}\right)$.

If $l = arg \; \min_l \{d_1, d_2\} = 1$ then we decode first the stream associated to $p = 1$ by doing

$$\widehat{\mathbf{m}}_{1,k} = \left[\begin{array}{c} \widehat{m}_{1,o} \\ \widehat{m}_{1,e} \end{array} \right]_k = \left[\begin{array}{c} \mathbf{g}_1^H \\ \mathbf{g}_2^H \end{array} \right]_k \mathbf{z}_k \tag{3.34}$$

and the second stream by doing the following steps:

$$\mathbf{z}_k' = \mathbf{z}_k - [\mathbf{h}_1 \; \mathbf{h}_2]_k \left[\begin{array}{c} \widehat{m}_{1,o} \\ \widehat{m}_{1,e} \end{array} \right]_k \tag{3.35}$$

$$\mathbf{H}_k' = [\mathbf{h}_3 \; \mathbf{h}_4]_k \tag{3.36}$$

$$\mathbf{H}_k'^H \mathbf{H}_k' = \frac{1}{|h_{12,o}^{(1)}|^2 + |h_{12,o}^{(2)}|^2 + |h_{22,o}^{(1)}|^2 + |h_{22,o}^{(2)}|^2} \mathbf{I}_2$$

$$= \frac{1}{\alpha} \mathbf{I}_2 \tag{3.37}$$

$$\widehat{\mathbf{m}}_{2,k} = \left[\begin{array}{c} \widehat{m}_{2,o} \\ \widehat{m}_{2,e} \end{array} \right]_k = \frac{1}{\alpha} \mathbf{H}_k'^H \mathbf{z}_k' \tag{3.38}$$

where $[\mathbf{h}_i]_k$ is the ith column of $\mathbf{H}_k$ and $\mathbf{I}_2$ is the 2×2 identity matrix. Equation (3.35) describes the cancellation operation, and in (3.37) neighboring subcarriers are assumed to have identical channel frequency response. Exactly the dual procedure of (3.34)÷(3.38) has to be applied if $l = arg \; \min_l \{d_1, d_2\} = 2$, to decode the second SM branch at the beginning

and then the first one.

3.3.1.2   SM-QSFBC-OFDM Transmission Scheme

Transmitter

Similar to SM-OSFBC scheme, Figure 3.1 explains the basic transmitter architecture for proposed SM-QSFBC system, with the receiver depicted in Figure 3.2. For $\Delta > 2$, such as $\Delta = 4$, we use quasi-orthogonal codes as in [12] for the studied SM-QSFBC system, so that SM-rate of P is maintained. For p^{th} SM branch, $\mathbf{m}_p$ is coded into Δ number of vectors, $\mathbf{m}_p^{(\delta)}$; $\delta = 1, \ldots, \Delta$. After SM and QSFBC operations, IFFT modulation is performed and CP is added before transmission via the respective transmit antenna. N subcarriers are divided into $N/4$ groups of 4 subcarriers and on each group QSFBC is performed. Note that $N_R \geq P$.

OSIC Receiver

The OSIC receiver for SM-QSFBC scheme is similar to the OSIC receiver for SM-OSFBC scheme described in Section 3.3.1.1. We can write the equivalent system model as follows:

$$\mathbf{z}_k = \mathbf{H}_k \mathbf{m}_k + \mathbf{n}_k \qquad k \in [1, \ldots, \frac{N}{4}] \tag{3.39}$$

where $\mathbf{z}_k$ and $\mathbf{n}_k$ are the concatenations of the received signals and noise, respectively, for the kth group of subcarriers. Here $\mathbf{z}_k = \left[\mathbf{z}_k^{(1)} \ldots \mathbf{z}_k^{(N_R)} \right]^T$, with $\mathbf{z}_k^{(q)} = \left[z_{4k-3}^{(q)}\ z_{4k-2}^{(q)*}\ z_{4k-1}^{(q)*}\ z_{4k}^{(q)} \right]^T$. Similarly, $\mathbf{m}_k = \left[\mathbf{m}_k^{(1)} \ldots \mathbf{m}_k^{(P)} \right]^T$, with $\mathbf{m}_k^{(p)} = \left[m_{4k-3}^{(p)}\ m_{4k-2}^{(p)}\ m_{4k-1}^{(p)}\ m_{4k}^{(p)} \right]$. $\mathbf{m}_x^{(y)}$ and $\mathbf{z}_x^{(y)}$ denote transmitted and received samples, respectively, for x^{th} subcarriers group on y^{th} SM branch or y^{th} receive antenna. $\mathbf{H}_k$ is shown in (3.40) as,

$$\mathbf{H}_k = \begin{bmatrix} [\mathbf{H}_{11}]_k & \cdots & [\mathbf{H}_{1P}]_k \\ \vdots & \ddots & \vdots \\ [\mathbf{H}_{N_R 1}]_k & \cdots & [\mathbf{H}_{N_R P}]_k \end{bmatrix} \tag{3.40}$$

where $[\mathbf{H}_{ij}]_k$, with $i \in \{1, \ldots, N_R\}$ and $j \in \{1, \ldots, P\}$, is:

$$[\mathbf{H}_{ij}]_k = \begin{bmatrix} h_{ij,4k-3}^{(1)} & h_{ij,4k-3}^{(2)} & h_{ij,4k-3}^{(3)} & h_{ij,4k-3}^{(4)} \\ h_{ij,4k-2}^{(2)*} & -h_{ij,4k-2}^{(1)*} & h_{ij,4k-2}^{(4)*} & -h_{ij,4k-2}^{(3)*} \\ h_{ij,4k-1}^{(3)*} & h_{ij,4k-1}^{(4)*} & -h_{ij,4k-1}^{(1)*} & -h_{ij,4k-1}^{(2)*} \\ h_{ij,4k}^{(4)} & -h_{ij,4k}^{(3)} & -h_{ij,4k}^{(2)} & h_{ij,4k}^{(1)} \end{bmatrix} \tag{3.41}$$

For ZF, we calculate the Moore-Penrose pseudo-inverse, $\mathbf{G}_k$, of the equivalent CTF, $\mathbf{H}_k$,

$$\begin{aligned} \mathbf{G}_k &= [\mathbf{g}_1 \ldots \mathbf{g}_{4N_R}]_k = \sqrt{\frac{\Delta P}{P_T}} \left\{ \mathbf{H}_k^H \mathbf{H}_k \right\}^{-1} \mathbf{H}_k^H \\ &= \sqrt{\frac{8}{P_T}} \left\{ \mathbf{H}_k^H \mathbf{H}_k \right\}^{-1} \mathbf{H}_k^H \end{aligned} \tag{3.42}$$

where P_T is total transmit power from all transmit antennas.

For the MMSE nulling operator, the pseudo-inverse is defined considering the noise variance [25], $\mathbf{G}_k = \sqrt{\frac{4P}{P_T}} \{ \mathbf{H}^H \mathbf{H} + \frac{4P}{\rho} \mathbf{I}_{4P} \}^{-1} \mathbf{H}^H$. Note that in our case, the number of transmit antennas is $\Delta P = 4P$. The SNR is $\rho = \frac{P_T}{\sigma^2}$, with σ^2 noise variance at each receive antenna. Using this definition of ρ, we finally obtain the MMSE nulling operator as

$$\begin{aligned} \mathbf{G}_k &= [\mathbf{g}_1 \ldots \mathbf{g}_{4N_R}]_k = \sqrt{\frac{\Delta P}{P_T}} \left\{ \mathbf{H}_k^H \mathbf{H}_k + \frac{\Delta P \sigma^2}{P_T} \mathbf{I}_{\Delta P} \right\}^{-1} \mathbf{H}_k^H \\ &= \sqrt{\frac{8}{P_T}} \left\{ \mathbf{H}_k^H \mathbf{H}_k + \frac{8\sigma^2}{P_T} \mathbf{I}_8 \right\}^{-1} \mathbf{H}_k^H \end{aligned} \tag{3.43}$$

where $[\mathbf{g}_i]_k$ is the ith column of $\mathbf{G}_k$, $\mathbf{I}_8$ is the 8×8 identity matrix and we have considered that $\Delta = 4$ and $P = 2$.

Let us define a vector, $\mathbf{\Omega}$ as $diag\left[\{ \mathbf{H}_k^H \mathbf{H}_k \}^{-1} \right]$ for ZF and $diag\left[\{ \mathbf{H}_k^H \mathbf{H}_k + \frac{8\sigma^2}{P_T} \mathbf{I}_8 \}^{-1} \right]$ for MMSE, where $diag\left[\mathbf{X} \right]$ is the vector containing all the diagonal components of matrix $\mathbf{X}$.

After that, then the ordering for layer-by-layer detection is done, by determining the strongest received signal branch. For this, we calculate the component of a vector,

$$
\begin{aligned}
\mathbf{d}(p) \ &= \ \mathbf{\Omega}(p) + \mathbf{\Omega}(p+P) + \mathbf{\Omega}(p+2P) + \dots \\
&+ \mathbf{\Omega}(p + (\Delta - 1)P)
\end{aligned}
\tag{3.44}
$$

where $\mathbf{\Omega}(p)$ and $\mathbf{d}(p)$ are the pth element of vector $\mathbf{\Omega}$ and $\mathbf{d}$, respectively. Clearly, $\mathbf{\Omega} \in \mathcal{C}^{[4P \times 1]}$ and $\mathbf{d} \in \mathcal{C}^{[P \times 1]}$. For example, when $\Delta = 4$ and $P = 2$, we can write that $\mathbf{d}(1) = \mathbf{\Omega}(1) + \mathbf{\Omega}(3) + \mathbf{\Omega}(5) + \mathbf{\Omega}(7)$ and $\mathbf{d}(2) = \mathbf{\Omega}(2) + \mathbf{\Omega}(4) + \mathbf{\Omega}(6) + \mathbf{\Omega}(8)$.

Using the vector $\mathbf{d}$, a new vector $\mathbf{\Phi}$ is defined, which represents the received strength of transmitted branches in descending order (i.e. the SM branches are arranged in descending order in this vector). We define, $\mathbf{\Phi}(1) = arg \ \min_l \{\mathbf{d}(l)\}, \forall \, l \in [1, \dots, P]$. Similarly, $\mathbf{\Phi}(2) = arg \ \min_l \{\mathbf{d}(l)\}, \forall \, l \in [1, \dots, P] \backslash \mathbf{\Phi}(1)$. This is continued until all P transmit branches are ordered. The metric to define the descending order of received SM branches in $\mathbf{\Phi}$ is found based on OSIC approach as explained in [25].

If $\mathbf{\Phi}(1) = 1$, then we extract the first receive stream by using ZF or MMSE nulling criterion, i.e. $\widehat{\mathbf{m}}_k^{(1)} = \mathbf{G}_{1,k} \mathbf{z}_k$, where $\widehat{\mathbf{m}}_k^{(1)} = \left[\widehat{m}_{4k-3}^{(1)} \ \widehat{m}_{4k-2}^{(1)} \ \widehat{m}_{4k-1}^{(1)} \ \widehat{m}_{4k}^{(1)} \right]_k^T$ and $\mathbf{G}_{1,k} = [\mathbf{g}_1 \ \mathbf{g}_2 \ \mathbf{g}_3 \ \mathbf{g}_4]_k^T$.

Once the strongest branch is extracted, then the contribution of this branch is subtracted from the remaining signal, and the new equivalent CTF is obtained:

$$
\mathbf{z}_k' = \mathbf{z}_k - [\mathbf{h}_1 \ \mathbf{h}_2 \ \mathbf{h}_3 \ \mathbf{h}_4]_k \, \widehat{\mathbf{m}}_k^{(1)} = \mathbf{H}_k' \left[\mathbf{m}_k^{(2)} \ \dots \ \mathbf{m}_k^{(P)} \right]^T
\tag{3.45}
$$

where $\mathbf{H}_k' = [\mathbf{h}_5 \ \mathbf{h}_6 \ \dots \ \mathbf{h}_{4P}]_k$ and $[\mathbf{h}_i]_k$ is the ith column of $\mathbf{H}_k$.

The next strongest branch is found as $\mathbf{\Phi}(2)$. A new nulling operator is defined as $\mathbf{G}_{\mathbf{\Phi}(2),k} = \left[\mathbf{g}_{4\mathbf{\Phi}(2)-3} \ \mathbf{g}_{4\mathbf{\Phi}(2)-2} \ \mathbf{g}_{4\mathbf{\Phi}(2)-1} \ \mathbf{g}_{4\mathbf{\Phi}(2)} \right]_k^T$. With this nulling operator and new CTF matrix as in (3.45), a new nulling criterion is defined and the second strongest branch is ex-

tracted from the remaining signal as shown below for ZF and MMSE solutions, respectively:

$$
\begin{aligned}
\widehat{\mathbf{m}}_k^{(\boldsymbol{\Phi}(2))} &= \mathbf{G}_{\boldsymbol{\Phi}(2),k}^{ZF}\mathbf{z}_k^{'} = \sqrt{\frac{\Delta P}{P_T}}\left\{\mathbf{H}_k^{''H}\mathbf{H}_k^{''}\right\}^{-1}\mathbf{H}_k^{''H}\mathbf{z}_k^{'} \\
&= \sqrt{\frac{8}{P_T}}\left\{\mathbf{H}_k^{''H}\mathbf{H}_k^{''}\right\}^{-1}\mathbf{H}_k^{''H}\mathbf{z}_k^{'}
\end{aligned}
\tag{3.46}
$$

$$
\begin{aligned}
\widehat{\mathbf{m}}_k^{(\boldsymbol{\Phi}(2))} &= \mathbf{G}_{\boldsymbol{\Phi}(2),k}^{MMSE}\mathbf{z}_k^{'} = \sqrt{\frac{\Delta P}{P_T}}\left\{\mathbf{H}_k^{''H}\mathbf{H}_k^{''} + \frac{\Delta P\sigma^2}{P_T}\mathbf{I}_\Delta\right\}^{-1}\mathbf{H}_k^{''H}\mathbf{z}_k^{'} \\
&= \sqrt{\frac{8}{P_T}}\left\{\mathbf{H}_k^{''H}\mathbf{H}_k^{''} + \frac{8\sigma^2}{P_T}\mathbf{I}_4\right\}^{-1}\mathbf{H}_k^{''H}\mathbf{z}_k^{'}
\end{aligned}
\tag{3.47}
$$

where $\mathbf{H}_k^{''} = \left[\mathbf{h}_{4\boldsymbol{\Phi}(2)-3}\ \mathbf{h}_{4\boldsymbol{\Phi}(2)-2}\ \mathbf{h}_{4\boldsymbol{\Phi}(2)-1}\ \mathbf{h}_{4\boldsymbol{\Phi}(2)}\right]_k^T$ in both (3.46) and (3.47), $\mathbf{I}_4$ is the 4×4 identity matrix. So far $\Delta = 4$ and $P = 2$ have been considered. When there are more than $P = 2$ transmitted streams, the whole procedure is continued until the last branch is detected.

3.3.2   Simulations and Discussions

We have used a simulation scenario with the system parameters shown in Table 3.1 [30]. We

Table 3.1: System Parameters

Parameter	Value
System bandwidth, B	1.25 MHz
Carrier frequency, f_c	3.5 GHz
OFDM sub-carriers, N	128
CP length, N_{CP}	16
Sampling rate, f_s	1.429 Msps
Symbol duration, $T_s = (N + N_{CP})/f_s$	100.77 μs
Number of symbols in a frame, N_f	5
Frame duration, $T_f = N_f T_s$	503.85 μs
Symbol mapping	QPSK
Channel coding	1/2-rate convolutional

assume two SM branches and dual receive antennas in all systems, i.e. $P = N_R = 2$. We have confined ourselves to the case of $\Delta = 2$ and 4 for each pth SM branch in SM-OSFBC and SM-QSFBC systems, respectively. Thus, we have 4×2 and 8×2 systems for SM-OSFBC and SM-QSFBC schemes, respectively. The tags used to denote different transmission and reception configurations are shown in Table 3.2.

We assume that perfect channel estimation values for each subcarrier for all the spatial channels are available at the receiver. We use the exponential model to generate the corresponding CIR and CTF of the channel. In our model, the power delay profile of the channel is exponentially distributed decay with gap between the first and the last impulse as -40 dB.

Table 3.2: Tags used in figures for corresponding schemes

Scheme	Tag
2×1 Alamouti SFBC scheme [11]	2×1 *SFBC*
2×2 VBLAST with ZF nulling [10]	2×2 *ZF-BLAST*
2×2 VBLAST with MMSE nulling [10]	2×2 *MMSE-BLAST*
2×2 SM system optimum ML reception	2×2 *ML*
4×2 SM-OSFBC transmitter and ZF based linear receiver [52]	4×2 *SM-OSFBC, ZF-Lin*
4×2 SM-OSFBC transmitter and MMSE based linear receiver [52]	4×2 *SM-OSFBC, MMSE-Lin*
4×2 SM-OSFBC transmitter and ZF based OSIC receiver [53]	4×2 *SM-OSFBC, ZF-OSIC*
4×2 SM-OSFBC transmitter and MMSE based OSIC receiver [53]	4×2 *SM-OSFBC, MMSE-OSIC*
8×2 SM-QSFBC transmitter and ZF based OSIC receiver	8×2 *SM-QSFBC, ZF-OSIC*
8×2 SM-QSFBC transmitter and MMSE based OSIC receiver	8×2 *SM-QSFBC, MMSE-OSIC*
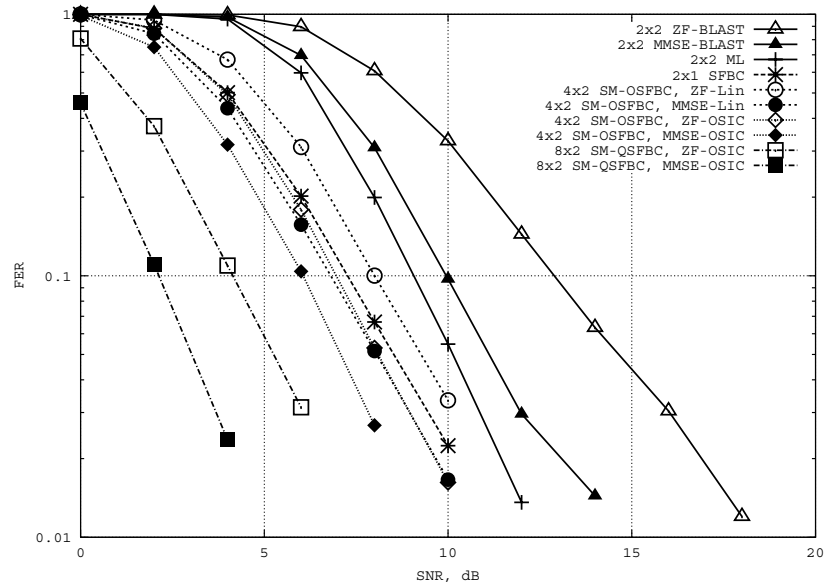
Figure 3.3: FER performance for the studied schemes

3.3.2.1   FER Performance

Figure 3.3 shows the coded FER results for the presented schemes. For various transmit antenna configurations, the total transmit power is kept constant, thus, the SNR at the x-axis reflects the total SNR. We have used Quadrature Phase Shift Keying (QPSK) modulation for all the systems. We know that 2×2 SM [10] performs worse in terms of FER compared to 2×1 SFBC system: in fact in the SM system, we get an higher rate, but we lose in diversity [42]. Considering this, we can see that 4×2 SM-OSFBC with OSIC receiver performs better than SFBC system in terms of FER. In this case, not only the diversity gain is achieved, but spatial multiplexing gain is also realized. We can see an even better gain in FER is obtained when 8×2 SM-QSFBC system is used. This clearly shows the benefits of using OSFBC or QSFBC at the transmission system.

If not differently specified, simulations were run for 5000 frames, thus as a rule of thumb we can say that results are statistically significant up to FER of $\frac{1}{5000e-2} = \frac{1}{50} \sim 0.01$.

3.3.2.2   Average Spectral Efficiency

Figure 3.4 shows the average spectral efficiency of the studied systems. The maximum rate with 1/2-rate convolutional coding, QPSK modulation ($bps = 2$ bits per symbol) and two spatially-multiplexed branches is $R_b = R_c \cdot bps \cdot P = 0.5 \cdot 2 \cdot 2 = 2$. We define the practical spectral efficiency as $SE = R_b (1 - FER)$, thus at the best case with current modulation and coding level along with MIMO rate, the maximum spectral efficiency of the JDM schemes is much higher than the 2×2 schemes at comparatively low SNR. As the SNR increases, the average spectral efficiency approaches to the maximum value (i.e. 2 bps/Hz) for all the schemes. It is noticed that for JDM schemes, maximum achievable spectral efficiency is obtained faster than other schemes when compared to increment in SNR. As expected, SM-QSFBC-MMSE-OSIC performs better than others in terms of average spectral efficiency, which is supported by its better FER performance seen in Figure 3.3.
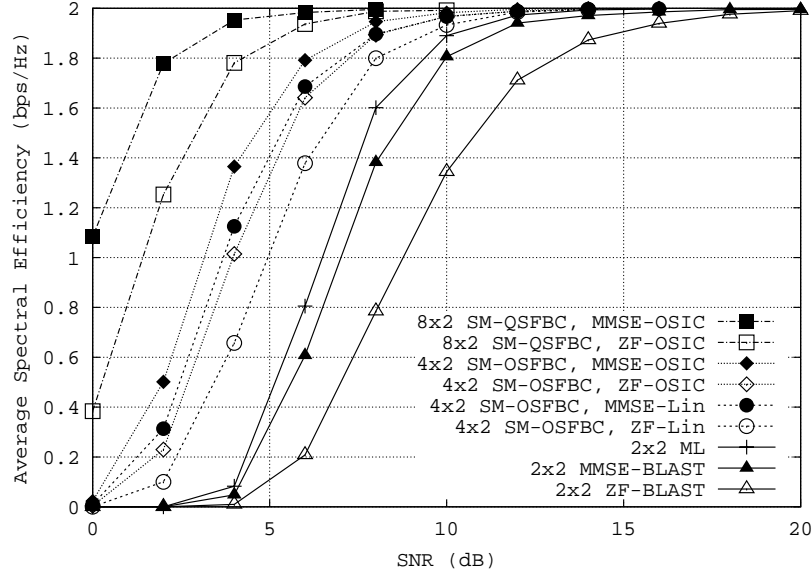
Figure 3.4: Average Spectral Efficiency for the studied systems

3.3.2.3   10% Outage Spectral Efficiency

Outage analysis is a form of reliability analysis. The 10% outage channel capacity is defined as the information rate that is guaranteed for 90% of the channel realizations, such that the probability that outage rate falls below the certain threshold rate is at most 10% [25]. The 10% outage spectral efficiencies for SM, SM-OSFBC and SM-QSFBC with different receiver configurations are given in Figure 3.5. At 0 dB of SNR, 10% outage spectral efficiency of SM-QSFBC-MMSE-OSIC and SM-QSFBC-ZF-OSIC schemes are 1.75 and 1 bps/Hz, respectively. The maximum achievable spectral efficiency with the set of parameters that we have used for these simulations is 2 bps/Hz (achieved with spatial rate of 2, QPSK modulation, channel coding rate of 1/2). For SM-QSFBC-OSIC schemes, the 10% outage spectral efficiency is almost close to maximum at any SNR more than than 4 dB. At that SNR, SM system obtains very low efficiency, whereas SM-OSFBC schemes obtain between
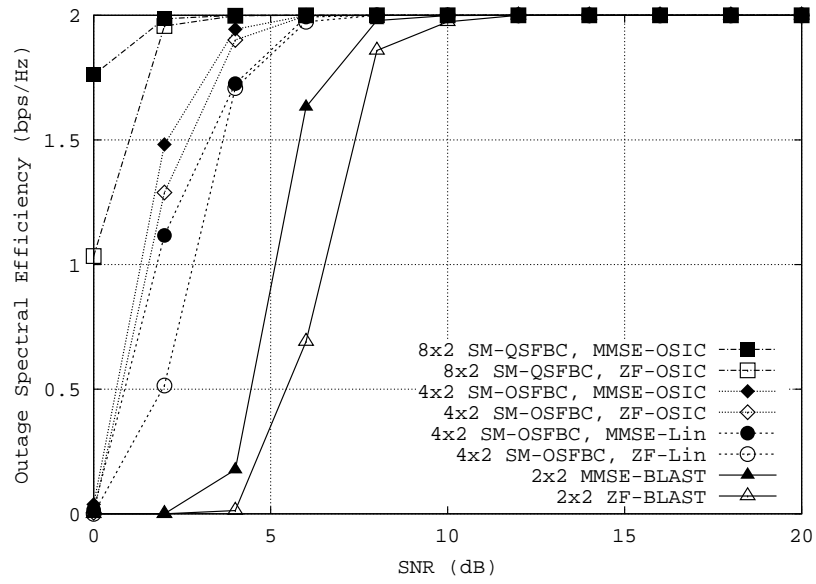
Figure 3.5: 10% Outage spectral efficiency in indoor scenario

Table 3.3: Correlation for corresponding spatial separation among antennas at 3.5 GHz of carrier frequency. R and d denote spatial correlation and separation in cm, respectively.

R	0.90	0.82	0.70	0.61	0.51	0.40	0.29	0.22	0.15
d(cm)	0.86	1.20	1.54	1.80	2.06	2.31	2.57	2.74	2.91

1.7 and 1.9 bps/Hz, which is quite impressive also. One conclusion that can be easily made is that added spatial dimensions at the transmitter side are exploited well in JDM schemes to improve system performance in terms of FER and outage spectral efficiency as seen in Figure 3.3 and Figure 3.5, respectively.

3.3.2.4 Effects of Spatial Correlation

The gains from transmit diversity and spatial multiplexing depend on the availability of spatially separable multipath. As a result, both spatial diversity and spatial multiplexing gains will be reduced in environments lacking spatial separability. The robustness of a particular design in such channels is therefore an important question [44]. The considered causes for spatial correlation in this work are:

- insufficient antenna spacing;

- LOS component.

Correlation due to Antenna Spacing

The spatial correlation in $\mathbf{H}$ is based on the inter-element distances in the transmit and receive antenna arrays, as it is done in [47]. We can model the spatial correlation across all subcarriers as

$$\mathbf{H}_k = \sqrt{\mathbf{R}_{k,rx}}\mathbf{H}_{w,k}\sqrt{\mathbf{R}_{k,tx}} \tag{3.48}$$

where $\mathbf{R}_{k,rx}$, $\mathbf{H}_{w,k}$ and $\mathbf{R}_{k,tx}$ are receive correlation matrix, uncorrelated channel matrix and transmit correlation matrix, respectively. For large values of the antenna spacing, the
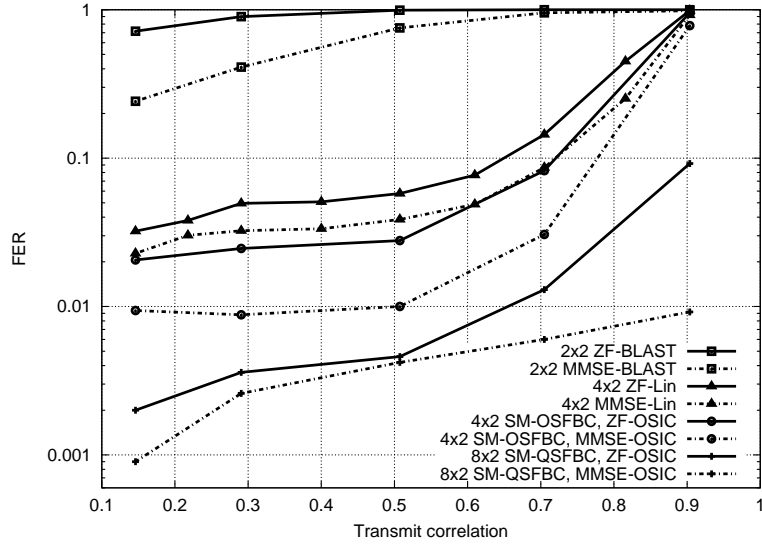
Figure 3.6: FER with respect to increasing transmit correlation (i.e. decreasing antenna spacing) and fixed receive correlation at system SNR of 12dB

correlation matrices will converge to the identity matrix, giving uncorrelated fading; for small values of the antenna spacing, the correlation matrices become rank deficient (eventually rank one) causing (fully) correlated fading [54]. The correlation coefficient between p_1 and p_2 transmit antennas can be written as:

$$[\mathbf{R}_{k,tx}]_{p_1,p_2} = \mathcal{J}_0 \left(\frac{2\pi(p_1 - p_2)d}{\lambda} \right) \tag{3.49}$$

where $p_1, p_2 \in [1, \ldots, P\Delta]$. $\mathcal{J}_0$ denotes the 0th order Bessel function of 1st kind, d is the distance between the elements and λ is the wavelength corresponding to the carrier frequency. Similar spatial correlation can be defined at the receiver.

In this Section, we investigate the impact of spatial correlation on FER and on outage spectral efficiency. For this, the receive (transmit) is fixed to 0.3 and transmit (receive) correlation is varied as shown in Table 3.3. This 0.3 of receive spatial correlation
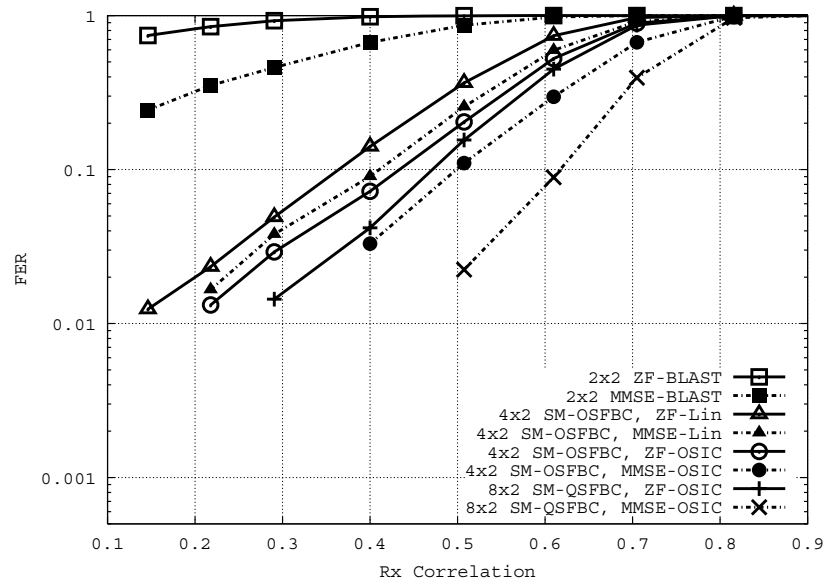
Figure 3.7: FER with respect to increasing receive correlation (i.e. decreasing antenna spacing) and fixed transmit correlation at system SNR of 12dB
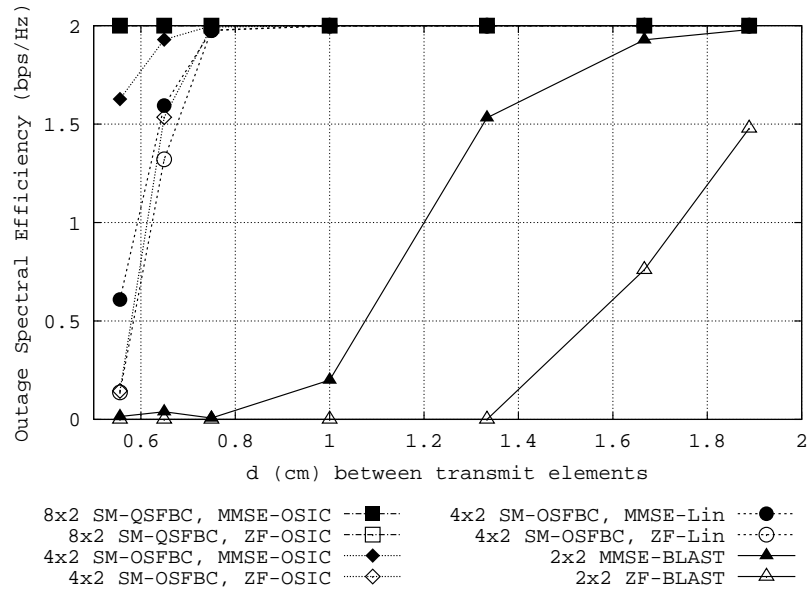
Figure 3.8: Outage spectral efficiency with respect to decreasing transmit correlation (i.e. increasing antenna spacing) and fixed receive correlation at system SNR of 12dB

corresponds to off-diagonal components in $\mathbf{R}_{k,rx}$, i.e. the spatial correlation between the neighboring elements is 0.3. The same applies for transmit side. The results are obtained for a particular SNR value, i.e. 12dB.

In Figures 3.6 and 3.7, FER results in presence of spatial correlation due to insufficient spatial separation between antenna elements are shown. In [49], impact of spatial correlation is studied for a system similar to SM-OSTBC scheme. For Figure 3.6, we varied the transmit correlation and fixed the receive correlation to 0.3, and the opposite is done for Figure 3.7. Note that we have dual receive antennas for all the schemes. One interesting conclusion that can be drawn from these figures is that receive correlation affects these systems much more than transmit correlation. This is because no extra diversity measures are taken at the receiver. From Figure 3.7, we see that the FERs increase very fast when the receive correlation increases. This is true for all the systems. From Figure 3.6, for increasing transmit correlation with a fixed receive correlation, the degradation in JDM schemes is gradual. Up to 60% of spatial correlation between the transmit antennas, the JDM schemes perform quite consistently, and their performance get worse only when the spatial correlation is further increased. Thus, as long as the transmit elements are separated by a spacing of at least 1.80 cm for our system (according to Table 3.3), the effect of spatial correlation in FER performance is not quite significant for JDM systems. While SM-QSFBC-OSIC with ZF and MMSE equalization performs the best for increasing transmit correlation, ZF-BLAST and MMSE-BLAST perform quite badly, when the spatial correlation is increased. Thus, it is evident that original VBLAST systems are not so robust in spatially correlated scenario as it was previously reported in [25].

Values in the order of 1.80 cm of spacing appear quite reasonable, since these distances fit with the current sizes of mobile phones, and would allow (considering only the correlation as impairing factor) to put either 2 or 4 antennas at the MS. Of course other considerations should be made in order to have a realistic evaluation of the multi-antenna

schemes, especially in the case of UL: as an example, let us assume two antennas at the MS, and that one hand of the person calling is covering one of the antennas, then there would not be any correlation between the two antennas, but there would not be any advantage deriving from multi-antenna configuration too.

To obtain more insight into the impact of transmit correlation, we have also performed simulations to measure the 10% outage spectral efficiency for all the schemes when transmit spatial correlation is increased steadily with a fixed receive spatial correlation. In Figure 3.8, the antenna spacing at the transmitter side is shown on x-axis: the higher the antenna spacing, the lower the spatial correlation experienced in the system. As shown in Figure 3.8, as soon as the antenna spacing at the transmitter starts to increase (i.e. the correlation starts to decrease), the outage efficiency for SM-QSFBC schemes reaches the highest spectral efficiency. Other JDM schemes also have high outage spectral efficiency. The reason for good outage spectral efficiency is the diversity benefit obtained in JDM schemes in parallel with the multiplexing gains. We know that any form of diversity benefit is bound to improve the outage scenario. It is worth noticing here that SM schemes provide very low outage efficiency even at low level of transmit correlation.

Correlation due to LOS

We model the wireless channel response having two distinct components [55],

1. a specular component (or LOS component) that illuminates the arrays uniformly and is thus spatially deterministic from antenna to antenna, we denote such a component as $\mathbf{H}_c$;

2. a scattered Rayleigh-distributed component that varies randomly from antenna to antenna, this component is denoted as $\mathbf{H}_w$.

The MIMO channel model for each subcarrier with the effect of LOS component can now be written as:

$$\mathbf{H}_k = \sqrt{\frac{K}{K+1}}\mathbf{H}_{c,k} + \sqrt{\frac{1}{K+1}}\mathbf{H}_{w,k} \tag{3.50}$$

where K is the Ricean K-factor of the system that is essentially the ratio of the power in the LOS component of the channel to the power in the multipath component. For small values of K ($K = 0$ corresponds to pure Rayleigh fading) clearly $\mathbf{H}_w$ dominates, giving uncorrelated fading, while for large values of K ($K = \infty$ corresponds to a pure non-fading channel), $\mathbf{H}_c$ dominates, causing correlated fading. The elements of normalized scattering component $\mathbf{H}_{w,k}$ are modelled as Zero Mean Circularly Symmetric Complex Gaussian (ZMCSCG) with unit variance [25]. The specular component is given by:

$$\mathbf{H}_c = \mathbf{a}(\theta_r)^T\mathbf{a}(\theta_t) \tag{3.51}$$

where $\mathbf{a}(\theta_t)$ and $\mathbf{a}(\theta_r)$ are the specular array responses at the transmitter and receiver, respectively. The array response corresponding to the transmit $P\Delta = 4P$ (or receive N_R)-element linear array is given by $\begin{bmatrix} 1 & e^{j2\pi d\cos(\theta)} & \dots & e^{j2\pi d(P\Delta-1)\cos(\theta)} \end{bmatrix} = \begin{bmatrix} 1 & e^{j2\pi d\cos(\theta)} & \dots & e^{j2\pi(4P-1)\cos(\theta)} \end{bmatrix}$, where θ is the Angle of Departure (AoD) at the transmitter (or Angle of Arrival (AoA) at the receiver) of the specular component and d is the antenna spacing in wavelengths [55].

Figure 3.9 shows the FER results when the strength of LOS component is steadily increased. This investigation is intended for indoor scenario, therefore θ_t and θ_r are taken to be 360 degrees. Spacing between antennas at both ends is taken as 2.57 cm (i.e. spatial correlation of 0.3). The impact of LOS on SM-QSFBC systems is much less compared to BLAST schemes. When the strength of LOS component is 10 (10 dB), then only SM-QSFBC schemes provide some reasonable FER (e.g. close to 10^{-2}). The other schemes show almost all frames in error.
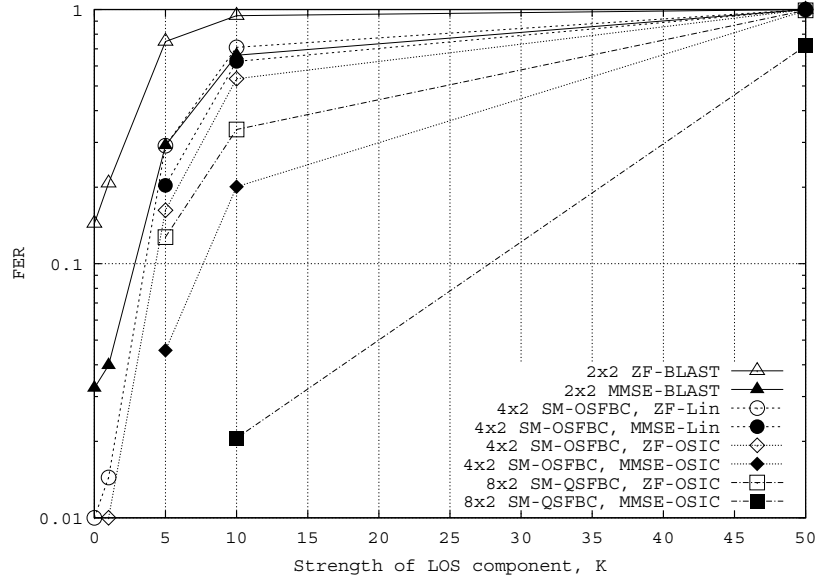
Figure 3.9: Impact of LOS on FER performances

Figure 3.10 shows the loss because of the LOS component in average spectral effi-
ciency. For brevity, only the results for MMSE based receivers are presented. Conforming
the results in Figure 3.9, it is found that spectral efficiency loss in *SM-QSFBC* system is
25% less compared to other schemes at $K = 50$ (i.e. ≈ 17 dB).

3.4   Conclusions

Original JDM schemes for OFDM systems have been presented, which allow to achieve both
diversity and multiplexing benefits at the same time. The performance of different receiver
strategies have been analyzed in realistic wireless conditions. The proposed JDM schemes
are in general robust to spatial correlation caused by inadequate spatial separation between
antenna elements. When spatial correlation is caused by the LOS scenario, then only SM-
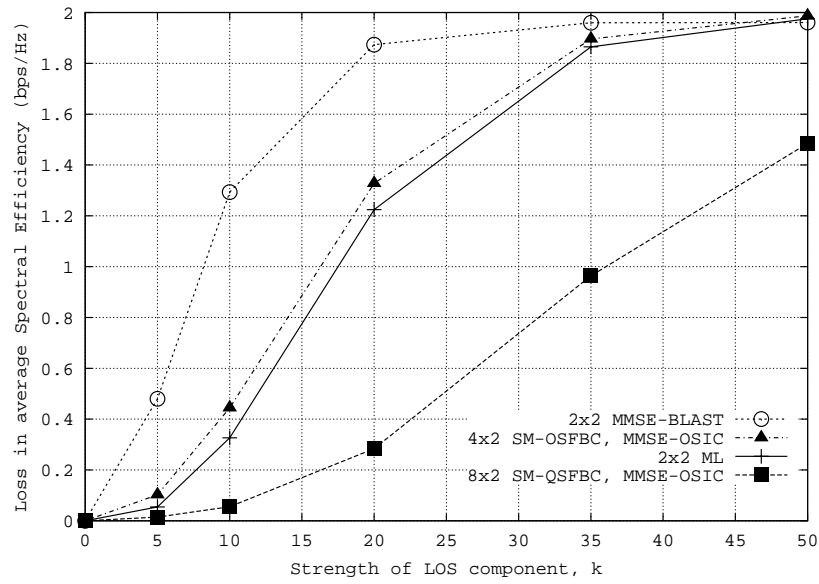
Figure 3.10: Loss in average spectral efficiency with respect to increasingly strong LOS component

QSFBC type JDM schemes show robustness in performance. All other JDM schemes fail with little increment in strength of LOS component in the wireless channel. For both ZF and MMSE, the VBLAST-based SM schemes [10] perform poorly in realistic wireless conditions.

Chapter 4

Multi-Antenna Schemes for SCFDE

4.1 Introduction

It has been shown that SCFDE is comparable to OFDM with respect to implementation effort and performance if MIMO extensions are applied [56]. However, between SCFDE and OFDM there are some important differences, i.e.

- the subcarriers access in SCFDE is not directly available: this creates problems for techniques that require subcarriers manipulation, such as SFBC;

- the trade-off diversity-multiplexing depends also on the sensitivity of the transmission technique with respect to coding in time or frequency, and since SCFDE and OFDM have different behaviors from this point of view, a different trade-off diversity-multiplexing for SCFDE and OFDM is expected.

In this Chapter, firstly the issue of extending SFBC to SCFDE systems, which is not straightforward as in case of STBC, is addressed and a low-complexity solution is proposed. Moreover, the proposed processing is used for applying a JDM SM-SFBC scheme to SCFDE system. To be able to apply SFBC and SFBC-based schemes to SCFDE systems is very important, since SFBCs show a great robustness to the time-selectivity caused by

users'mobility, and they work well for a wider range of propagation scenarios with respect to STBCs.

4.2 Space-Frequency Block Coding for SCFDE

The STBC extension to SCFDE proposed in [13] cannot be directly mapped to space and frequency domains. To overcome this problem, in this Section a new low-complexity SCFDE-SFBC scheme will be introduced which allows to code across antennas and subcarriers. One has to notice that the subcarriers domain is not directly accessible at the transmitter of a SCFDE system, but the novel scheme introduced hereafter makes possible the access to frequency domain by properly organizing the information in the time domain over the two antennas. SCFDE-SFBC is shown to outperform SCFDE-STBC technique over fast fading channels caused by high mobility speed. We compare these two schemes in terms of uncoded BER for different levels of time and frequency selectivity. Uncoded BER was here chosen as a metric to study the behavior of the proposed scheme in a simplified case, i.e. to see the potential gain due to the scheme itself, rather than to the impact of channel coding.

4.2.1 System Model

Figure 4.1 and Figure 4.2 show the transmitter and the receiver respectively, of the proposed 2×1 transmit diversity scheme. The data stream to be transmitted is organized in 4 sequences by properly combining the even and the odd sequences of the original data stream, as it is described in 4.2.1.1; 2 of the 4 sequences are multiplied by a *phase vector* **w** and then contemporarily transmitted over two transmit antennas after the insertion of the Cyclic Prefix (CP).

At the receiver, after the CP removal, the FFT operation is performed. Then, MMSE-FDE is performed each two consecutive sub-carriers. Two N/2-points IFFT convert back to the time domain the even and odd sequences, which are then multiplexed to obtain the
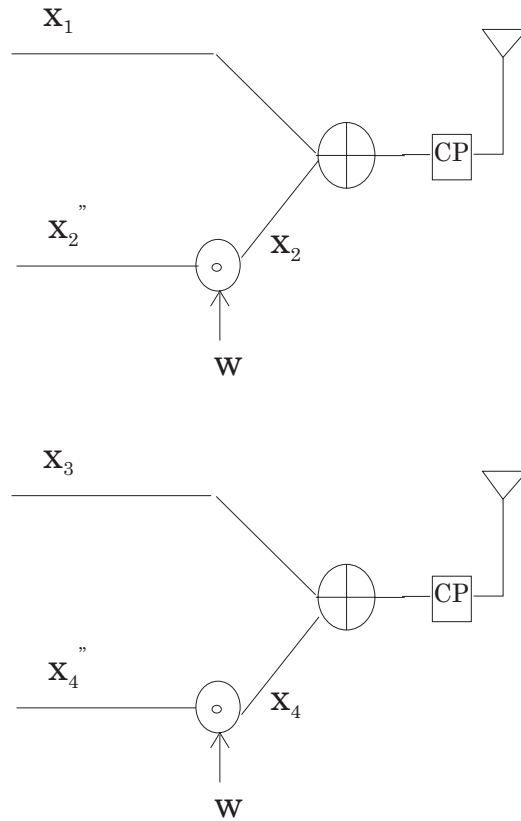
Figure 4.1: Transmitter model of the proposed 2x1 SCFDE transmit diversity scheme samples used for the decision process.

4.2.1.1   Transmitter

Let us consider a data stream $\mathbf{s}$ of N symbols:

$$\mathbf{s} = [s_1, s_2, \ldots, s_N]^T \tag{4.1}$$

which is split in the odd sequence $\mathbf{o}$ and even sequence $\mathbf{e}$:

$$\mathbf{o} = [s_1, s_3, \ldots, s_{N-1}]^T \tag{4.2}$$

$$\mathbf{e} = [s_2, s_4, \ldots, s_N]^T \tag{4.3}$$
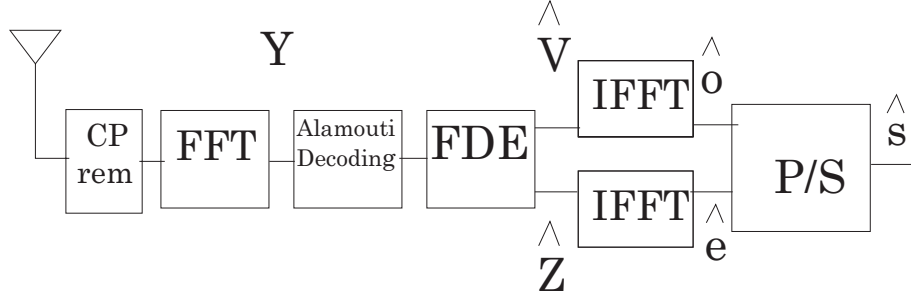
Figure 4.2: Receiver model of the proposed 2x1 SCFDE transmit diversity scheme

Let us form the following four N-long sequences: $\mathbf{x}_1 = \left[\mathbf{o}^T, \mathbf{o}^T\right]^T$, $\mathbf{x}_2' = \left[-\mathbf{e}^{*T}, -\mathbf{e}^{*T}\right]^T$, $\mathbf{x}_3 = \left[\mathbf{e}^T, \mathbf{e}^T\right]^T$, $\mathbf{x}_4' = \left[\mathbf{o}^{*T}, \mathbf{o}^{*T}\right]^T$, and let us rewrite them in terms of the original sequence $\mathbf{s}$:

$$\mathbf{x}_1 = [s_1, s_3, \ldots, s_{N-1}, s_1, s_3, \ldots, s_{N-1}]^T \tag{4.4}$$

$$\mathbf{x}_2' = [-s_2^*, -s_4^*, \ldots, -s_N^*, -s_2^*, -s_4^*, \ldots, -s_N^*]^T \tag{4.5}$$

$$\mathbf{x}_3 = [s_2, s_4, \ldots, s_N, s_2, s_4, \ldots, s_N]^T \tag{4.6}$$

$$\mathbf{x}_4' = [s_1^*, s_3^*, \ldots, s_{N-1}^*, s_1^*, s_3^*, \ldots, s_{N-1}^*]^T \tag{4.7}$$

It is evident that $\mathbf{x}_2' = -\mathbf{x}_3^*$ and $\mathbf{x}_4' = \mathbf{x}_1^*$. Starting from $\mathbf{x}_2'$ and $\mathbf{x}_4'$, the vectors $\mathbf{x}_2''$ and $\mathbf{x}_4''$ are built as:

$$\mathbf{x}_2'' = [-s_2^*, -s_N^*, \ldots, -s_4^*, -s_2^*, -s_N^*, \ldots, -s_4^*]^T \tag{4.8}$$

$$\mathbf{x}_4'' = [s_1^*, s_{N-1}^*, \ldots, s_3^*, s_1^*, s_{N-1}^*, \ldots, s_3^*]^T \tag{4.9}$$

The sequences transmitted simultaneously on the first transmit antenna (see Equations (4.4)-(4.8)) are $\mathbf{x}_1$ and:

$$\mathbf{x}_2 = \mathbf{w} \odot \mathbf{x}_2'' \tag{4.10}$$

while the sequences transmitted from the second transmit antenna (see Equations (4.6)-(4.9)) are $\mathbf{x}_3$ and:

$$\mathbf{x}_4 = \mathbf{w} \odot \mathbf{x}_4^{''} \tag{4.11}$$

where $\odot$ means component-wise product and $\mathbf{w}$ is the $N \times 1$ vector:

$$\mathbf{w} = \left[1, e^{j\pi/\frac{N}{2}}, \ldots, e^{j(\frac{N}{2}-1)\pi/\frac{N}{2}}, -1, -e^{j\pi/\frac{N}{2}}, \ldots, -e^{j(\frac{N}{2}-1)\pi/\frac{N}{2}}\right]^T \tag{4.12}$$

4.2.1.2   Receiver

The received vector is:

$$\mathbf{y} = \mathbf{H}_1\left(\mathbf{x}_1 + \mathbf{x}_2\right) + \mathbf{H}_2\left(\mathbf{x}_3 + \mathbf{x}_4\right) + \mathbf{n} \tag{4.13}$$

where $\mathbf{H}_1$ and $\mathbf{H}_2$ are $N \times N$ circulant channel matrices. Using the eigen-value decomposition:

$$\mathbf{y} = \mathbf{Q}^H \mathbf{\Lambda}_1 \mathbf{Q}\left(\mathbf{x}_1 + \mathbf{x}_2\right) + \mathbf{Q}^H \mathbf{\Lambda}_2 \mathbf{Q}\left(\mathbf{x}_3 + \mathbf{x}_4\right) + \mathbf{n} \tag{4.14}$$

where $\mathbf{Q}$ is the orthonormal $N \times N$ FFT matrix, i.e. $\mathbf{Q}(i,j) = \frac{1}{\sqrt{N}}e^{-j\frac{2\pi}{N}(i-1)(j-1)}$, $1 \leq i, j \leq N$. After the FFT block, it can be written (frequency domain):

$$
\begin{aligned}
\mathbf{Y} &= \mathbf{Q}\mathbf{y} & (4.15) \\
&= \mathbf{\Lambda}_1 \mathbf{Q}\left(\mathbf{x}_1 + \mathbf{x}_2\right) + \mathbf{\Lambda}_2 \mathbf{Q}\left(\mathbf{x}_3 + \mathbf{x}_4\right) + \mathbf{Q}\mathbf{n} & (4.16) \\
&= \mathbf{\Lambda}_1 \left(\mathbf{X}_1 + \mathbf{X}_2\right) + \mathbf{\Lambda}_2 \left(\mathbf{X}_3 + \mathbf{X}_4\right) + \mathbf{N} & (4.17)
\end{aligned}
$$

where $\mathbf{\Lambda}_i$, $i = 1, 2$ are $N \times N$ diagonal matrices whose $(l, l)^{th}$ entries are equal to the lth FFT coefficients of the CIRs $\mathbf{h}_i$, $i = 1, 2$, and $\mathbf{X}_j$, $j = 1, \ldots, 4$ and $\mathbf{N}$ are $N \times 1$ vectors representing the FFT transforms of transmitted vectors $\mathbf{x}_j$, $j = 1, \ldots, 4$ and noise

n, respectively. In particular, for the FFT transforms of the transmitted vectors:

$$\mathbf{X}_1 = \mathbf{Q}\mathbf{x}_1 = \left[V_1, 0, \ldots, V_{N/2}, 0\right]^T \tag{4.18}$$

$$\mathbf{X}_2 = \mathbf{Q}\mathbf{x}_2 = \left[0, -Z_1^*, \ldots, 0, -Z_{N/2}^*\right]^T \tag{4.19}$$

$$\mathbf{X}_3 = \mathbf{Q}\mathbf{x}_3 = \left[Z_1, 0, \ldots, Z_{N/2}, 0\right]^T \tag{4.20}$$

$$\mathbf{X}_4 = \mathbf{Q}\mathbf{x}_4 = \left[0, V_1^*, \ldots, 0, V_{N/2}^*\right]^T \tag{4.21}$$

from which it is possible to recognize the Alamouti-like structure in the space and frequency domains [11][45]. For the k-th couple of subcarriers, with $k = 1, \ldots, \frac{N}{2}$:

$$\begin{bmatrix} Y_{2k-1} \\ Y_{2k}^* \end{bmatrix} = \begin{bmatrix} \Lambda_{1,2k-1} & \Lambda_{2,2k-1} \\ \Lambda_{2,2k}^* & -\Lambda_{1,2k}^* \end{bmatrix} \begin{bmatrix} V_k \\ Z_k \end{bmatrix} + \begin{bmatrix} N_{2k-1} \\ N_{2k}^* \end{bmatrix} \tag{4.22}$$

Let us assume the two channels constant for two adjacent subcarriers:

$$\Lambda_{j,2k-1} = \Lambda_{j,2k} = \Lambda_{j,k}, \ j = 1, 2, \ k = 1, \ldots, \frac{N}{2} \tag{4.23}$$

then (4.22) can be rewritten as:

$$\begin{bmatrix} Y_{2k-1} \\ Y_{2k}^* \end{bmatrix} = \begin{bmatrix} \Lambda_{1,k} & \Lambda_{2,k} \\ \Lambda_{2,k}^* & -\Lambda_{1,k}^* \end{bmatrix} \begin{bmatrix} V_k \\ Z_k \end{bmatrix} + \begin{bmatrix} N_{2k-1} \\ N_{2k}^* \end{bmatrix} \tag{4.24}$$

By doing a MRC processing:

$$\begin{bmatrix} \widetilde{Y}_{2k-1} \\ \widetilde{Y}_{2k} \end{bmatrix} = \begin{bmatrix} \Lambda_{1,k}^* & \Lambda_{2,k} \\ \Lambda_{2,k}^* & -\Lambda_{1,k} \end{bmatrix} \begin{bmatrix} Y_{2k-1} \\ Y_{2k}^* \end{bmatrix}$$

$$= \begin{bmatrix} \tilde{\Lambda} & 0 \\ 0 & \tilde{\Lambda} \end{bmatrix} \begin{bmatrix} V_k \\ Z_k \end{bmatrix} + \begin{bmatrix} \widetilde{N}_1 \\ \widetilde{N}_2 \end{bmatrix} \tag{4.25}$$

where $\widetilde{\Lambda} = |\Lambda_{1,k}|^2 + |\Lambda_{2,k}|^2$, $\widetilde{N}_1 = \Lambda_{1,k}^* N_{2k-1} + \Lambda_{2,k} N_{2k}^*$, and $\widetilde{N}_2 = \Lambda_{2,k}^* N_{2k-1} - \Lambda_{1,k} N_{2k}^*$. After the MMSE-FDE equalization [38]:

$$\begin{bmatrix} \widehat{V}_k \\ \widehat{Z}_k \end{bmatrix} = \sqrt{\frac{N_T}{P_T}} \begin{bmatrix} 1/\left(\widetilde{\Lambda} + \frac{N_T}{\rho}\right) & 0 \\ 0 & 1/\left(\widetilde{\Lambda} + \frac{N_T}{\rho}\right) \end{bmatrix} \begin{bmatrix} \widetilde{Y}_{2k-1} \\ \widetilde{Y}_{2k} \end{bmatrix}$$

where $\rho = P_T/\sigma^2$, and P_T is the total power of the transmitted signal, while σ^2 is the total variance of the complex Gaussian noise process. Therefore, we have recovered:

$$\widehat{\mathbf{V}} = \left[\widehat{V}_1, \widehat{V}_2, \ldots, \widehat{V}_{N/2}\right]^T \tag{4.26}$$

$$\widehat{\mathbf{Z}} = \left[\widehat{Z}_1, \widehat{Z}_2, \ldots, \widehat{Z}_{N/2}\right]^T \tag{4.27}$$

and we go back into the time-domain through two $\frac{N}{2}$-points IFFT, with a coefficient of normalization $\frac{1}{2}$:

$$\widehat{\mathbf{o}} = [\widehat{s}_1, \widehat{s}_3, \ldots, \widehat{s}_{N-1}]^T = \frac{1}{2} IFFT(\widehat{\mathbf{V}}) \tag{4.28}$$

$$\widehat{\mathbf{e}} = [\widehat{s}_2, \widehat{s}_4, \ldots, \widehat{s}_N]^T = \frac{1}{2} IFFT(\widehat{\mathbf{Z}}) \tag{4.29}$$

After a Parallel to Serial (P/S) converter, and a proper multiplexing of the two sequences, the estimation of the transmitted sequence $\mathbf{s}$ is achieved:

$$\widehat{\mathbf{s}} = [\widehat{s}_1, \widehat{s}_2, \ldots, \widehat{s}_N]^T \tag{4.30}$$

4.2.2 Simulations and Discussions

We present here the comparison of SCFDE-STBC and the proposed SCFDE space-frequency transmit scheme in terms of uncoded BER and complexity. Simulation parameters are shown in Table 4.1. Ideal time and frequency synchronization is assumed. We also assume perfect

channel estimation at the receiver. An L-taps frequency selective channel is assumed, with exponential decay. In particular, we consider: a low frequency selective channel characterized by $L = 8$ taps, corresponding to a maximum delay spread of $\tau_{max} = 4.90 \mu s$; a high frequency selective channel with $L = 30$, i.e. a maximum delay spread of $\tau_{max} = 20.29 \mu s$; a quasi-static channel with normalized Doppler frequency $f_d T_s = 0.001$, corresponding to a velocity of 3 kmph; a high time-selective channel with normalized Doppler frequency $f_d T_s = 0.03$, i.e. velocity of 90 kmph.

Table 4.1: Simulation Parameters

Parameters	Value
System bandwidth, B	1.25 MHz
Sampling frequency, f_s	1.429 MHz
Carrier frequency, f_c	3.5 GHz
Symbols per block, N	128
Subcarrier spacing, Δf	9.77 KHz
CP length, N_{CP}	16
Data symbol mapping	BPSK
FDE Equalizer	MMSE
Channel coding scheme	1/2-rate convolutional coding

Figure 4.3 shows the uncoded BER of a SCFDE-STBC transmit diversity scheme with respect to the proposed scheme in a low frequency selective channel. As expected, when the channel is quasi-static the two schemes show almost identical performance. However, in a fast varying channel ($f_d T_s = 0.03$) the proposed scheme outperforms the SCFDE-STBC transmit diversity scheme, which shows a floor in the uncoded BER. As in a OFDM-SFBC scheme, the proposed scheme assumes the channel constant over two consecutive subcarriers. Therefore, the performance of the proposed scheme are expected to show a degradation over high frequency selective channels. More insight into sensitivity of the two transmit diversity schemes over different propagation conditions are provided by Figure 4.4 and Figure 4.5. In particular, Figure 4.4 shows the performance degradation of the two schemes when the normalized coherence bandwidth (defined as $B_{c,norm} = \frac{1}{\tau_{max} \Delta f}$) decreases, i.e. when the
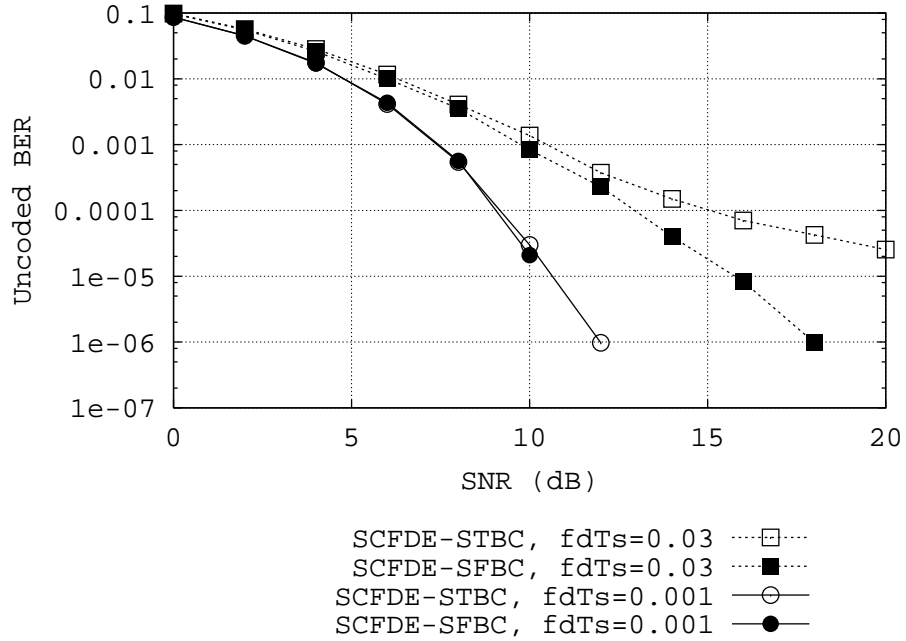
Figure 4.3: SCFDE-STBC vs the proposed scheme in low and high time selective channels

channel frequency selectivity increases. First of all, we observe that the STBC scheme is not very sensitive to the increase of the frequency selectivity. Moreover, when the channel is quasi-static the STBC scheme always outperforms the proposed scheme. However, the performance gap of the two schemes is quite low for a wide range of frequency selectivity conditions. In presence of a high time-selective channel, the proposed scheme noticeably outperforms the STBC scheme for a big range of frequency selectivity.

While STBC has very low sensitivity with respect to the frequency selectivity of the channel, the time-selectivity has a greater impact on the performance of the proposed scheme, especially when the frequency selectivity is low. This is shown in Figure 4.5, which plots the uncoded BER of the two schemes for increasing normalized Doppler frequency, i.e.
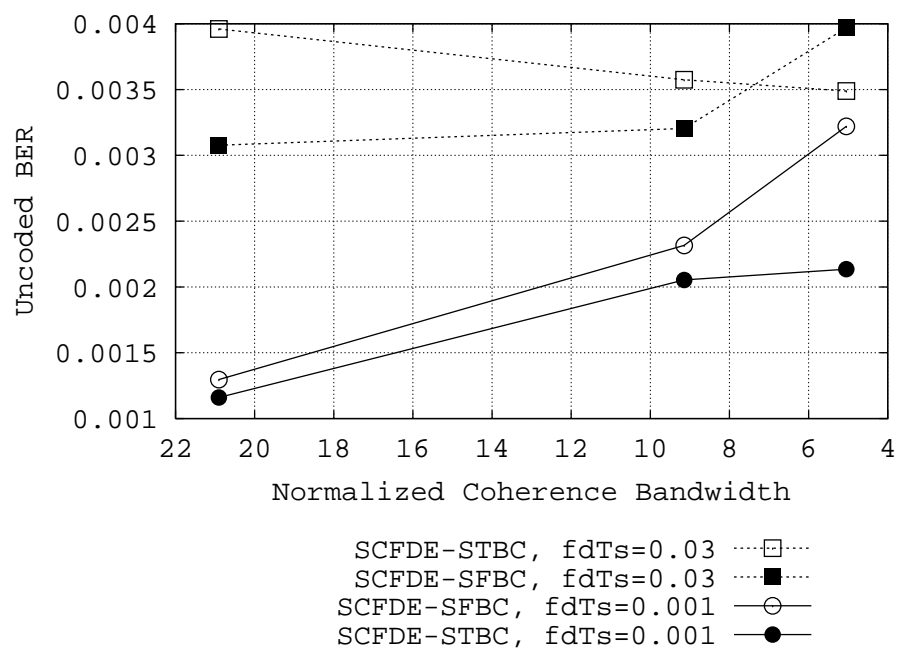
Figure 4.4: Uncoded BER vs. normalized coherence bandwidth at the SNR of 8 dB
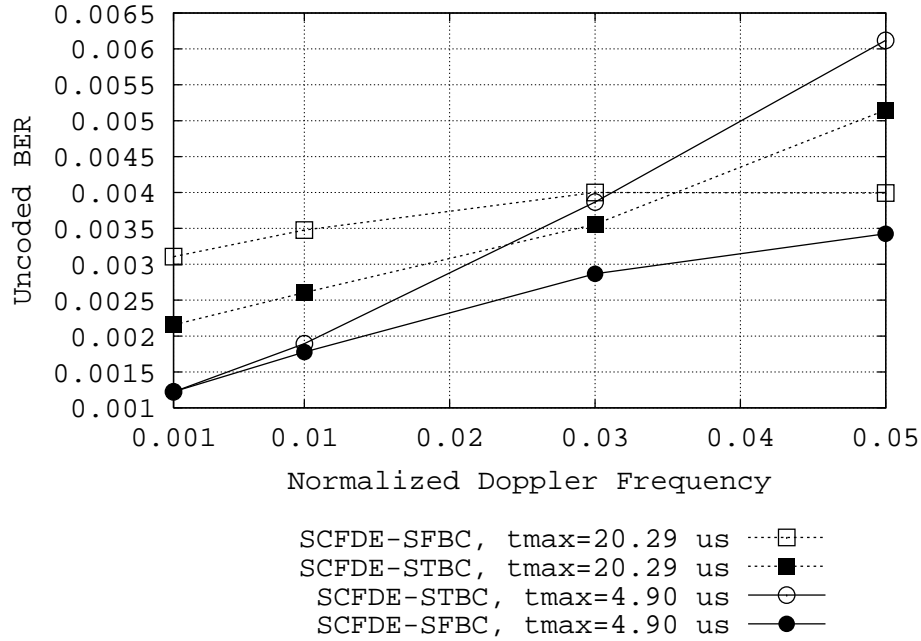
Figure 4.5: Uncoded BER vs. normalized Doppler frequency at the SNR of 8 dB

increasing time-variability. However, the sensitivity of the STBC scheme with respect to the time-variability is much greater and the proposed scheme outperforms the STBC scheme over highly time-varying channels also when the frequency selectivity is high.

It is interesting to notice from Figures 4.4 and 4.5 that when SCFDE-STBC scheme fails because of high velocity (high normalized Doppler frequency), this scheme recovers in BER performance in presence of frequency selectivity (high maximum delay spread), since SCFDE is able to exploit the frequency diversity without channel coding, differently from OFDM. The same does not hold for SFBC since for this scheme the frequency selectivity is detrimental (hypothesis of channel constance over adjacent subcarriers).

4.2.3 Computational Complexity

The computational complexities, in terms of the overall number of complex multiplications (considering transmitter and receiver) of SCFDE-SFBC and SCFDE-STBC are, respectively:

$$
\begin{aligned}
C^{SC-SF} &= N_T N^2 + (N_R + 1)\frac{N}{2}log_2 N - \frac{N}{2} \\
C^{SC-ST} &= N_T N^2 + (N_R + 1)\frac{N}{2}log_2 N
\end{aligned}
$$

The complexity for the 2×1 case is shown in Table 4.2. The parameters in this case are $N_T = 2$, $N_R = 1$.

Table 4.2: Complexity in terms of complex multiplications for 2x1 case

scheme	N=64	N=128
SCFDE-SF	8544	33600
SCFDE-ST	8576	33664

Therefore, the presented transmit diversity scheme has a slightly less complexity than STBC. As SCFDE is considered as a possible alternative to OFDM transmission in the uplink of future broadband wireless systems, the possibility of implementing SCFDE-SFBC without increasing the complexity at the mobile is a positive aspect.

4.3 Combining Diversity and Multiplexing in SCFDE

The trade-off diversity-multiplexing, which has been studied for OFDM systems [52]-[40]-[44], to the best of our knowledge has not yet been investigated for SCFDE. Basically, techniques that try to combine diversity and multiplexing, use the available antennas to get either more diversity gain or more multiplexing (rate) gain, according to the desired trade-off. Since this trade-off depends also on the sensitivity of the transmission technique with respect to coding in time or frequency, and SCFDE and OFDM have different behaviors from

this point of view, we also expect a different trade-off diversity-multiplexing for SCFDE and OFDM. The pre-processing technique which allows a low complexity extension of SFBC technique to SCFDE is used to implement a 4×2 scheme which combines SM with SFBC, where the four antennas are divided in two groups of two antennas: the SM is applied to the two groups of antennas, while SFBC is applied to the two antennas of each group.

4.3.1   System Model

In the presented 4×2 SCFDE SF-JDM system, the four transmit antennas are divided in two groups of two antennas each. Signals over the two groups of antennas are sent simultaneously and recovered via a SM approach, whilst over the two antennas of each group, a SFBC processing is applied. The system model is depicted in Figure 4.6, considering also the ST case. The objective is to get both multiplexing and diversity gain.

4.3.1.1   4x2 SCFDE SF-JDM

Four sequences are transmitted through the first two antennas, implementing a SCFDE-SFBC scheme, and other four sequences are transmitted in the same way via the third and fourth transmit antennas.

The vector received at the ith receive antenna is $\mathbf{y}_i = \sum_{j=1}^{4} \mathbf{H}_{ij}\mathbf{t}_j = \mathbf{H}_{i1}\left(\mathbf{x}_{1,1} + \mathbf{x}_{1,2}\right) + \mathbf{H}_{i2}\left(\mathbf{x}_{1,3} + \mathbf{x}_{1,4}\right) + \mathbf{H}_{i3}\left(\mathbf{x}_{2,1} + \mathbf{x}_{2,2}\right) + \mathbf{H}_{i4}\left(\mathbf{x}_{2,3} + \mathbf{x}_{2,4}\right) + \mathbf{n}_i$, $i = 1, 2$ where $\mathbf{H}_{ij}$, $i = 1, 2$, $j = 1, \ldots, 4$ are $N \times N$ circulant channel matrices and $\mathbf{x}_{i,j}$, $i = 1, 2$, $j = 1, \ldots, 4$ are the SFBC transmitted vectors, defined as in (4.4)-(4.6)-(4.10)-(4.11). After eigen-value decomposing the circulant channel matrices, i.e. $\mathbf{H}_{ij} = \mathbf{Q}^H \boldsymbol{\Lambda}_{ij} \mathbf{Q}$ and the FFT block at the receiver, we have $\mathbf{Y}_i = \mathbf{Q}\mathbf{y}_i$. For the kth couple of subcarriers, with $k = 1, \ldots, \frac{N}{2}$, after some simple linear algebra manipulation, it is possible to obtain:

$$\mathbf{Y}_k^{'} = \boldsymbol{\Lambda}_k \mathbf{X}_k + \mathbf{N}_k \tag{4.31}$$
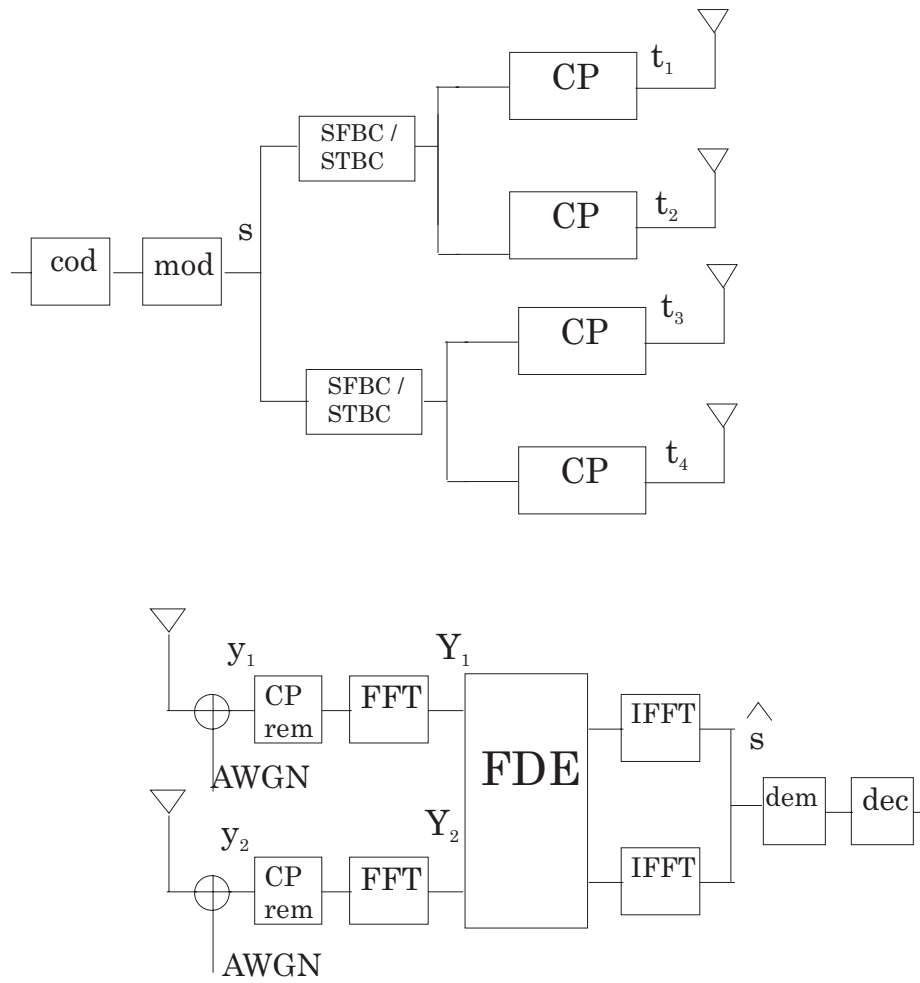
Figure 4.6: 4x2 SCFDE JDM system model

where $\mathbf{Y}'_k = \left[Y_{1,2k-1}, Y_{2,2k-1}, Y^*_{1,2k}, Y^*_{2,2k}\right]^T$, $\mathbf{X}_k = [V_{1,2k-1}, Z_{1,2k-1}, V_{2,2k-1}, Z_{2,2k-1}]^T$, $\mathbf{N}_k = \left[N_{1,2k-1}, N_{2,2k-1}, N^*_{1,2k}, N^*_{2,2k}\right]^T$, and:

$$
\mathbf{\Lambda}_k = \begin{bmatrix}
\Lambda_{11,k} & \Lambda_{12,k} & \Lambda_{13,k} & \Lambda_{14,k} \\
\Lambda_{21,k} & \Lambda_{22,k} & \Lambda_{23,k} & \Lambda_{24,k} \\
\Lambda^*_{12,k} & -\Lambda^*_{11,k} & \Lambda^*_{14,k} & -\Lambda^*_{13,k} \\
\Lambda^*_{22,k} & -\Lambda^*_{21,k} & \Lambda^*_{24,k} & -\Lambda^*_{23,k}
\end{bmatrix}
\tag{4.32}
$$

where the CTF is assumed identical over two adjacent subcarriers. At this point, $\mathbf{Y}'_k$ is MMSE equalized, i.e.

$$
\widehat{\mathbf{X}}_k = \mathbf{G}^{MMSE}_k \mathbf{Y}'_k
\tag{4.33}
$$

where:

$$
\mathbf{G}^{MMSE}_k = \sqrt{\frac{N_T}{P_T}} \left(\mathbf{\Lambda}^H_k \mathbf{\Lambda}_k + \frac{N_T}{\rho} \mathbf{I}_{N_T} \right)^{-1} \mathbf{\Lambda}^H_k
\tag{4.34}
$$

where $\rho = P_T/\sigma^2$, with P_T total power of the transmitted signal and σ^2 noise variance at one receive antenna. After this, the IFFT operation is performed.

4.3.1.2   4x2 SCFDE ST-JDM

Let us consider a 4×2 system, with 2 SM branches and on each SM branch an STBC block, such that both multiplexing and diversity gains can be realized, through SM and STBC, respectively. At time t, the vectors $\mathbf{x}_i(t) = [x_{i,1}, x_{i,2}, \ldots, x_{i,N}]^T$, $i = 1, \ldots, 4$ are sent from the four transmit antennas. At time $t + T$, the special encoding rule introduced in [13] is applied, i.e. $\mathbf{x}_i(t + T) = \left[-x^*_{j,1}, -x^*_{j,N}, \ldots, -x^*_{j,2}\right]^T$, $i = 1, 3$, $j = 2, 4$ are transmitted from antennas 1 and 3, and $\mathbf{x}_i(t + T) = \left[x^*_{j,1}, x^*_{j,N}, \ldots, x^*_{j,2}\right]^T$, $i = 2, 4$, $j = 1, 3$ from antennas 2 and 4. Analogously to SCFDE SF-JDM, and following the same procedure as in [44], it

can be written, for k^{th} subcarrier, $k = 1, \ldots, N$:

$$\mathbf{Y}_k^{'} = \mathbf{\Lambda}_k \mathbf{X}_k + \mathbf{N}_k \tag{4.35}$$

where $\mathbf{Y}_k^{'} = \left[Y_{1,k}(n), Y_{2,k}(n), Y_{1,k}^*(n+1), Y_{2,k}^*(n+1) \right]^T$, $\mathbf{X}_k = [V_{1,k}(n), Z_{1,k}(n), V_{2,k}(n), Z_{2,k}(n)]^T$, $\mathbf{N}_k = \left[N_{1,k}(n), N_{2,k}(n), N_{1,k}^*(n+1), N_{2,k}^*(n+1) \right]^T$, and:

$$\mathbf{\Lambda}_k(n) = \begin{bmatrix} \Lambda_{11,k}(n) & \Lambda_{12,k}(n) & \Lambda_{13,k}(n) & \Lambda_{14,k}(n) \\ \Lambda_{21,k}(n) & \Lambda_{22,k}(n) & \Lambda_{23,k}(n) & \Lambda_{24,k}(n) \\ \Lambda_{12,k}^*(n+1) & -\Lambda_{11,k}^*(n+1) & \Lambda_{14,k}^*(n+1) & -\Lambda_{13,k}^*(n+1) \\ \Lambda_{22,k}^*(n+1) & -\Lambda_{21,k}^*(n+1) & \Lambda_{24,k}^*(n+1) & -\Lambda_{23,k}^*(n+1) \end{bmatrix} \tag{4.36}$$

with n identifying the nth time instant. Assuming $\Lambda_{i,j}(n) = \Lambda_{i,j}(n+1)$, i.e., assuming a quasi-static channel, Equations (4.32), (4.33) and (4.34) still hold, but instead of $\frac{N}{2}$ couples of subcarriers, this time N subcarriers have to be considered.

4.3.1.3 4x2 SCFDE QOD Schemes

In the next Section, the SF and ST-JDM schemes previously presented are compared with 4×2 antennas SF and ST-QOD schemes. The QOD transmitter is shown in Figure 4.7, with the receiver part that is the same as in Figure 4.6. The QOD schemes use the 4-antennas code proposed in [12]. The SF-QOD code can be achieved in SCFDE in a similar way to the 2-antennas code SFBC presented in Section 4.2. It is worth noting that QOD codes provide a full rate of 1, but present a loss in orthogonality. The rate of 1 is provided by sending four symbols over the transmit antennas in four subcarriers, for SF-QOD, and in four block durations, for ST-QOD.
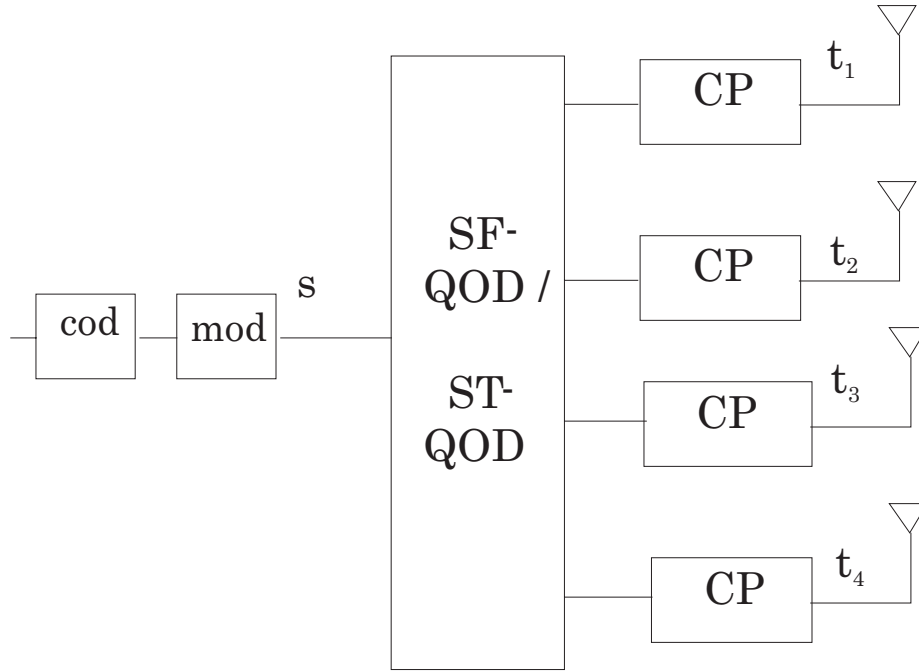
Figure 4.7: 4x2 SCFDE QOD system model: transmitter

4.3.2 Simulations and Discussions

Simulation parameters have been shown in Table 4.1. Ideal time and frequency synchronization and perfect channel estimation are assumed at the receiver. The channel is a L-taps frequency selective channel with exponentially distributed power decay. This Section presents results achieved in terms of average Spectral Efficiency (SE), without and with channel coding ($\frac{1}{2}$-rate convolutional coding). The average spectral efficiency is defined in terms of rate R and FER, as $SE = R(1 - FER)$, where R considers modulation order, spatial rate, and channel coding rate. The average SE is a good metric of the achievable trade-off multiplexing-diversity, since it considers both rate and reliability.

Figure 4.8: Uncoded Average SE for low frequency selectivity ($\tau_{max} = 2.80~\mu s$) and high time selectivity ($f_d T_s = 0.03$)

4.3.2.1   Space-Frequency Schemes

Figure 4.8 shows the uncoded average SE of SF-JDM schemes with respect to SF-QOD diversity schemes, with the same 4×2 antennas configuration and same rate $R = 2$ (i.e. BPSK modulation for SF-JDM schemes that have spatial rate of 2, and QPSK for SF-QOD that have spatial rate of 1), in highly time-variant channels ($f_d T_s = 0.03$ corresponding to $v = 90$ kmph) with low frequency selectivity. Both SCFDE and OFDM systems are considered in the comparison. Figure 4.8 shows that for low frequency selective channels, it is more efficient to use the redundancy introduced by the 4 transmit antennas in order to maximize the diversity gain. This holds both for SCFDE and OFDM systems. It is expected that the frequency selectivity of the channel severely degrades the performance of SF schemes, which are based on the assumption that the channel is constant over two or more consecutive subcarriers. In particular, for the 4×2 SF-QOD scheme, the channel is supposed to be constant over 4 subcarriers.

However, as it is shown in Figures 4.9 and 4.10, in SCFDE systems, the combination of SM and SFBC is more robust to the frequency selectivity with respect to QOD. Already for moderate frequency selective channels, the SF-JDM scheme begins to outperform the SF-QOD scheme in terms of SE. Moreover, JDM keeps on working for high frequency selective channels where the QOD performance are severely degraded and the SE is almost half of the maximum that is achievable for that configuration. Also for OFDM systems, the SF-JDM scheme is more robust to the frequency selectivity of the channel, since it requires the channel to be constant over less consecutive subcarriers. However, the performance of both OFDM schemes are severely degraded by the frequency selectivity of the channel. This is expected since the uncoded OFDM is not able to exploit the frequency selectivity of the channel as it is a SCFDE transmission scheme. Therefore, for uncoded OFDM the frequency selectivity has only a negative impact, even if it is less negative for the JDM scheme.

Figure 4.11 shows the coded average SE comparison. The maximum achievable rate

is 1, since also the channel coding rate of $\frac{1}{2}$ is taken into account. The negative effect of frequency selectivity on SF schemes is very much mitigated by channel coding, particularly for OFDM schemes and SCFDE SF-QOD. Therefore, in the coded case, it is more convenient to use the available antennas to provide only diversity, using higher order constellations, instead of providing both diversity and multiplexing, using lower order symbol mappings.

Finally, we also consider the sensitivity of the JDM scheme with respect to spatial correlation. The spatial correlation is modelled according to the interelement distances in the transmit and receive antenna arrays, as it is done in [47]. Correlation at both the transmit and receive arrays is considered, with values between 0, for no correlation, and 1, for full correlation. The impact of spatial correlation on the performance of SCFDE-SF-JDM and SCFDE-SF-QOD for moderate frequency selectivity in terms of uncoded average SE is shown in Figures 4.12. As expected, the JDM scheme is quite sensitive to the spatial correlation. Nevertheless, QOD scheme is also affected by spatial correlation, though its drop in performance is less impressive than for JDM. If channel coding is used (see Figure 4.13), QOD scheme is much less impacted by the spatial correlation than JDM scheme.

4.3.2.2 Space-Time Schemes

The dual propagation scenarios are considered when comparing ST schemes, i.e. a high frequency selectivity ($\tau_{max} = 18.20\ \mu s$) and increasing time selectivity. In Figure 4.14 the case for low time selectivity is shown ($f_d T_s = 0.001$ corresponding to $v = 3$ kmph): the QOD schemes outperform the JDM schemes, and the ones with SCFDE modulation are better than the ones with OFDM.

As shown in Figures 4.15 and 4.16, corresponding to moderate ($f_d T_s = 0.015$, $v = 45$ kmph) and severe ($f_d T_s = 0.03$, $v = 90$ kmph) time selectivity, the SCFDE ST-JDM scheme performs the best, in uncoded case, as SCFDE SF-JDM was doing among the SF schemes in the harsh scenario of high time and frequency variability. In Figure 4.16, also the SCFDE
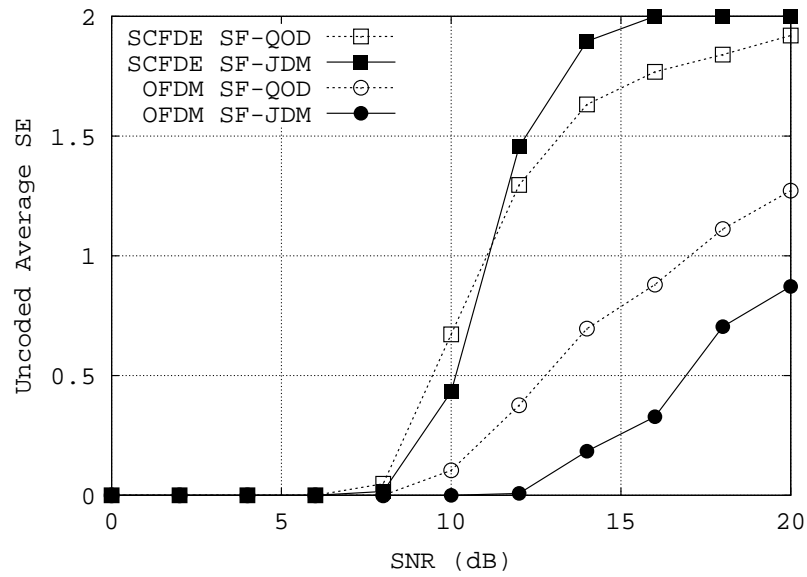
Figure 4.9: Uncoded Average SE for moderate frequency selectivity ($\tau_{max} = 14.70~\mu s$) and high time selectivity ($f_d T_s = 0.03$)
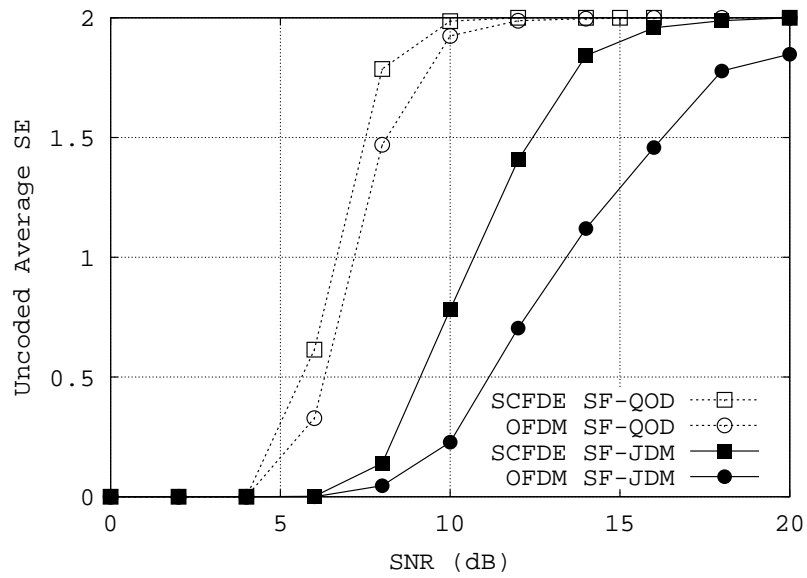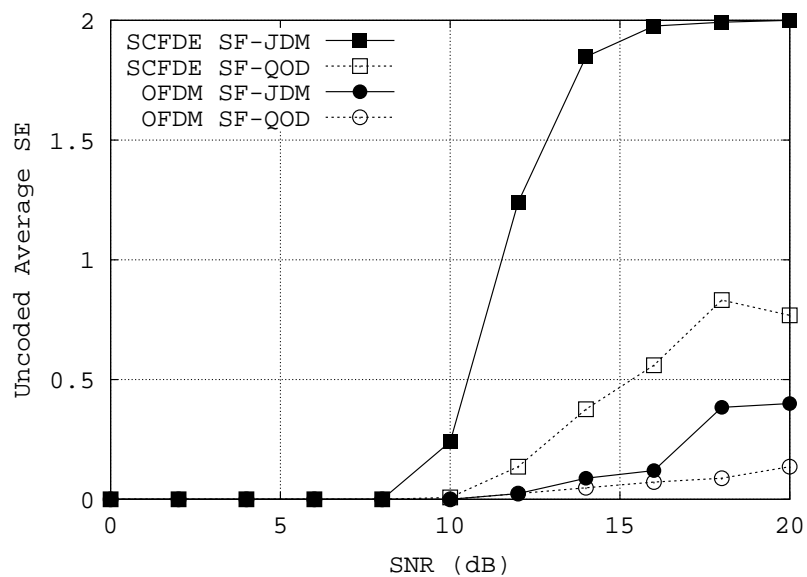
Figure 4.10: Uncoded Average SE for high frequency selectivity ($\tau_{max} = 18.20 \ \mu s$) and high time selectivity ($f_d T_s = 0.03$)
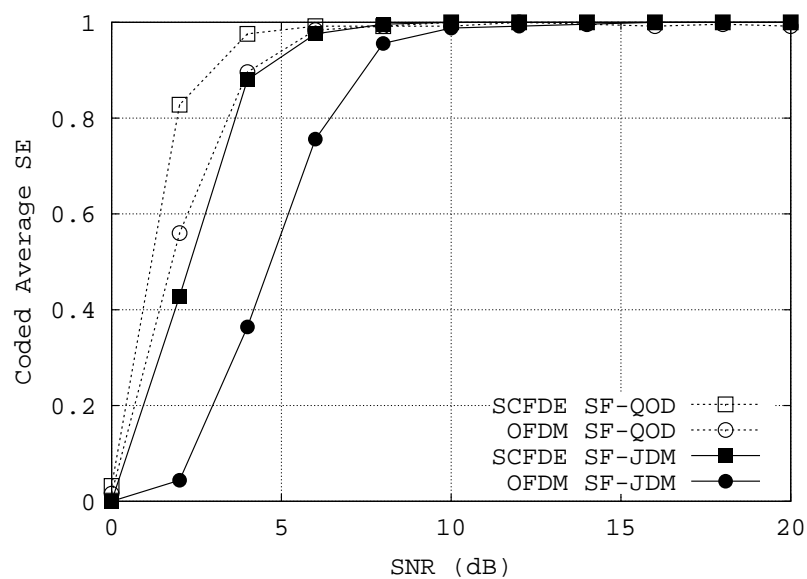
Figure 4.11: Coded Average SE for high frequency selectivity ($\tau_{max} = 18.20\ \mu s$) and high time selectivity ($f_d T_s = 0.03$)
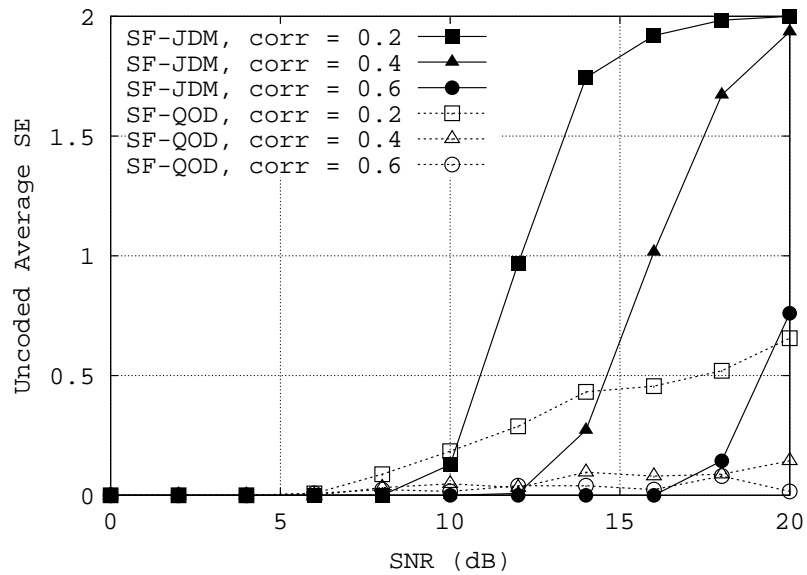
Figure 4.12: Uncoded Average SE in presence of spatial correlation (at both transmit and receive arrays) and moderate frequency selectivity ($\tau_{max} = 14.70 \ \mu s$) and high time selectivity ($f_d T_s = 0.03$)
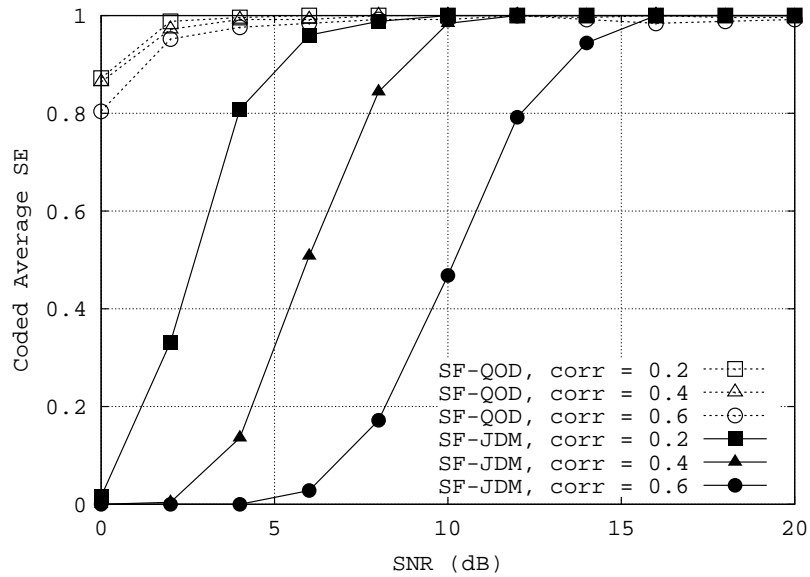
Figure 4.13: Coded Average SE in presence of spatial correlation (at both transmit and receive arrays) and moderate frequency selectivity ($\tau_{max} = 14.70\ \mu s$) and high time selectivity ($f_d T_s = 0.03$)
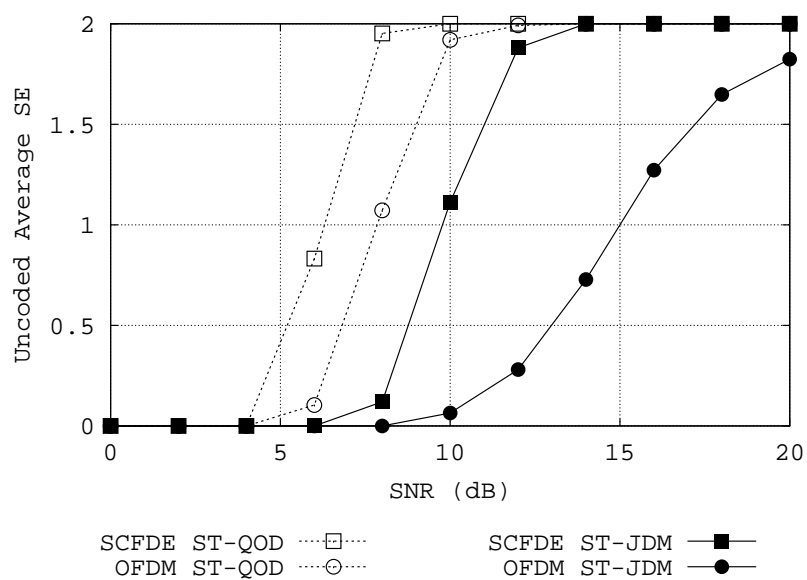
Figure 4.14: Uncoded Average SE for low time selectivity ($f_d T_s = 0.001$) and high frequency selectivity ($\tau_{max} = 18.20 \ \mu s$)
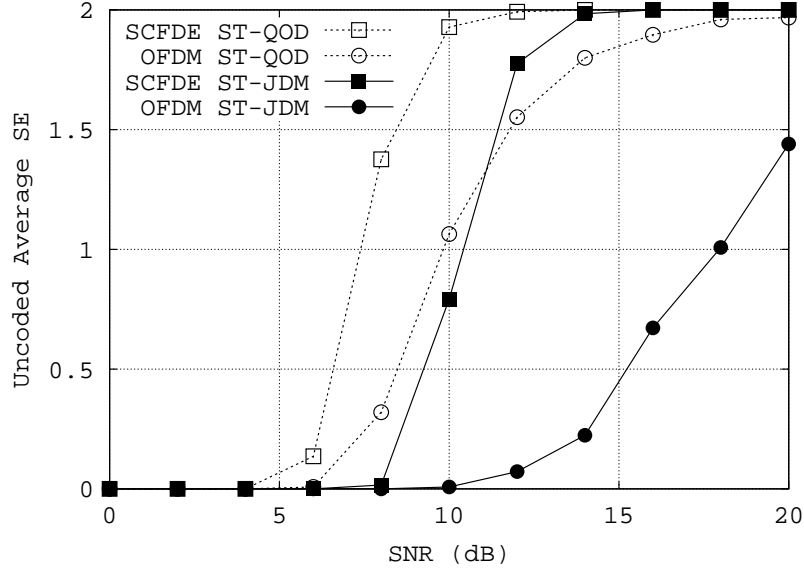
Figure 4.15: Uncoded Average SE for moderate time selectivity ($f_d T_s = 0.015$) and high frequency selectivity ($\tau_{max} = 18.20~\mu s$)

SF-JDM and QOD schemes have been included, to compare them with the correspondent ST schemes. The SF and ST-JDM schemes perform practically the same, whilst SF-QOD is performing much worse than ST-QOD, suggesting that the impact of frequency selectivity is more important than the impact of time variability. The OFDM schemes perform the worst, since as already mentioned, OFDM does need channel coding, differently from SCFDE that can get frequency diversity gain without coding. Once again, the introduction of channel coding suggests a very different conclusion with respect to the uncoded case (see Figure 4.17): the QOD schemes perform better than JDM schemes. Comparing SF and ST-QOD, and SF and ST-JDM, ST schemes perform slightly better. Still SCFDE modulation shows better behavior than OFDM.

An important aspect to mention is that by using ST schemes an extra processing delay is introduced with respect to SF schemes. In fact, ST-QOD needs to wait four symbol
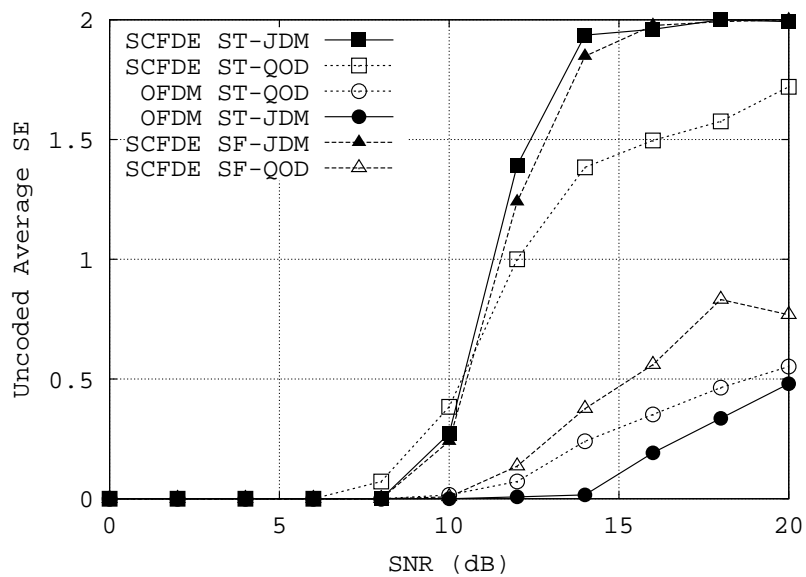
Figure 4.16: Uncoded Average SE for high time selectivity ($f_d T_s = 0.03$) and high frequency selectivity ($\tau_{max} = 18.20\ \mu s$)
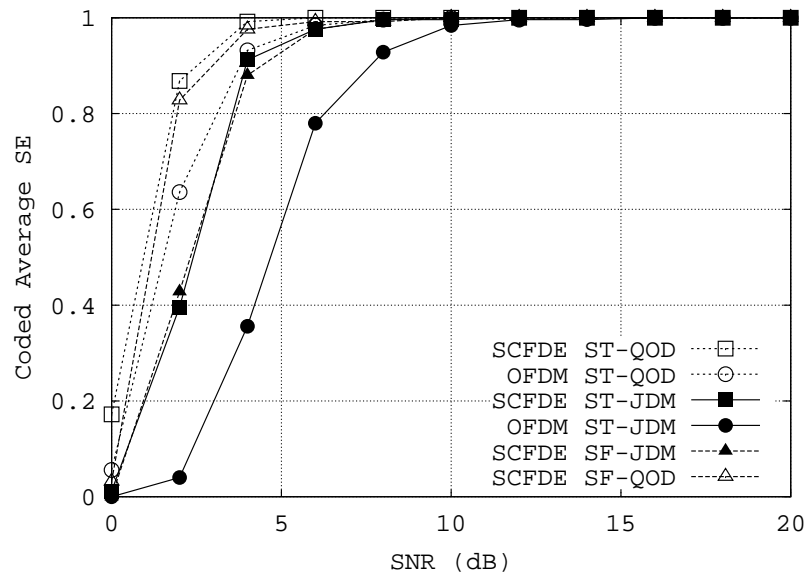
Figure 4.17: Coded Average SE for high time selectivity ($f_d T_s = 0.03$) and high frequency selectivity ($\tau_{max} = 18.20\ \mu s$)

periods at the receiver before completing the detection process, while ST-JDM needs to wait for two periods. In real-time applications this could be an obstacle to the use of ST schemes, even if they are the ones shown to have the best performance. Therefore the SCFDE SF-QOD and SF-JDM, which process the symbols period by period, without added delay, appear to be appealing solutions especially for real-time applications, preferring the SF-QOD for coded case, and preferring SF-JDM for uncoded case.

4.4 Conclusions

A new low-complexity SCFDE-SFBC scheme has been presented which allows to code across antennas and subcarriers, even if the subcarriers domain is not directly accessible at the transmitter of a SCFDE system. The proposed scheme has been shown to be more robust than SCFDE-STBC in highly time-varying channels.

The above mentioned SCFDE-SFBC scheme has then been applied to a JDM scheme (combined SM and SFBC). It has been shown that for SCFDE it is very efficient to use the available antennas to get multiplexing gain, since the resulting JDM scheme is robust to both the frequency and time selectivity of the channel. In case channel coding is present, it is more convenient to use the available antennas to provide only diversity instead of both diversity and multiplexing.

Chapter 5

Linear Dispersion Codes for SCFDE

5.1 Introduction

LDC are considered as one of attractive advanced multiple antennas techniques for future wireless systems [57]. Proposed in [4], they represent a space-time transmission scheme that has many of the coding and diversity advantages of previously designed codes, but has also the decoding simplicity of VBLAST at high data rates. Moreover, with respect to VBLAST, they work with arbitrary number of transmit and receive antennas and both VBLAST and pure transmit diversity schemes can be considered as a special case of LDC.

In the present Chapter, the application of space-frequency LDC to SCFDE systems is addressed. As for SFBC schemes (see Chapter 4), which are a special case of LDC, the application of space-frequency LDC schemes to SCFDE is not straightforward. Moreover, in case of LDC, the dispersion in frequency instead of in time might be even more beneficial than in other multi-antenna techniques since the hypothesis of channel constant over a certain number of symbol intervals might be more stringent. The main contribution of this work is the definition of the dispersion matrices to be applied at the transmitter of a SCFDE system to achieve the desired SF dispersion. To the best of our knowledge, so far no work

has investigated SF-LDC in SCFDE systems.

5.2 Linear Dispersion Codes

Multiple-antenna systems that operate at high rates require simple yet effective space-time transmission schemes to handle the large traffic volume in real time. At rates of tens of bits per second per hertz, VBLAST, where every antenna transmits its own independent substream of data, has been shown to have good performance and simple encoding and decoding. Yet VBLAST suffers from its inability to work with fewer receive antennas than transmit antennas - this deficiency is especially important for modern cellular systems, where a base station typically has more antennas than the mobile handsets. Furthermore, because VBLAST transmits independent data streams, on its antennas there is no built-in spatial coding to guard against deep fades from any given transmit antenna.

On the other hand, there are many previously proposed space-time codes that have good fading resistance and simple decoding, but these codes generally have poor performance at high data rates or with many antennas.

In [4] one proposes a high-rate coding scheme that can handle any configuration of transmit and receive antennas and that subsumes both VBLAST and many proposed space-time block codes as special cases. The scheme breaks the data stream into substreams that are dispersed in linear combinations over space and time. These codes are designed to optimize the mutual information between the transmitted and received signals. Because of their linear structure, the codes retain the decoding simplicity of VBLAST, and because of their information-theoretic optimality, they possess many coding advantages. The Authors in [4] refer to these codes as LDC. The LDC have the following properties:

1. they subsume, as special cases, both VBLAST [58] and the space block codes of [59];

2. they generally outperform both VBLAST and the space block codes;

3. they can be used for any number of transmit and receive antennas;

4. they are very simple to encode;

5. they can be decoded in a variety of ways;

6. they are designed with the numbers of both the transmit and receive antennas in mind;

7. they satisfy the following information-theoretic optimality criterion: *the codes are designed to maximize the mutual information between the transmit and receive signals.*

Let us assume N_T number of transmit antennas, N_R number of receive antennas, and an interval of T symbols where the propagation channel is constant and known to the receiver. The transmitted signal can then be written as a $T \times N_T$ matrix $\mathbf{S}$ that governs the transmission over the N_T antennas during the interval. Let us assume that the data sequence has been broken into Q substreams and that $s_1, \ldots, s_Q$ are the complex symbols chosen from an arbitrary, say r-PSK or r-QAM, constellation. A rate $R = \frac{Q}{T} log_2 r$ linear dispersion code is a code for which $\mathbf{S}$ obeys

$$\mathbf{S} = \sum_{q=1}^{Q} (\alpha_q \mathbf{A}_q + j\beta_q \mathbf{B}_q) \tag{5.1}$$

where the scalars (α_q, β_q) are determined by

$$s_q = \alpha_q + j\beta_q \tag{5.2}$$

The design of LDC depends crucially on the choices of the parameters T,Q and of the dispersion matrices $(\mathbf{A}_q, \mathbf{B}_q)$. To choose $(\mathbf{A}_q, \mathbf{B}_q)$, [4] proposes to optimize the mutual information between the transmitted signals (α_q, β_q) and the received signal.

5.3 Space-Frequency LDC for SCFDE

The application of LDC is problematic for highly variable channels. In fact, as it has been shown in [4], LDC are more efficient than pure transmit diversity schemes for a wide range of SNRs, when the required rate is high. To get high data rate, when the dispersion is done over time and space, the channel must be supposed constant over a number T of symbol intervals that is usually higher than 2 (as it is in a simple Alamouti scheme), hypothesis that might not hold in realistic propagation environment. In fact, when applied to OFDM systems T symbol intervals mean T OFDM symbols, that can be quite a long time.

This motivated the study of SF-LDC in OFDM systems: originally designed for flat fading channels, LDC have been extended to frequency selective channels in combination with OFDM. In [60] the transmitted symbols are dispersed over uncorrelated subchannels instead of adjacent subchannels, to take advantage of multipath diversity, provided that the subcarriers inside a subchannel behave the same. Actually, when extended to frequency domain, LDC could also be used to disperse the symbols over time and frequency instead of time and space, in order to exploit the multipath diversity of the channel [61].

Some effort has recently been spent, where LDC are applied in the time and frequency domains for SCFDE systems [62]. However, as stated in [62], application of LDC to frequency-domain for SCFDE systems is not straightforward since there is no direct access to subcarriers at the transmitter. The same problem has been observed in Chapter 4 for the easier case of SFBC and a solution has been provided.

This Chapter proposes a general solution for applying SF-LDC to SCFDE systems, which includes as special case the processing proposed in Chapter 4. As it is shown in this Chapter, SF-LDC are more efficient solutions in high-data-rate and high-mobility environment with respect to ST-LDC or pure transmit diversity schemes. The sensitivity of SF-LDC with respect to the frequency selectivity and time selectivity of the channel is also investigated, to better identify the range of propagation conditions in which SF-LDC are a

suitable solution.

The computational complexity of the proposed solution (SCFDE SF-LDC) is analyzed and compared with SCFDE ST-LDC and OFDM SF-LDC.

5.3.1 System Model

Firstly, in Section 5.3.1.1 the system model for the original LDC proposed in [4] is recalled, as a starting point for developing a general system model for SF-LDC in SCFDE, presented in Section 5.3.1.2. Then, in Section 5.3.1.3 some specific examples on the application of the proposed procedure are presented, such as 2-antennas Alamouti [45] [11] and Hassibi codes [4], and 4-antennas Jafarkhani [12] and Hassibi [4] codes.

5.3.1.1 Original LDC

The design method proposed in [4] consists of the following two steps:

1. choose $Q \leq N_R T$ (typically $Q = min\,(N_T, N_R) \cdot T$)

2. choose $(\mathbf{A}_q, \mathbf{B}_q)$ that solve the optimization problem

$$C_{LD}\,(\rho, T, N_T, N_R) = \max_{\mathbf{A}_q, \mathbf{B}_q, q=1,\ldots,Q} \frac{1}{2T} E \, log \, det \left(\mathbf{I}_{2N_R T} + \frac{\rho}{N_T} \mathcal{H}\mathcal{H}^T \right) \qquad (5.3)$$

for an SNR ρ of interest, subject to one of the following constraints:

(a) $\sum_{q=1}^{Q} \left(tr\mathbf{A}_q^*\mathbf{A}_q + tr\mathbf{B}_q^*\mathbf{B}_q \right) = 2TN_T$

(b) $tr\mathbf{A}_q^*\mathbf{A}_q = tr\mathbf{B}_q^*\mathbf{B}_q = \frac{TN_T}{Q}, q = 1, \ldots, Q$

(c) $\mathbf{A}_q^*\mathbf{A}_q = \mathbf{B}_q^*\mathbf{B}_q = \frac{T}{Q}\mathbf{I}_{N_T}, q = 1, \ldots, Q$

where $\mathcal{H}$ is given by (5.4) with the $\mathbf{h}_n$ having independent $\mathcal{N}\left(0, \frac{1}{2}\right)$ entries

$$\mathcal{H} = \begin{bmatrix} \mathcal{A}_1 \mathbf{h}_1 & \mathcal{B}_1 \mathbf{h}_1 & \cdots & \mathcal{A}_Q \mathbf{h}_1 & \mathcal{B}_Q \mathbf{h}_1 \\ \vdots & \vdots & \ddots & \vdots & \vdots \\ \mathcal{A}_1 \mathbf{h}_N & \mathcal{B}_1 \mathbf{h}_N & \cdots & \mathcal{A}_Q \mathbf{h}_N & \mathcal{B}_Q \mathbf{h}_N \end{bmatrix} \tag{5.4}$$

where

$$\mathcal{A}_q = \begin{bmatrix} \mathbf{A}_{R,q} & -\mathbf{A}_{I,q} \\ \mathbf{A}_{I,q} & \mathbf{A}_{R,q} \end{bmatrix} \tag{5.5}$$

$$\mathcal{B}_q = \begin{bmatrix} -\mathbf{B}_{I,q} & -\mathbf{B}_{R,q} \\ \mathbf{B}_{R,q} & -\mathbf{B}_{I,q} \end{bmatrix} \tag{5.6}$$

with

$$\mathbf{A}_q = \mathbf{A}_{R,q} + j\mathbf{A}_{I,q} \tag{5.7}$$

$$\mathbf{B}_q = \mathbf{B}_{R,q} + j\mathbf{B}_{I,q} \tag{5.8}$$

and

$$\mathbf{h}_n = \begin{bmatrix} \mathbf{h}_{R,n} \\ \mathbf{h}_{I,n} \end{bmatrix}, \; n = 1, \ldots, N_R \tag{5.9}$$

with $\mathbf{h}_{R,n}$ and $\mathbf{h}_{I,n}$ n-th columns of $\mathbf{H}_R$ and $\mathbf{H}_I$, and $\mathbf{H} = \mathbf{H}_R + j\mathbf{H}_I$ ($N_T \times N_R$ matrix).

For $T = 2, N_T = 2, N_R = 1$, one solution to (5.3), for any of the constraints (a)-(c), is the orthogonal design (Alamouti structure [45]). This holds because the mutual information of this particular orthogonal design achieves the actual channel capacity $C(\rho, N_T = 2, N_R = 1)$, thus Alamouti for the $N_T \times N_R = 2 \times 1$ cannot be defeated by LDC. Let us move to more than one receive antenna ($N_R > 1$).

When $N_R \geq N_T$ and $Q = N_T T$, [4] provides an explicit solution to (5.3) subject to the constraint (c). For $T = N_T$, one such set of matrices is given by

$$\mathbf{A}'_{N_T(k-1)+l} = \mathbf{B}'_{N_T(k-1)+l} = \frac{1}{\sqrt{N_T}}\mathbf{D}^{k-1}\mathbf{\Pi}^{l-1}, k = 1,\ldots,N_T, l = 1,\ldots,N_T \qquad (5.10)$$

where

$$\mathbf{D} = \begin{bmatrix} 1 & 0 & \cdots & & 0 \\ 0 & e^{j\frac{2\pi}{N_T}} & 0 & & \cdots \\ \vdots & & \ddots & & \\ 0 & & & & e^{j\frac{2\pi(N_T-1)}{N_T}} \end{bmatrix}_{N_T \times N_T} \qquad (5.11)$$

and

$$\mathbf{\Pi} = \begin{bmatrix} 0 & \cdots & & 0 & 1 \\ 1 & 0 & \cdots & & 0 \\ 0 & 1 & 0 & \cdots & 0 \\ \vdots & & \ddots & & \vdots \\ 0 & \cdots & 0 & 1 & 0 \end{bmatrix}_{N_T \times N_T} \qquad (5.12)$$

5.3.1.2   General Space-Frequency LDC for SCFDE

The system model is depicted in Figure 5.1. The $B \times N_T$ space-frequency dispersion matrix (after the FFT) is the same replicated for $N_S = N/B$ subchannels, with N number of subcarriers, B number of subcarriers per subchannel, and N_T number of transmit antennas, and for the real part corresponds to:

$$\mathbf{A}_q^f = \begin{bmatrix} a_{11}^q & a_{12}^q & \cdots & a_{1N_T}^q \\ a_{21}^q & a_{22}^q & \cdots & a_{2N_T}^q \\ \vdots & \vdots & \vdots & \vdots \\ a_{B1}^q & a_{B2}^q & \cdots & a_{BN_T}^q \end{bmatrix}, \; q = 1,\ldots,Q^f \qquad (5.13)$$
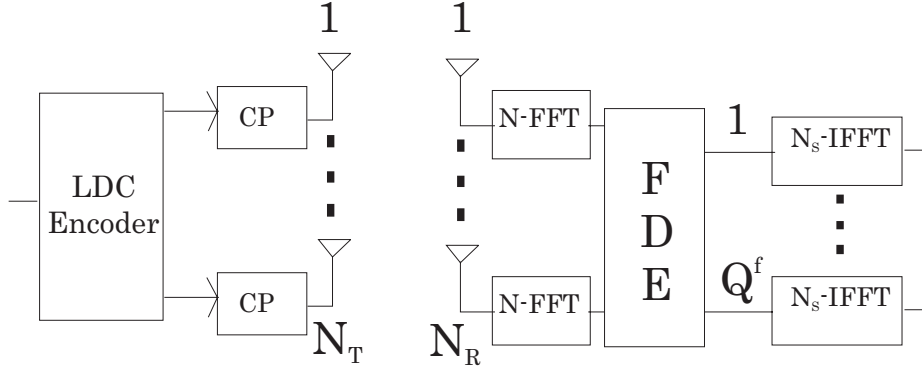
Figure 5.1: Space-Frequency LDC Transceiver

For the nth transmit antenna, in SF domain:

$$\sum_{q=1}^{Q^f}\sum_{i=n}^{B} a_{i,n}^q \mathbf{s}_i^q = \sum_{q=1}^{Q^f}\left(a_{1,n}^q \mathbf{s}_1^q + \cdots + a_{B,n}^q \mathbf{s}_B^q\right) \tag{5.14}$$

which corresponds in ST domain to:

$$\sum_{q=1}^{Q^f}\sum_{i=1}^{B} a_{i,n}^q \widehat{\mathbf{s}}_i^q = \sum_{q=1}^{Q^f}\left(a_{1,n}^q IFFT(\mathbf{s}_1^q) + \cdots + a_{B,n}^q IFFT(\mathbf{s}_B^q)\right) \tag{5.15}$$

where the $\mathbf{s}_i^q$ have the structure as follows:

$$\mathbf{s}_1^q = \left[\alpha_{q,1}^f, \underbrace{0,\cdots}_{(B-1)\ 0s},\cdots, \alpha_{q,N_S}^f, \underbrace{0,\cdots}_{(B-1)\ 0s}\right]^T \tag{5.16}$$

$$\vdots$$

$$\mathbf{s}_B^q = \left[\underbrace{\cdots,0}_{(B-1)\ 0s}, \alpha_{q,1}^f,\cdots, \underbrace{\cdots,0}_{(B-1)\ 0s}, \alpha_{q,N_S}^f\right]^T \tag{5.17}$$

and the $\widehat{\mathbf{s}}_i^q$, $i = 1, \ldots, B$ have the structure as in Equation (5.18).

$$
\widehat{\mathbf{s}}_i^q =
\begin{bmatrix}
1^{st}\ subperiod
\begin{cases}
\alpha_{q,1}^t \\
\alpha_{q,2}^t e^{j\frac{(i-1)\pi}{B}} \\
\vdots \\
\alpha_{q,N_S}^t e^{j\frac{(N_S-1)(i-1)\pi}{B}}
\end{cases} \\
\vdots \\
B^{th}\ subperiod
\begin{cases}
\alpha_{q,1}^t e^{j\frac{(N-N_S)(i-1)\pi}{B}} \\
\alpha_{q,2}^t e^{j\frac{(N-N_S+1)(i-1)\pi}{B}} \\
\vdots \\
\alpha_{q,N_S}^t e^{j\frac{(N-1)(i-1)\pi}{B}}
\end{cases}
\end{bmatrix}
\tag{5.18}
$$

The $\widehat{\mathbf{s}}_i^q$ vectors can be written as:

$$
\widehat{\mathbf{s}}_i^q = \sum_{k=1}^{N_S} \alpha_{q,k}^t \mathbf{p}_{k,i}
\tag{5.19}
$$

where the $N \times 1$ phase vectors $\mathbf{p}_{k,i}$ are as follows:

$$
\mathbf{p}_{1,i} = \left[\underbrace{1, 0, \cdots}_{1^{st}}, \cdots, \underbrace{e^{j\frac{(N-N_S)(i-1)\pi}{B}}, 0, \cdots}_{B^{th}} \right]^T
\tag{5.20}
$$

$$
\mathbf{p}_{2,i} = \left[\underbrace{0, e^{j\frac{(i-1)\pi}{B}}, \cdots}_{1^{st}}, \cdots, \underbrace{0, e^{j\frac{(N-N_S+1)(i-1)\pi}{B}}, \cdots}_{B^{th}} \right]^T
\tag{5.21}
$$

$$
\vdots
$$

$$
\mathbf{p}_{N_S,i} = \left[\underbrace{\cdots, 0, e^{j\frac{(N_S-1)(i-1)\pi}{B}}}_{1^{st}}, \cdots, \underbrace{\cdots, 0, e^{j\frac{(N-1)(i-1)\pi}{B}}}_{B^{th}} \right]^T
\tag{5.22}
$$

Equation (5.15) can then be rewritten as:

$$\sum_{q=1}^{Q^f}\sum_{i=1}^{B} a_{i,n}^q \widehat{\mathbf{s}}_i^q = \sum_{q=1}^{Q^f}\sum_{i=1}^{B} a_{i,n}^q \sum_{k=1}^{N_S} \alpha_{q,k}^t \mathbf{p}_{k,i} \tag{5.23}$$

and inverting the order of sums in i and k:

$$\sum_{q=1}^{Q^f}\sum_{i=1}^{B} a_{i,n}^q \widehat{\mathbf{s}}_i^q = \sum_{q=1}^{Q^f}\sum_{k=1}^{N_S} \alpha_{q,k}^t \sum_{i=1}^{B} a_{i,n}^q \mathbf{p}_{k,i} \tag{5.24}$$

Equation (5.24) means it is possible to define the $N \times N_T$ space-time dispersion matrix $\mathbf{A}_{q,k}$, to be applied to the real part of the N symbols at the transmitter, as the matrix where the nth column, with $n = 1, \ldots, N_T$, is given by $\mathbf{A}_{q,k}(:,n) = \alpha_{q,k}^t \sum_{i=1}^{B} a_{i,n}^q \mathbf{p}_{k,i}$. Therefore, given the desired dispersion matrices in the space and frequency domain, it is possible to define the dispersion matrices to be applied at the transmitter in the space and time domain. The same can be done for the dispersion matrices for the imaginary part. The total number of space-time dispersion matrices is $2Q^f N_S$.

5.3.1.3 Some examples

The general procedure just introduced will be applied to some known LDC. The features of the considered schemes are listed up in Table 5.1.

2x2 SCFDE SF-LDC

For the 2-transmit antennas Hassibi code (Equation (31) [4]) it is $N_S = \frac{N}{2}$, $B = 2$, and $Q^f = 4$. The space-frequency dispersion matrices are:

$$\mathbf{A}_1^f = \mathbf{B}_1^f = \begin{bmatrix} 1 & 0 \\ 0 & 1 \end{bmatrix} , \ \mathbf{A}_2^f = \mathbf{B}_2^f = \begin{bmatrix} 0 & 1 \\ 1 & 0 \end{bmatrix} , \ \mathbf{A}_3^f = \mathbf{B}_3^f = \begin{bmatrix} 1 & 0 \\ 0 & -1 \end{bmatrix} , \ \mathbf{A}_4^f = \mathbf{B}_4^f = \begin{bmatrix} 0 & 1 \\ -1 & 0 \end{bmatrix}$$
$$\tag{5.25}$$

Table 5.1: Schemes characteristics

Scheme	2x2 LDC	2x2 OD	4x4 LDC	4x4 QOD
No. transmit antennas, N_T	2	2	4	4
No. transmit antennas, N_R	2	2	4	4
No. symbols dispersed per sub-channel (period), Q^f (Q^t)	4	2	16	4
No. "subcarriers" per subchannel, B (symbols per period, T)	2	2	4	4
Rate, $R = \frac{Q^f}{B}log_2 r$ $\left(R = \frac{Q^t}{T}log_2 r\right)$, r=mod. order	$2log_2 r$	$log_2 r$	$4log_2 r$	$log_2 r$
Reference Equation	(31) [4]	Table I [45]	(31) [4]	(5) [12]

and the phase vectors of Equations (5.20)-(5.21)-(5.22) are, for $i = 1$:

$$\mathbf{p}_{1,1} = \left[\underbrace{1, 0, \cdots}_{1^{st}}, \underbrace{1, 0, \cdots}_{2^{nd}}\right]^T \tag{5.26}$$

$$\mathbf{p}_{2,1} = \left[\underbrace{0, 1, \cdots}_{1^{st}}, \underbrace{0, 1, \cdots}_{2^{nd}}\right]^T \tag{5.27}$$

$$\vdots$$

$$\mathbf{p}_{N/2,1} = \left[\underbrace{\cdots, 0, 1}_{1^{st}}, \underbrace{\cdots, 0, 1}_{2^{nd}}\right]^T \tag{5.28}$$

and for $i = B = 2$:

$$
\mathbf{p}_{1,2} = \left[\underbrace{1, 0, \cdots}_{1^{st}}, \underbrace{e^{j\frac{(N-N/2)\pi}{2}}, 0, \cdots}_{2^{nd}} \right]^T \tag{5.29}
$$

$$
\mathbf{p}_{2,2} = \left[\underbrace{0, e^{j\frac{\pi}{2}}, \cdots}_{1^{st}}, \underbrace{0, e^{j\frac{(N-N/2+1)\pi}{2}}, \cdots}_{2^{nd}} \right]^T \tag{5.30}
$$

$$
\vdots
$$

$$
\mathbf{p}_{N/2,2} = \left[\underbrace{\cdots, 0, e^{j\frac{(N/2-1)\pi}{2}}}_{1^{st}}, \underbrace{\cdots, 0, e^{j\frac{(N-1)\pi}{2}}}_{2^{nd}} \right]^T \tag{5.31}
$$

2x2 SCFDE SF-OD

For the 2-transmit antennas Orthogonal Design (OD) it is $N_S = \frac{N}{2}$, $B = 2$, and $Q^f = 2$. The space-frequency dispersion matrices are:

$$
\mathbf{A}_1^f = \begin{bmatrix} 1 & 0 \\ 0 & 1 \end{bmatrix} , \ \mathbf{B}_1^f = \begin{bmatrix} 1 & 0 \\ 0 & -1 \end{bmatrix} , \ \mathbf{A}_2^f = \begin{bmatrix} 0 & 1 \\ -1 & 0 \end{bmatrix} , \ \mathbf{B}_2^f = \begin{bmatrix} 0 & 1 \\ 1 & 0 \end{bmatrix} \tag{5.32}
$$

and the phase vectors are the same as for 2×2 SCFDE SF-LDC.

4x4 SCFDE SF-QOD and SF-LDC

The 4-transmit antennas SF schemes considered (Equation (31) [4] and Equation (5) [12]) are straightforward extensions of the $N_T = 2$ case. The QOD code of [12] was chosen because it provides a sufficient high spatial rate of 1, with no need to go for too high (unrealistic) modulation orders, with respect to OD (e.g. the OD (38) of [59] has spatial rate of 1/2 and needs 256-QAM to achieve $R = 4$, while LDC only BPSK, and needs 65536-QAM (!!!) to achieve $R = 8$, while LDC only QPSK). As an example the space-frequency dispersion

matrices for Jafarkhani QOD code (in this case it is $N_S = \frac{N}{4}$, $B = 4$, and $Q^f = 4$) are:

$$
\mathbf{A}_1^f = \begin{bmatrix} 1 & 0 & 0 & 0 \\ 0 & 1 & 0 & 0 \\ 0 & 0 & 1 & 0 \\ 0 & 0 & 0 & 1 \end{bmatrix}, \; \mathbf{B}_1^f = \begin{bmatrix} 1 & 0 & 0 & 0 \\ 0 & -1 & 0 & 0 \\ 0 & 0 & -1 & 0 \\ 0 & 0 & 0 & 1 \end{bmatrix} \tag{5.33}
$$

$$
\mathbf{A}_2^f = \begin{bmatrix} 0 & 1 & 0 & 0 \\ -1 & 0 & 0 & 0 \\ 0 & 0 & 0 & 1 \\ 0 & 0 & -1 & 0 \end{bmatrix}, \; \mathbf{B}_2^f = \begin{bmatrix} 0 & 1 & 0 & 0 \\ 1 & 0 & 0 & 0 \\ 0 & 0 & 0 & -1 \\ 0 & 0 & -1 & 0 \end{bmatrix} \tag{5.34}
$$

$$
\mathbf{A}_3^f = \begin{bmatrix} 0 & 0 & 1 & 0 \\ 0 & 0 & 0 & 1 \\ -1 & 0 & 0 & 0 \\ 0 & -1 & 0 & 0 \end{bmatrix}, \; \mathbf{B}_3^f = \begin{bmatrix} 0 & 0 & 1 & 0 \\ 0 & 0 & 0 & -1 \\ 1 & 0 & 0 & 0 \\ 0 & -1 & 0 & 0 \end{bmatrix} \tag{5.35}
$$

$$
\mathbf{A}_4^f = \begin{bmatrix} 0 & 0 & 0 & 1 \\ 0 & 0 & -1 & 0 \\ 0 & -1 & 0 & 0 \\ 1 & 0 & 0 & 0 \end{bmatrix}, \; \mathbf{B}_4^f = \begin{bmatrix} 0 & 0 & 0 & 1 \\ 0 & 0 & 1 & 0 \\ 0 & 1 & 0 & 0 \\ 1 & 0 & 0 & 0 \end{bmatrix} \tag{5.36}
$$

and the phase vectors of Equations (5.20)-(5.21)-(5.22) are, for $i = 1$:

$$\mathbf{p}_{1,1} \;=\; \left[\underbrace{1,0,\cdots,}_{1^{st}}\cdots,\underbrace{1,0,\cdots}_{4^{th}}\right]^{T} \tag{5.37}$$

$$\mathbf{p}_{2,1} \;=\; \left[\underbrace{0,1,\cdots,}_{1^{st}}\cdots,\underbrace{0,1,\cdots}_{4^{th}}\right]^{T} \tag{5.38}$$

$$\vdots$$

$$\mathbf{p}_{N/4,1} \;=\; \left[\underbrace{\cdots,0,1,}_{1^{st}}\cdots,\underbrace{\cdots,0,1}_{4^{th}}\right]^{T} \tag{5.39}$$

up to $i = B = 4$:

$$\mathbf{p}_{1,4} \;=\; \left[\underbrace{1,0,\cdots,}_{1^{st}}\cdots,\underbrace{e^{j\frac{(N-N/4)3\pi}{4}},0,\cdots}_{4^{th}}\right]^{T} \tag{5.40}$$

$$\mathbf{p}_{2,4} \;=\; \left[\underbrace{0,e^{j\frac{3\pi}{4}},\cdots,}_{1^{st}}\cdots,\underbrace{0,e^{j\frac{(N-N/4+1)3\pi}{4}},\cdots}_{4^{th}}\right]^{T} \tag{5.41}$$

$$\vdots$$

$$\mathbf{p}_{N/4,4} \;=\; \left[\underbrace{\cdots,0,e^{j\frac{(N/4-1)3\pi}{4}},}_{1^{st}}\cdots,\underbrace{\cdots,0,e^{j\frac{(N-1)3\pi}{4}}}_{4^{th}}\right]^{T} \tag{5.42}$$

5.3.1.4 Equalization

As in [4] the single real system of equations (5.43) can be written, and in more compact form as in Equation (5.44):

$$\mathbf{Y}_k = \sqrt{\frac{P_T}{N_T}}\mathcal{H}_k^f \mathbf{s}_k^f + \mathbf{N}_k, \; k = 1, \dots, N_S \tag{5.44}$$

where $\mathbf{Y}_k$, $k = 1, \dots, N_S$ is a $2BN_R \times 1$ vector, $\mathcal{A}_j^f$ and $\mathcal{B}_j^f$, $j = 1, \dots, Q^f$ are $2B \times 2N_T$ matrices, $\mathcal{H}_k^f$ is a $2BN_R \times 2Q^f$ matrix, $\mathbf{s}_k^f$ is a $2Q^f \times 1$ vector, and $\mathbf{N}_k$ is a $2BN_R \times 1$ vector.

$$\begin{bmatrix} \mathbf{Y}_{R,1,k} \\ \mathbf{Y}_{I,1,k} \\ \vdots \\ \mathbf{Y}_{R,N_R,k} \\ \mathbf{Y}_{I,N_R,k} \end{bmatrix} = \sqrt{\frac{P_T}{N_T}} \begin{bmatrix} \mathcal{A}_1^f \mathbf{h}_{1,k} & \mathcal{B}_1^f \mathbf{h}_{1,k} & \cdots & \mathcal{A}_Q^f \mathbf{h}_{1,k} & \mathcal{B}_Q^f \mathbf{h}_{1,k} \\ \vdots & \vdots & \ddots & \vdots & \vdots \\ \mathcal{A}_1^f \mathbf{h}_{N_R,k} & \mathcal{B}_1^f \mathbf{h}_{N_R,k} & \cdots & \mathcal{A}_Q^f \mathbf{h}_{N_R,k} & \mathcal{B}_Q^f \mathbf{h}_{N_R,k} \end{bmatrix} \begin{bmatrix} \alpha_{1,k}^f \\ \beta_{1,k}^f \\ \vdots \\ \alpha_{Q,k}^f \\ \beta_{Q,k}^f \end{bmatrix} + \begin{bmatrix} \mathbf{N}_{R,1,k} \\ \mathbf{N}_{I,1,k} \\ \vdots \\ \mathbf{N}_{R,N_R,k} \\ \mathbf{N}_{I,N_R,k} \end{bmatrix}$$

$$(5.43)$$

$$\mathbf{H}_k = \mathbf{H}_{R,k} + j\mathbf{H}_{I,k} = \begin{bmatrix} \mathbf{H}_{1,1}\left((k-1)B+1\right) & \cdots & \mathbf{H}_{1,N_R}\left((k-1)B+1\right) \\ \vdots & \ddots & \vdots \\ \mathbf{H}_{N_T,1}\left((k-1)B+1\right) & \cdots & \mathbf{H}_{N_T,N_R}\left((k-1)B+1\right) \end{bmatrix}, \ k = 1, \ldots, N_S$$

$$(5.46)$$

The vector $\mathbf{Y}_{R,j,k}$ is built as follows:

$$\mathbf{Y}_{R,j,k} = \begin{bmatrix} \mathbf{Y}_{R,j,k}(1) \\ \vdots \\ \mathbf{Y}_{R,j,k}(B) \end{bmatrix}, \ k = 1, \ldots, N_S, j = 1, N_R \qquad (5.45)$$

and analogously for $\mathbf{Y}_{I,j,k}$. $\mathbf{Y}_{R,j,k}$ and $\mathbf{Y}_{I,j,k}$ are $B \times 1$ vectors.

The matrices $\mathcal{A}_q^f$ and $\mathcal{B}_q^f$, $q = 1, \ldots, Q^f$ are defined as in [4], using the $B \times N_T$ matrices $\mathbf{A}_q^f$ and $\mathbf{B}_q^f$, $q = 1, \ldots, Q^f$.

Regarding the channel, let us suppose it constant over k-th subchannel, as in Equation (5.46) where $\mathbf{H}_{m,n}(i)$ is the CTF between m-th transmit antenna and n-th receive antenna for the i-th subcarrier, and $\mathbf{H}_k$, $\mathbf{H}_{R,k}$, $\mathbf{H}_{I,k}$ are all $N_T \times N_R$ matrices. The following $2N_T \times 1$ vector is then built:

$$\mathbf{h}_{j,k} = \begin{bmatrix} \mathbf{h}_{R,j,k} \\ \mathbf{h}_{I,j,k} \end{bmatrix}, \ k = 1, \ldots, N_S, \ j = 1, \ldots, N_R \qquad (5.47)$$

where $\mathbf{h}_{R,j,k}$ and $\mathbf{h}_{I,j,k}$ are the j-th columns of $\mathbf{H}_{R,k}$ and $\mathbf{H}_{I,k}$, respectively.

The $B \times 1$ noise vector $\mathbf{N}_{R,j,k}$ is built as:

$$\mathbf{N}_{R,j,k} = \begin{bmatrix} \mathbf{N}_{R,j,k}(1) \\ \vdots \\ \mathbf{N}_{R,j,k}(B) \end{bmatrix}, \ k = 1, \ldots, N_S, \ j = 1, \ldots, N_R \tag{5.48}$$

and analogously for $\mathbf{N}_{I,j,k}$.

The linear relation in (5.44) allows us to use a linear receiver, i.e.

$$\widehat{\mathbf{s}}_k = \mathbf{G}_k \mathbf{Y}_k, \ k = 1, \ldots, N_S \tag{5.49}$$

where for ZF

$$\mathbf{G}_k = \mathbf{G}_{ZF,k} = \sqrt{\frac{N_T}{P_T}} \left(\mathcal{H}_k^H \mathcal{H}_k \right)^{-1} \mathcal{H}_k^H \tag{5.50}$$

and for MMSE

$$\mathbf{G}_k = \mathbf{G}_{MMSE,k} = \sqrt{\frac{N_T}{P_T}} \left(\mathcal{H}_k^H \mathcal{H}_k + \frac{N_T}{\rho} \mathbf{I}_{N_T} \right)^{-1} \mathcal{H}_k^H \tag{5.51}$$

where $\rho = P_T / \sigma^2$.

5.3.2 Simulations and Discussions

The simulations parameters are shown in Table 5.2, and consider a WiMAX scenario [30] with values for maximum delay spread and velocity taken from the ITU Vehicular A channel model [63]. In Figure 5.2 we show the uncoded BER for 2×2 schemes, LDC and OD, both ST and SF. The rate is $R = 8$, which means 16-QAM for LDC and 256-QAM for OD. As we can see in ITU Vehicular A channel model, the ST schemes show worse performance than the SF schemes, since the assumption they make of channel identical over two time

Table 5.2: Simulation Parameters

Parameters	Value
System bandwidth, B	1.25 MHz
Sampling frequency, f_s	1.429 MHz
Carrier frequency, f_c	3.5 GHz
Symbols per block, N	128
Subcarrier spacing, Δf	9.77 KHz
CP length, N_{CP}	16
Max delay spread, τ_{max}	2.51 μs
Velocity	30 Kmph
FDE Equalizer	MMSE
Channel coding scheme	1/2-rate convolutional coding

periods [45] does not hold anymore, already at a moderate velocity of 30 kmph. The SF schemes instead, show a much more robust behavior to the time-variability of the channel. We can note that even though the SF-LDC scheme outperforms SF-OD up to SNR=22 dB, OD behaves better for higher SNR: this diversity loss of the LDC can be explained by the fact that the code used satisfies more the mutual information criterion than the diversity criterion [4].

In Figure 5.3 we compare 4×4 LDC and QOD pure-diversity systems, both ST and SF. It is interesting to notice that the impact of time-selectivity is much higher for 4×4 ST-LDC than for any other scheme considered. This is due to the fact that the assumption of channel constant over four time periods is not realistic already for moderate velocities. This is also confirmed by Figure 5.4, which shows the impact of increasing time-selectivity on the studied systems. The velocity considered in the ITU Vehicular A model is correspondent to a normalized Doppler frequency $f_d T_s = 0.01$.

Finally, the impact of frequency-selectivity is shown in Figure 5.5. The normalized coherence bandwidth is defined as $B_{c,norm} = \frac{1}{\tau_{max}\Delta f}$. The dual behavior of Figure 5.4 can be seen, and the big degradation in performance of SF-LDC is due to the non-realistic assumption of channel constant over four subcarriers, in case of high frequency-selectivity.
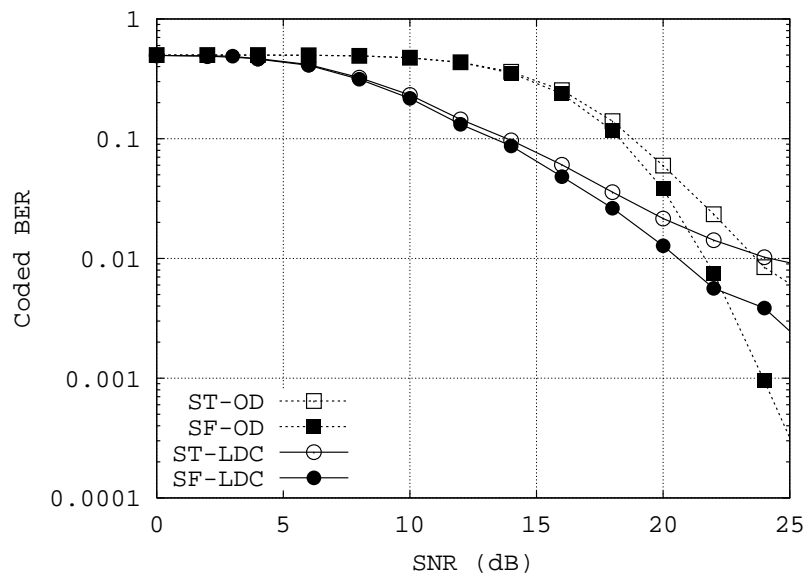
Figure 5.2: Coded BER performance for 2x2 ST and SF-LDC vs. ST and SF-OD, rate = 8, B = T = 2, ITU vehicular A channel
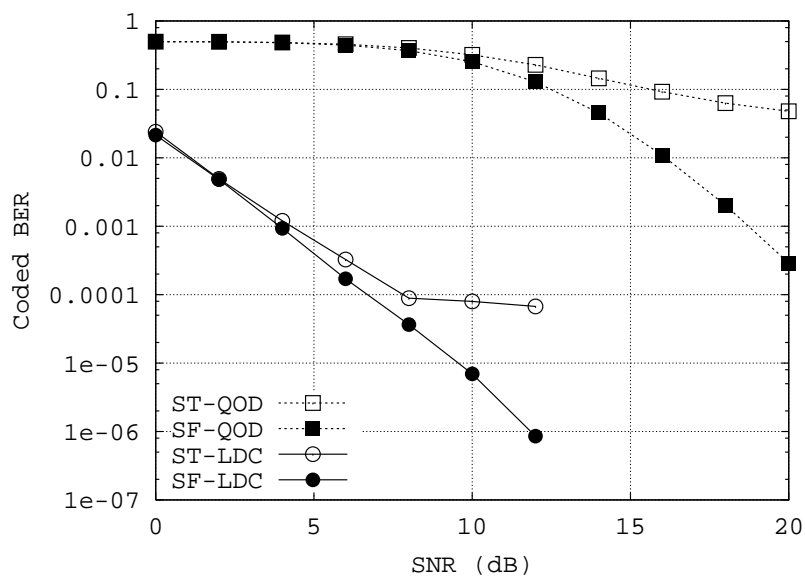
Figure 5.3: Coded BER performance for 4x4 ST and SF-LDC vs. ST and SF-QOD, rate = 8, B = T = 4, ITU vehicular A channel
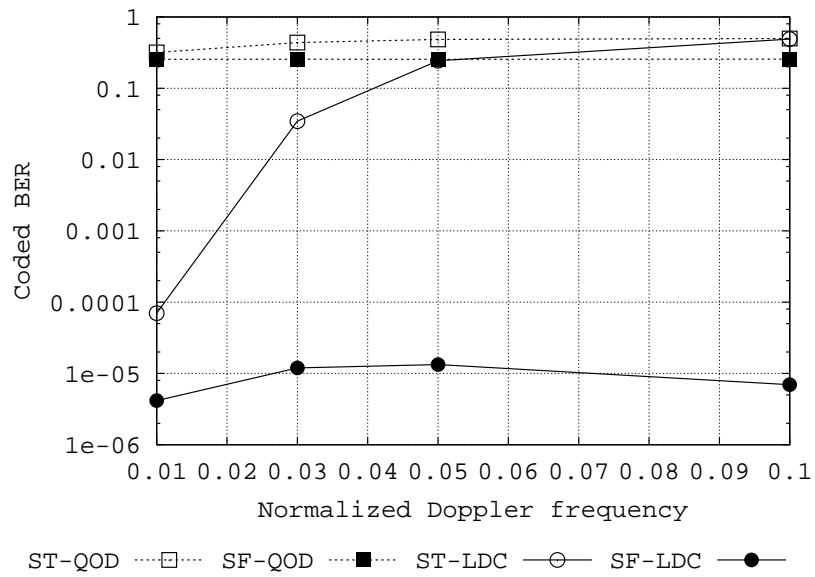
Figure 5.4: Impact of time-selectivity for 4x4 ST and SF-LDC vs. ST and SF-QOD, rate = 8, B = T = 4, SNR = 10 dB
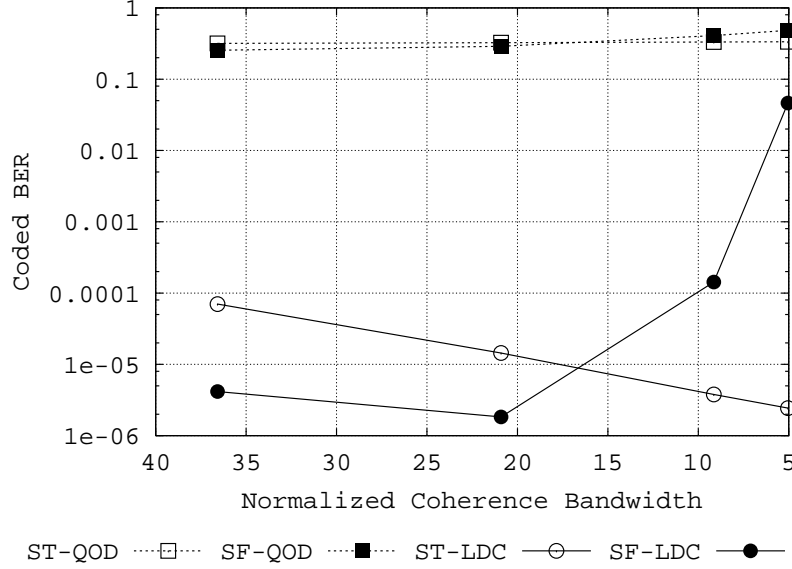
Figure 5.5: Impact of frequency-selectivity for 4x4 ST and SF-LDC vs. ST and SF-QOD, rate = 8, B = T = 4, SNR = 10 dB

The maximum delay spread considered in the ITU Vehicular A model is correspondent to a normalized coherence bandwidth $B_{c,norm} = 36.58$. From Figure 5.5, we can notice that both ST and SF-LDC for SCFDE systems show a higher frequency diversity gain as the coherence bandwidth decreases. However, in the case of SF-LDC, the diversity gain is compensated by the performance degradation due to the hypothesis of channel constance over B consecutive subcarriers. This explains the minimum in the curve of SF-LDC.

The influence of correlation, due either to insufficient antennas spacing or to the presence of LOS component, was not investigated for LDC and is left for future investigations.

5.3.3   Computational Complexity

The complexities for SCFDE-SF-LDC, SCFDE-ST-LDC, and OFDM-SF-LDC are, respectively:

$$C^{SC-SF} = 2\frac{Q^f N_S N N_T}{B} + N_R \frac{N}{2} log_2 N + Q^f \frac{N_S}{2} log_2 N_S \qquad (5.52)$$

$$C^{SC-ST} = 2\frac{Q^t \frac{N_P}{T} N N_T}{T} + N_R \frac{N}{2} log_2 N + \frac{Q^t}{T} \frac{N_P}{2} log_2 N_P \qquad (5.53)$$

$$C^{MC-SF} = 2\frac{N_S Q^f N_S B N_T}{B} + N_T \frac{N}{2} log_2 N + N_R \frac{N}{2} log_2 N \qquad (5.54)$$

where the number of subchannels for SF codes is $N_S = N/B$ and the number of symbols periods for ST codes is $N_P = N$.

The complexity for the 2×2 case is shown in Table 5.3. The parameters in this case are: $N_T = N_R = 2$, $B = T = 2$. Moreover, it is $Q^f = Q^t = B = T = 2$ for Alamouti, and $Q^f = Q^t = N_T B = N_T T = 4$ for Hassibi.

Table 5.3: Complexity in terms of complex multiplications for 2x2 case

scheme	Hassibi N=64	Hassibi N=128	Alamouti N=64	Alamouti N=128
SCFDE-SF	17088	67200	8736	34048
SCFDE-ST	17152	67328	8768	34112
OFDM-SF	17152	67328	8960	34560

The complexity for the 4×4 case is shown in Table 5.4. The parameters in this case are: $N_T = N_R = 4$, $B = T = 4$. Moreover, it is $Q^f = Q^t = B = T = 4$ for Jafarkhani, and $Q^f = Q^t = N_T B = N_T T = 16$ for Hassibi.

Therefore, the proposed SCFDE-SF schemes are slightly less complex than the correspondent SCFDE-ST and OFDM-SF schemes.

Table 5.4: Complexity in terms of complex multiplications for 4x4 case

scheme	Hassibi N=64	Hassibi N=128	Jafarkhani N=64	Jafarkhani N=128
SCFDE-SF	34048	134144	9088	34880
SCFDE-ST	34304	134656	9152	35008
OFDM-SF	34304	134656	9728	36352

5.4   SD, SM and JDM as special cases of LDC

In this Section it is explicitly shown how the schemes considered in the former Chapters, i.e. 2-transmit antennas Alamouti SD, 2-transmit antennas SM, and 4-transmit antennas JDM, can all be incorporated in the LDC theoretical framework.

In the case of Alamouti SD with $N_T = T = 2$ (or $N_T = B = 2$), the matrix $\mathbf{S}$ of Equation (5.1) can be written as:

$$
\mathbf{S}_{SD} = \begin{bmatrix} s_1 & s_2 \\ -s_2^* & s_1^* \end{bmatrix} \tag{5.55}
$$

$$
= \begin{bmatrix} \alpha_1 + j\beta_1 & \alpha_2 + j\beta_2 \\ -\alpha_2 + j\beta_2 & \alpha_1 - j\beta_1 \end{bmatrix} \tag{5.56}
$$

$$
= \alpha_1 \begin{bmatrix} 1 & 0 \\ 0 & 1 \end{bmatrix} + j\beta_1 \begin{bmatrix} 1 & 0 \\ 0 & -1 \end{bmatrix} + \alpha_2 \begin{bmatrix} 0 & 1 \\ -1 & 0 \end{bmatrix} + j\beta_2 \begin{bmatrix} 0 & 1 \\ 1 & 0 \end{bmatrix} \tag{5.57}
$$

$$
= \alpha_1 \mathbf{A}_1 + j\beta_1 \mathbf{B}_1 + \alpha_2 \mathbf{A}_2 + j\beta_2 \mathbf{B}_2 \tag{5.58}
$$

For SM with $N_T = 2$ and $T = 1$ (or $B = 1$), the matrix $\mathbf{S}$ of Equation (5.1) can be written

as:

$$\mathbf{S}_{SM} = \begin{bmatrix} s_1 & s_2 \end{bmatrix} \tag{5.59}$$

$$= \begin{bmatrix} \alpha_1 + j\beta_1 & \alpha_2 + j\beta_2 \end{bmatrix} \tag{5.60}$$

$$= \alpha_1 \begin{bmatrix} 1 & 0 \end{bmatrix} + j\beta_1 \begin{bmatrix} 1 & 0 \end{bmatrix} + \alpha_2 \begin{bmatrix} 0 & 1 \end{bmatrix} + j\beta_2 \begin{bmatrix} 0 & 1 \end{bmatrix} \tag{5.61}$$

$$= \alpha_1 \mathbf{A}_1 + j\beta_1 \mathbf{B}_1 + \alpha_2 \mathbf{A}_2 + j\beta_2 \mathbf{B}_2 \tag{5.62}$$

In the case of JDM with $N_T = 4$ and $T = 2$ (or $B = 2$), the matrix $\mathbf{S}$ of Equation (5.1) can be written as:

$$\mathbf{S}_{JDM} = \begin{bmatrix} s_1 & s_2 & s_3 & s_4 \\ -s_2^* & s_1^* & -s_4^* & s_3^* \end{bmatrix} \tag{5.63}$$

$$= \begin{bmatrix} \alpha_1 + j\beta_1 & \alpha_2 + j\beta_2 & \alpha_3 + j\beta_3 & \alpha_4 + j\beta_4 \\ -\alpha_2 + j\beta_2 & \alpha_1 - j\beta_1 & -\alpha_4 + j\beta_4 & \alpha_3 - j\beta_3 \end{bmatrix} \tag{5.64}$$

$$= \alpha_1 \begin{bmatrix} 1 & 0 & 0 & 0 \\ 0 & 1 & 0 & 0 \end{bmatrix} + j\beta_1 \begin{bmatrix} 1 & 0 & 0 & 0 \\ 0 & -1 & 0 & 0 \end{bmatrix} \tag{5.65}$$

$$+ \alpha_2 \begin{bmatrix} 0 & 1 & 0 & 0 \\ -1 & 0 & 0 & 0 \end{bmatrix} + j\beta_2 \begin{bmatrix} 0 & 1 & 0 & 0 \\ 1 & 0 & 0 & 0 \end{bmatrix}$$

$$+ \alpha_3 \begin{bmatrix} 0 & 0 & 1 & 0 \\ 0 & 0 & 0 & 1 \end{bmatrix} + j\beta_3 \begin{bmatrix} 0 & 0 & 1 & 0 \\ 0 & 0 & 0 & -1 \end{bmatrix}$$

$$+ \alpha_4 \begin{bmatrix} 0 & 0 & 0 & 1 \\ 0 & 0 & -1 & 0 \end{bmatrix} + j\beta_4 \begin{bmatrix} 0 & 0 & 0 & 1 \\ 0 & 0 & 1 & 0 \end{bmatrix}$$

$$= \alpha_1 \mathbf{A}_1 + j\beta_1 \mathbf{B}_1 + \alpha_2 \mathbf{A}_2 + j\beta_2 \mathbf{B}_2 + \alpha_3 \mathbf{A}_3 + j\beta_3 \mathbf{B}_3 + \alpha_4 \mathbf{A}_4 + j\beta_4 \mathbf{B}_4 \tag{5.66}$$

5.5   Conclusions

A general procedure has been introduced to derive the dispersion matrices to be applied at the transmitter of a SCFDE system, to achieve the desired space-frequency dispersion. To the best of Authors' knowledge, no other work before has addressed the issue of applying LDC in the frequency domain to SCFDE systems. It has been shown that the dispersion in frequency is more suitable than the dispersion in time, already at moderate terminal speeds and for a wide range of frequency selectivity of the channel.

Part IV

Summary and Conclusions

Chapter 6

Summary and Conclusions

This Thesis has investigated several kinds of multiple antenna transceiver architectures in FDE, especially addressing the SCFDE case and the application of SF multi-antenna schemes.

The main contributions of the Thesis are two:

- the efficient (low-complexity) application of space-frequency diversity techniques in SCFDE systems;

- original JDM techniques for both OFDM and SCFDE systems, which achieve a trade-off between diversity and multiplexing gains.

6.1 Space-Frequency Diversity Techniques for SCFDE Systems

This work proposed several solutions to the application to SCFDE systems of SF diversity techniques, which are recognized to be important in future wireless systems targeting also high mobility environments (i.e., highly time variable channels). However, their "straight" application to SCFDE system would require the introduction of high complexity processing,

especially at the transmit terminal (the mobile terminal in case of the application of SCFDE to the uplink). The proposed solutions overcome this issue. Moreover, the investigation carried out in this Thesis showed that SF techniques are very suitable in a wide range of propagation scenarios.

6.1.1 SCFDE-SFBC

A new low-complexity SCFDE-SFBC transmit diversity scheme has been presented, which has been shown to be more robust than SCFDE-STBC transmit diversity scheme in highly time-varying channels. As SFBC schemes in OFDM-based transmissions, the proposed scheme processes simultaneously two adjacent subcarriers at the receiver, and hence, it is expected to work well in low frequency selective channel. However, the performance comparison between STBC and the proposed scheme in different channel conditions showed that STBC is outperformed by SFBC over highly time-varying channels also when the frequency selectivity is high.

6.1.2 Linear Dispersion Codes for SCFDE

The application of a SF approach appears to be even more important when high rate LDC are used. A general procedure has been introduced to derive the dispersion matrices to be applied at the transmitter of a SCFDE system, to achieve the desired space-frequency dispersion. This is the main contribution of this Thesis. With the derived procedure, LDC can be applied in the frequency domain of SCFDE systems as the LDC in the time domain (same transmitter and complexity) by simply changing the dispersion matrices.

This procedure can be applied also to diversity or spatial multiplexing schemes, which are special cases of LDC. As expected, LDC in the frequency domain work better than LDC in the time domain in highly time variable channels but their performance degrade as high frequency selectivity is experienced. However, it is worth outlining (from the shown

performance results) that the dispersion in frequency instead of in time is more suitable, already at moderate terminal speeds and for a wide range of frequency selectivity of the channel.

6.2 JDM Techniques for FDE-based Systems

6.2.1 Combining Diversity and Multiplexing in OFDM

Two JDM schemes for OFDM systems have been proposed. They showed robustness to the spatial correlation caused by the inadequate spatial separation between antenna elements. When spatial correlation is caused by the LOS scenario, then only SM-QSFBC type JDM schemes show robustness in performance. All other JDM schemes fail with little increment in strength of the LOS component in the wireless channel. For both ZF and MMSE, the VBLAST-based SM schemes [10] perform poorly in realistic wireless conditions.

The proposed JDM schemes appear to be a suitable solution when SM is used at any cellular access point, as they allow to increase the coverage in terms of radius where SM can be supported.

6.2.2 Combining Diversity and Multiplexing in SCFDE

The JDM schemes proposed for OFDM in Chapter 3 have been extended to the SCFDE case. In particular, the combination of SM and SFBC for SCFDE systems is studied in highly time variable channels, where the application of the coding across antennas and time (ST coding) is known to have poor performance. The above-introduced low-complexity implementation of SFBC in SCFDE systems is applied to a JDM scheme (combined SM and SFBC).

A different behavior between OFDM systems and SCFDE systems has been observed in terms of diversity-multiplexing trade-off. In fact, it has been shown that space-frequency-based diversity schemes in OFDM systems are very sensitive to the frequency selectivity of

Table 6.1: Dissemination of the Ph.D work

Chapter	Journals	Conferences	Deliverables
2		WPMC Sep 04	Jade Del 3.1.1 Jul 04
			Jade Del 3.2.1 Sep 04
3	IEE Letters Aug 06	OFDM Workshop Aug-Sep 05	Jade Del Jun 05
	Eurasip JWCN Jul 07	IEEE ISWCS Sep 05	
		IEEE VTC fall Sep 06	
4	Wiley WCMC Fall 07	IEEE ICC Jun 07	
		IST Jul 07	
5	IEEE TW Comm Fall 07	IEEE PIMRC Sep 07	
	Wiley WCMC Fall 07		

the channel and "coding less" across subcarriers by using part of the available antennas to get SM gain does not help much in reducing the negative impact of the frequency selectivity. On the other hand, for SCFDE it is very efficient to use the available antennas to get multiplexing gain since the resulting scheme is robust to both the frequency selectivity, and the time selectivity of the channel (by using SFBC instead of STBC). As expected, the spatial correlation of the channel negatively impacts the performance of the JDM schemes. However, for moderate and high frequency selective channels, the proposed JDM scheme still outperforms diversity-only schemes in uncoded systems.

On the other hand, when channel coding is present, the detrimental effect of frequency selectivity on SF schemes is much mitigated, and it is shown that it is more convenient to use the available antennas to provide only diversity instead of both diversity and multiplexing.

6.3   Dissemination

The state-of-the-art surveys and original contributions presented in this Thesis have been disseminated in international journals and conferences, and project deliverables, as indicated in Table 6.1. The percentage of personal contribution to the presented work is quantified in Table 6.2.

Table 6.2: Percentage of personal contribution to the presented work

Chapter	Personal Contribution
2	25%
3	50%
4	80%
5	80%

6.4   Future Work

The work presented in this Ph.D. Thesis can be extended towards several directions, and some of them are:

- Study of time-frequency codes (advantage: one avoids the complexity due to spatial domain, i.e. to multiple antennas) and of space-time-frequency codes (in this case, despite of the complexity, one would achieve the best possible code in terms of performance) for SCFDE;

- Universal FDE-based MIMO transceiver: inclusion of beam-forming techniques [32] in the FDE-based JDM or LDC schemes to achieve all the possible gains provided by an array of antennas (diversity, multiplexing and array gains) [25] [64];

- System Level evaluation, where one will be considered: a multi-user scenario considering SCFDE as modulation for the UL and OFDM for the DL, LDC and JDM schemes providing a multiplexing-diversity trade-off as an effective option in the intermediate region of the cell;

- Alternative design approach to the pragmatic one of the present work: one could instead start from principles and establish bounds on performance. This alternative approach would be analogous to the one already taken to study coding in space-frequency domain for OFDM [40];

- A more complete complexity analysis could be addressed, comparing the computational complexities calculated for the schemes presented in this work with the current hardware state of the art. In this perspective, it would be also relevant to address the complexity of the SCFDE implementation with direct access to the frequency domain (Discrete Fourier Transform (DFT)-spread OFDM) and compare it with the proposed schemes;

- One of the main arguments to go for SC modulation in UL is the reduced PAPR, compared to OFDM; as ST and SF encoding imply to add and subtract different versions of the same symbols, which could originate an increase in PAPR, this aspect could be verified, to validate also from this aspect the efficacy of the proposed multi-antenna coding techniques for SCFDE.

Part V

Appendices

Appendix A

List of Publications Produced during the Ph.D. Studies

A.1 Journals

1. N. Marchetti, E. Cianca, and R. Prasad, "Advanced Spatial Coding for Single Carrier-Frequency Domain Equalization", *Wiley Journal on Wireless Communications and Mobile Computing* (in preparation), Fall 2007

2. N. Marchetti, E. Cianca, and R. Prasad, "Space-Frequency Linear Dispersion Codes for Single Carrier-Frequency Domain Equalization", *IEEE Transaction on Wireless Communications* (submitted), Fall 2007

3. M.I. Rahman, N. Marchetti, E. de Carvalho, and R. Prasad, "Joint Diversity and Multiplexing Schemes for MIMO-OFDM Systems", *Eurasip Journal on Wireless Communications and Networking* (accepted with major revisions), July 2007

4. M.I. Rahman, N. Marchetti, E. de Carvalho, and R. Prasad, "Spatially Multiplexed Quasi-orthogonal SFBC System", IEE Electronics Letters, Volume 42, Issue 18, Au-

gust 2006 Page(s):59 - 60

A.2   Conference Papers

5. N. Marchetti, E. Cianca, and R. Prasad, "Linear Dispersion Codes in Space-Frequency Domain for SCFDE: a General Framework", *Personal, Indoor and Mobile Radio Communications (PIMRC)*, Athens, Greece, September 2007

6. N. Marchetti, E. Cianca, and R. Prasad, "Combining Spatial Multiplexing and Transmit Diversity in SCFDE Systems in High-Mobility Environment", *IST Mobile & Wireless Communications Summit*, Budapest, Hungary, July 2007

7. N. Marchetti, E. Cianca, and R. Prasad, "Low complexity transmit diversity scheme for SCFDE transmissions over time-selective channels", *IEEE International Conference on Communications (ICC)*, Glasgow, Scotland, June 2007

8. M.I. Rahman, N. Marchetti, E. de Carvalho, and R. Prasad, "Joint Quasi-orthogonal SFBC and Spatial Multiplexing in OFDM-MIMO Systems", *IEEE Vehicular Technology Conference (VTC)-fall*, Montreal, Canada, September 2006

9. M.I. Rahman, N. Marchetti, F. Fitzek, and R. Prasad, "Non-Linear Detection for Joint Space-Frequency Block Coding and Spatial Multiplexing in OFDM-MIMO Systems", *IEEE International Symposium on Wireless Communication Systems (ISWCS)*, Siena, Italy, September 2005

10. M.I. Rahman, N. Marchetti, S.S. Das, F. Fitzek, and R. Prasad, "Combining Space-Frequency Block Coding and Spatial Multiplexing in MIMO-OFDM System", *International OFDM Workshop*, Hamburg, Germany, August-September 2005

11. D.V.P. Figueiredo, M.I. Rahman, N. Marchetti, F. Fitzek, M. Katz, Y. Cho, and R. Prasad, "Transmit Diversity vs Beamforming for Multi-user OFDM Systems", *Wire-*

less Personal Multimedia Communications (WPMC), Abano Terme, Italy, September 2004

A.3 Technical Reports

12. M.I. Rahman, N. Marchetti, et al., "Joint Diversity and Multiplexing Schemes for MIMO-OFDM Systems", JADE Project 6-months Deliverable, Center for TeleInFrastruktur, Aalborg University, June 2005

13. M.I. Rahman, N. Marchetti, et al. "Multi-antenna techniques in Multi-user OFDM Systems", JADE Project Deliverable 3.2.1, Center for TeleInFrastruktur, Aalborg University, September 2004

14. JADE Working Group 3, "Comparison of Various Modulation and Access Schemes under Ideal Channel Conditions", JADE Project Deliverable 3.1.1, Center for TeleInFrastruktur, Aalborg University, July 2004

A.4 Other Publications

These are other publications made during the Ph.D. work:

15. COMET Project Group, "Emerging Directions in Wireless Location: Vista from the COMET Project", *IST Mobile & Wireless Communications Summit*, Budapest, Hungary, July 2007

16. M. Kaneko, N. Marchetti, et al., "Multi-user Diversity in Scheduling", JADE Project Deliverable 3.2.2, Center for TeleInFrastruktur, Aalborg University, January 2005

17. N. Marchetti, R. Veronesi, and V. Tralli, "Allocation and Adaptation Techniques for Protocol Performance Improvement in Multicellular Wireless Packet Networks with

MIMO links", *IEEE Global Communications Conference (Globecom)*, Dallas, USA, November-December 2004

18. N. Marchetti, R. Veronesi, and V. Tralli, "On the impact of Allocation and Adaptation Techniques for Protocol Performance Improvement in Multicellular MIMO Wireless Packet Networks", *IEEE Vehicular Technology Conference (VTC)-fall*, Los Angeles, USA, September 2004

Appendix B

General Definitions

Frequency Domain: it is the subcarrier domain. While for OFDM it is directly accessible at the transmitter, this does not hold for SCFDE;

Spatial Coding: coding applied to the space domain, domain which is identified by the array of transmit antennas. This term includes a variety of schemes, from SM which just multiplexes the input streams over the transmit antennas to block coding, or more advanced codes, such as LDC;

Diversity gain: a scheme is said to have a diversity gain d if its average error probability decays like $1/\rho^d$, where ρ is the SNR;

Multiplexing gain: a scheme is said to have a spatial multiplexing gain r if its rate scales like $rlog\rho$, where ρ is the SNR.

Appendix C

Physical Characteristics of Multipath Channels

Wireless channel is always very unpredictable with harsh and challenging propagation situations. Wireless channel differs from wire line channel in a lot of ways. One of the most unique characteristics of wireless channel is multipath reception. Together with multipath, there are other serious impairments present at the channel, namely propagation path loss, shadow fading, Doppler spread, time dispersion or delay spread, etc.

C.1   Multipath Scenario

Multipath is the result of reflection of wireless signals by objects in the environment between the transmitter and receiver. The objects can be anything present on the signal traveling path, e.g. buildings, trees, vehicles, hills or even human beings. Thus, multipath scenario includes random number of received signal from the same transmission source; depending on the location of transmitter and receiver, a direct transmission path referred to as the Line of Sight (LOS) path may be present or may not be present. When LOS component is present (or when one of the components is much stronger than others), then the environment is

modeled as Ricean channel, and when no LOS signal is present, the environment is described as Rayleigh channel [65, 66].

Multipaths arrive at the receiver with random phase offsets, because each reflected wave follows a different path from transmitter to reach the receiver. The reflected waves interfere with direct LOS wave, and cause a severe degradation of network performance. This results in random signal fades as the reflections destructively (and/or constructively) superimpose one another, which effectively cancels part of signal energy for a brief period of time. The severity of fading will depend on delay spread of the reflected signal, as embodied by their relative phases and their relative power [65].

A common approach to represent the multipath channel is as the CIR. The channel baseband equivalent impulse response function, $\tilde{h}_u(t)$ is defined as

$$\tilde{h}_u(\tau, t) = \sum_{l=0}^{L} h_{u,l}(t)\delta_c(\tau - \tau_l) \tag{C.1}$$

where $h_{u,l}(t) = A_{t,l}\exp(-j\theta_{t,l})$ is the complex gain of the lth multipath component at time t. Here, $A_{t,l}$, $\theta_{t,l}$ and τ_l are the amplitude, phase and delay of the lth path. The CIR given by Eq.(C.1) is also called Power Delay Profile (PDP), which is shown in Figure C.1.

Delay spread is the time spread between the arrival of the first and last multipath signal seen by receiver. The time dispersion in a channel is commonly measured by the Root Mean Square (RMS) delay spread τ_{rms}. It is the square root of the second central moment of the PDP as defined below [65]:

$$\tau_{rms} = \left[\bar{\tau^2} - (\bar{\tau})^2\right]^{\frac{1}{2}} \tag{C.2}$$
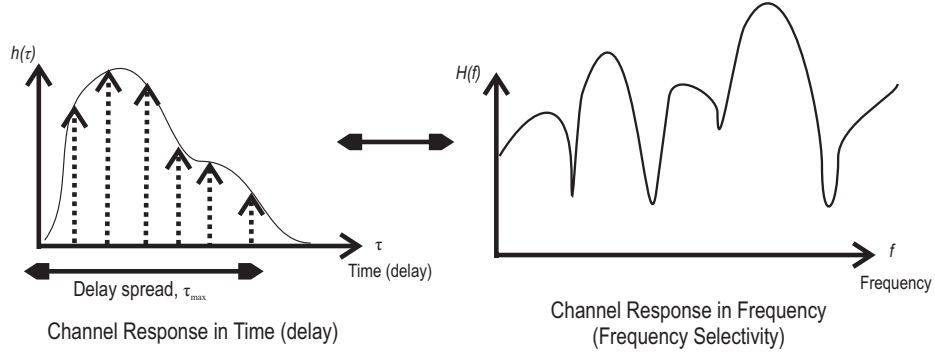
Figure C.1: Channel impulse responses and corresponding frequency response

where,

$$
\bar{\tau^2} = \frac{\sum_{l=1}^{L} A_l^2 \tau_l^2}{\sum_{l=1}^{L} A_l^2} = \frac{\sum_{l=1}^{L} P(\tau_l)\tau_l^2}{\sum_{l=1}^{L} P(\tau_l)} \tag{C.3}
$$

$$
\bar{\tau} = \frac{\sum_{l=1}^{L} A_l^2 \tau_l}{\sum_{l=1}^{L} A_l^2} = \frac{\sum_{l=1}^{L} P(\tau_l)\tau_l}{\sum_{l=1}^{L} P(\tau_l)} \tag{C.4}
$$

For clarity, we can remove the time index from the expressions related to CIR, as the CIR can be assumed to be time invariant, or at least to be wide sense stationary over a small-scale time or distance interval. $\bar{\tau}$ in Eq.(C.4) is the mean excess delay, defined as the first moment of PDP; $\bar{\tau^2}$ is the excess delay spread, defined as the first moment of squared delays. Eqs.(C.2 - C.4) do not depend on the absolute power level of $P(\tau_l)$, rather they only consider the relative amplitude between the first and later multipaths. In practice, values for τ_{rms}, $\bar{\tau^2}$ and $\bar{\tau}$ depend on the choice of noise threshold used to process $P(\tau_l)$.

The corresponding frequency-domain Channel Transfer Function (CTF), $H_u(f,t)$, can then be found using Fourier transformation:

$$
\begin{aligned}
H_u(f,t) &= \mathcal{F}\left\{\tilde{h}_u(\tau,t)\right\} \\
&= \int_{-\infty}^{\infty} \tilde{h}_u(\tau,t)e^{-j2\pi f\tau}d\tau
\end{aligned} \tag{C.5}
$$

Related to delay spread is *Coherence Bandwidth*, which is used to define channel frequency selectivity level [65]. If the coherence bandwidth is defined as the bandwidth over which the frequency correlation function is above 0.5, then the coherence bandwidth is approximately, $B_c = \frac{1}{5\tau_{rms}}$ [66]. Based on this, we can define the values for coherence bandwidth as shown in Table C.1. If the system bandwidth is much smaller compared to the coherence bandwidth, then the channel is said to be frequency non selective. In this case, the correlation coefficient is almost 1 for the frequencies within the system bandwidth. Physically, the frequency response within the system bandwidth is almost flat, so this kind of fading is also called flat fading. On the other hand, if the system bandwidth is larger than the coherence bandwidth, then the channel is said to be frequency selective.

RMS delay spread	Coherence bandwidth
τ_{rms}	B_c
50ns	4MHz
100ns	2MHz
0.5μs	400kHz
1.0μs	200kHz
2.0μs	100kHz
3.0μs	66.67kHz
5.0μs	40kHz

Table C.1: Channel coherence bandwidth with respect to different RMS delay spread

In a digital system, the delay spread can lead to ISI. In Figure C.1, the delay spread amounts to τ_{max}. It is noted that delay spread is always measured with respect to the first arriving component. Let's assume a system transmitting in the time intervals T_{sym}. The longest path with respect to the earliest path arrives at the receiver with a delay of τ_{max}; in other words, the last path arrives τ_{max} seconds after the first path arrives. This means that a received symbol can theoretically be influenced by previous symbols, which is termed as ISI. With high data rate, T_{sym} can be very small; thus the number of symbols that are affected by ISI can be in multiple of tens or more. Combating the influence of such large ISI

at the receiver is very challenging and sometimes may become unattainable at very severe channel conditions [67].

C.2   Doppler Effect

The Doppler effect is caused by the relative motion of transmitter and receiver. For example, in an urban environment in the city center, the vehicles are always moving; the walking pedestrians are also changing their locations continuously, thus their movements affect the transmission medium. The Doppler effect is expressed with so called Doppler shift or Doppler frequency which happens when there is a relative movement between the transmitter and receiver with a velocity v. The Doppler shift can be defined as:

$$f_d = \frac{1}{2\pi} \frac{\Delta\phi}{\Delta t} = \frac{v}{\lambda} cos\theta \tag{C.6}$$

where $\Delta\phi$ is the change of phase, defined as:

$$\Delta\phi = \frac{2\pi\Delta l}{\lambda} = \frac{2\pi v \Delta t}{\lambda} cos(\theta) \tag{C.7}$$

where, Δt is the time taken by the receiver to travel from one place to another and Δl is the difference in the pathlengths from the transmitter to these two locations of the mobile receiver. θ is the angle of arrival of the signal component. Although the receiver has moved from one place to another, the change in θ can be neglected assuming that the transmitter and receiver are located far away. It is obvious that the maximum Doppler shift is $f_m = \frac{v}{\lambda}$. Fourier transform of Doppler spread gives Doppler power spectral density.

Related to Doppler spread is a term, namely coherence time, which is inversely proportional to maximum Doppler frequency, thus, the time variance of the channel is directly related the relative motion of transmitter and receiver. Coherence Time (T_c) is a measure of the time-variance of a channel. If it is defined as the time over which the time

correlation function is 0.5, then the coherence time is approximately, $T_c = \sqrt{\frac{9}{16\pi f_d^2}} = \frac{0.4231}{f_d}$, when $f_d = \frac{v}{c} f_c$ is maximum Doppler shift. Here v, c and f_c are user velocity, speed of light and carrier frequency respectively. From Table C.2, we can get an estimate of the largest allowable symbol duration for the channel to be quasi-static over one multi-carrier symbol duration.

	2.0GHz		3.5GHz	
v, kmph	f_d, Hz	T_c, ms	f_d, Hz	T_c, ms
3	5.56	76.2	9.72	43.5
10	18.52	22.8	32.41	13.1
20	37.04	11.4	64.82	6.5
50	92.59	4.6	162.04	2.6
100	185.19	2.3	324.08	1.3
150	277.78	1.5	486.11	0.9
200	370.37	1.1	648.15	0.7
250	462.96	0.9	810.19	0.5

Table C.2: Channel coherence time at 2.0GHz and 3.5GHz of carrier frequency with respect to receiver mobility

A high Doppler can be experienced when a user is located in a fast moving car or in a speedy train, because the relative motion will be higher when either transmitter or receiver is moving very fast. This relative motion of transmitter and receiver changes the received signal from the original transmitted signal. When they are moving towards each other, the frequency of the received signal is higher than the source and when they moving away from each other, the received frequency decreases. When the relative speed is higher, then Doppler shift can be very high, and thus the receiver may become unable to detect the transmitted signal frequency. Even at lower relative motion when the Doppler shift is usually very little, if the transmission and reception technique is very sensitive to carrier frequency offset, then the system may fail.

Appendix D

Channel Model

In this section, the code used to simulate the wireless channel is reported. In the main simulator, one calls the function *Freq_ CH_ gen*, which provide both the CTF and the CIR, providing as inputs: the number of subcarriers N and the number of multipaths L, the normalized Doppler frequency $f_d T_s$, the number of OFDM symbols/SC blocks in a frame (frame length), and the Power Delay Profile (PDP) profile.

$hh \ = \ zeros(LEN\_FRAME, \ L);$

$H \ = \ zeros(LEN\_FRAME, \ N);$

$[ctf, \ cir] \ = \ Freq\_CH\_gen(N, \ L, \ fdTs, \ LEN\_FRAME, \ D\_PROFILE);$

$hh \ = \ cir(:, \ 1:L);$

$H \ = \ ctf(:, \ 1:N);$

The function *Freq_ CH_ gen* is as follows:

function $[CH\_F, \ cir] \ = \ Freq\_CH\_gen(N\_fft, \ L, \ fdTs, \ N\_s, \ D\_PROFILE)$
if $D\_PROFILE \ == \ 1$

% Exponential channel weighting

$weight\_t \ = \ exp(-4.6 * (0 : L - 1)/L);$

$weight \ = \ weight\_t/norm(weight\_t);$

else

$weight \ = \ ones(1, L)/sqrt(L);$

end

% channel generation

for $n = 1 : L$

$CH(n, :) \ = \ jakes(N\_s, \ fdTs);$

end

% Get the CIR

for $m = 1 : N\_s$

$cir(m, :) = (weight.'. * CH(:, m)).';$

end

%Get the CTF

for $m = 1 : N\_s$

$CH_F(m, :) = fft(weight.'. * CH(:, m), \ N\_fft).';$

end

where it is used the function *jakes*, reported below, to which the frame length and the normalized Doppler frequency are provided as inputs:

function $y \ = \ jakes(len, \ fdT)$

$N \ = \ 34;$

$N0 \ = \ (N/2 \ - \ 1)/2;$

$alpha \ = \ pi/4;$

$xc \;=\; zeros(len, \; 1);$

$xs \;=\; zeros(len, \; 1);$

$sc \;=\; sqrt(2) * cos(alpha);$

$ss \;=\; sqrt(2) * sin(alpha);$

$ts \;=\; 0 : (len - 1);$

$ts \;=\; ts \;+\; randint(1, \; 1, \; round(len/fdT)) * 100 * randint(1, 1, 100);$

$wd \;=\; 2 * pi * fdT;$

$xc \;=\; sc. * cos(wd. * ts);$

$xs \;=\; ss. * cos(wd. * ts);$

for $lx \;=\; 1 : N0$

$wn \;=\; wd * cos(2 * pi * lx/N);$

$xc \;=\; xc \;+\; (2 * cos(pi * lx/N0)). * cos(wn. * ts);$

$xs \;=\; xs \;+\; (2 * sin(pi * lx/N0)). * cos(wn. * ts);$

end;

$y \;=\; (xc \;+\; i. * xs)./sqrt(2 * (N0 + 1));$

$y \;=\; y/sqrt(y * y'/len)$

Appendix E

Abbreviations

AMC	Adaptive Modulation and Coding
AoA	Angle of Arrival
AoD	Angle of Departure
AP	Access-Point
BER	Bit Error Rate
BF	Beamforming
BLAST	Bell labs LAyered Space Time
BPSK	Binary Phase Shift Keying
BS	Base Station
CIR	Channel Impulse Response
CP	Cyclic Prefix
CSI	Channel State Information

CTF	Channel Transfer Function
DFT	Discrete Fourier Transform
DL	Downlink
DoA	Direction of Arrival
ECC	Error Correction Coding
FDD	Frequency Division Duplex
FDE	Frequency Domain Equalization
FDM	Frequency-Division Multiplexing
FEC	Forward Error Correction
FER	Frame Error Rate
FFT	Fast Fourier Transform
IFFT	Inverse Fast Fourier Transform
ISI	Inter-Symbol Interference
JDM	Joint Diversity and Multiplexing
LDC	Linear Dispersion Codes
LMS	Least Mean Square
LOS	Line of Sight
LS	Least Squares
MC	Multi-Carrier

MIMO	Multiple Input Multiple Output
ML	Maximum Likelihood
MMSE	Minimum Mean Square Error
MRC	Maximal Ratio Combining
MS	Mobile Station
OD	Orthogonal Design
OFDM	Orthogonal Frequency Division Multiplexing
OFDMA	Orthogonal Frequency Division Multiple Access
OSFBC	Orthogonal Space-Frequency Block Code
OSIC	Ordered Successive Interference Cancellation
PAPR	Peak to Average Power Ratio
PDP	Power Delay Profile
P/S	Parallel to Serial
QAM	Quadrature Amplitude Modulation
QOD	Quasi-Orthogonal Design
QoS	Quality of Service
QPSK	Quadrature Phase Shift Keying
QSFBC	Quasi-orthogonal Space-Frequency Block Code
RF	Radio Frequency

RLS	Recursive Least Squares
RMS	Root Mean Square
SC	Single Carrier
SCFDE	Single Carrier - Frequency Domain Equalization
SD	Space Diversity
SE	Spectral Efficiency
SF	Space-Frequency
SFBC	Space-Frequency Block Code
SIC	Successive Interference Cancellation
SISO	Single Input Single Output
SM	Spatial Multiplexing
SM-OSFBC	Spatially-Multiplexed Orthogonal Space-Frequency Block Coding
SM-OSTBC	Spatially-Multiplexed Orthogonal Space-Time Block Coding
SM-QSFBC	Spatially-Multiplexed Quasi-orthogonal Space-Frequency Block Coding
SM-QSTBC	Spatially-Multiplexed Quasi-orthogonal Space-Time Block Coding
SNR	Signal to Noise Ratio
S-PARC	Selective Per-Antenna Rate Control
ST	Space-Time

STBC	Space-Time Block Code
STC	Space-Time Coding
SVD	Singular Value Decomposition
TCM	Trellis Coded Modulation
TCP	Transmission Control Protocol
TD	Transmit Diversity
TDD	Time Division Duplex
TDE	Time Domain Equalization
TDMA	Time Division Multiple Access
UL	Uplink
UT	User Terminal
VBLAST	Vertical - Bell Labs LAyered Space-Time Architecture
WCDMA	Wideband Code Division Multiple Access
ZF	Zero Forcing
ZMCSCG	Zero Mean Circularly Symmetric Complex Gaussian

Bibliography

[1] https://www.ist-winner.org.

[2] M. C. X. Yu, G. Chen and X. Gao, "Toward Beyond 3G: The FuTURE Project in China," *IEEE Commun. Magazine*, January 2005.

[3] S. Abeta, H. Atarashi, and M. Sawahashi, "Broadband packet wireless access incorporating high-speed IP packet transmission," in *VTC fall*, 2002.

[4] B. Hassibi and B.M. Hochwald, "High-Rate Codes That Are Linear in Space and Time," *IEEE Trans. Info. Theory*, vol. 48, no. 7, pp. 1804–1824, December 2002.

[5] R. Prasad, *OFDM for Wireless Communications Systems.* Artech House Publishers, September 2004.

[6] H. Sari et al., "Frequency Domain Equalization of Mobile Radio and Terrestrial Broadcast Channels," in *IEEE International Conference on Global Communications*, 1994, pp. 1–5.

[7] H. Sari, G. Karam, and I. Jeanclaude, "Transmission techniques for digital terrestrial TV broadcasting," *IEEE Commun. Magazine*, vol. 33, pp. 100–109, February 1995.

[8] E. Dahlman et al., "A Framework for Future Radio Access," in *IEEE VTC Spring 2005*, Stockholm, Sweden, May-June 2005.

[9] S.T. Chung, A. Lozano, and H.C. Huang, "Approaching Eigenmode Channel Capacity using V-BLAST with Rate and Power Feedback," in *VTC fall*, October 2001.

[10] P.W. Wolniansky et al., "V-BLAST: An Architecture for Realizing Very High Data Rates Over the Rich-Scattering Wireless Channel," in *Proc. IEEE-URSI International Symposium on Signals, Systems and Electronics*, Pisa, Italy, May 1998.

[11] K.F. Lee, & D.B. Williams, "A Space-Frequency Transmitter Diversity Technique for OFDM Systems," in *IEEE GLOBECOM*, vol. 3, November-December 2000, pp. 1473–1477.

[12] Hamid Jafarkhani, "A Quasi-Orthogonal Space-Time Block Code," *IEEE Trans. Comm.*, vol. 49, no. 1, pp. 1–4, January 2001.

[13] N. Al-Dhahir, "Single-Carrier Frequency-Domain Equalization for Space-Time Block-Coded Transmissions Over Frequency-Selective Fading Channels," *IEEE Communications Letters*, vol. 5, no. 7, July 2001.

[14] G. Kadel, "Diversity and Equalization in Frequency Domain - a Robust and Flexible Receiver Technology for Broadband Mobile Communication Systems," in *IEEE VTC Spring*, May 1997.

[15] S.U.H. Qureshi, "Adaptive Equalization," in *Proc. IEEE*, 1985.

[16] F. Falconer, S.L. Ariyavisitakul, A. Benyamin-Seeyar & B. Eidson, "Frequency Domain Equalization for Single-Carrier Broadband Wireless Systems," *IEEE Comm. Magazine*, April 2002.

[17] S. Haykin, *Adaptive Filter Theory*, 3rd ed. Prentice-Hall, December 1996.

[18] M.V. Clark, "Adaptive Frequency-Domain Equalization and Diversity Combining for Broadband Wireless Communications," *IEEE JSAC*, pp. 1385–95, October 1998.

[19] A. Benyamin-Seeyar et al., "Harris Corporation Inc." http://www.ieee802.org/16/tg3/contrib/802163$c - 01$_32.pdf, 2001.

[20] L. Zheng and D.N.C. Tse, "Diversity and multiplexing: A fundamental tradeoff in multiple antenna channels," *IEEE Trans. Info. Theory*, vol. 49, no. 4, pp. 1073–1096, May 2003.

[21] G. J. Foschini, "Layered Space-Time Architecture for Wireless Communication in a Fading Environment When Using Multiple Antennas," *Bell Labs Technical Journal*, pp. 41–59, Autumn 1996.

[22] I. Telatar, "Capacity of Multi-Antenna Gaussian Channels," *European Trans. Telecomm.*, November 1999.

[23] R. Heath, Jr., and A. Paulraj, "Switching between multiplexing and diversity based on constellation distance," in *Proc. Allerton Conf. Communication, Control and Computing*, 2000.

[24] G. L. Stuber et al., "Broadband MIMO-OFDM Wireless Communications," in *Proceedings of the IEEE*, vol. 92, no. 2, February 2004, pp. 271–294.

[25] A.J. Paulraj, R. Nabar, and D. Gore, *Introduction to Space-Time Wireless Communications*, 1st ed. Cambridge University Press, September 2003.

[26] H. Bolcskei, D. Gesbert, and A. J. Paulraj, "On the Capacity of OFDM-Based Spatial Multiplexing Systems," *IEEE Trans. Commun.*, vol. 50, no. 2, pp. 225–234, February 2002.

[27] IST-Winner Consortium, "Assesment of Adavnced Beamforming and MIMO Technologies," http://www.ist-broadway.org/documents/deliverables/broadway-wp1-d2.pdf, Tech. Rep.

[28] M.I. Rahman, N. Marchetti, et al., "Multi-antenna Techniques in Multi-user OFDM Systems," Aalborg University, Denmark, JADE project Deliverable D3.2[1], September 2004.

[29] D. Gesbert, M. Shafi et al., "From Theory to Practice: An Overview of MIMO Space-Time Coded Wireless Systems," *IEEE JSAC*, vol. 21, no. 3, pp. 281–302, April 2003.

[30] H. Yaghoobi, "Scalable OFDMA Physical Layer in IEEE 802.16 WirelessMAN," *Intel Technical Journal*, August 2004.

[31] T.S. Rappaport, *Wireless Communications Principles and Practice.* Prentice-Hall, January 1996.

[32] D.V.P. Figueiredo, M.I. Rahman, N. Marchetti et al., "Transmit Diversity Vs beamforming for Multi-User OFDM Systems," in *WPMC*, Abano Terme, Italy, September 2004.

[33] J. Coon et al., "Adaptive frequency-domain equalization for single-carrier MIMO systems," in *IEEE ICC*, June 2004.

[34] Y. Zhu and K.B. Letaief, "A Hybrid Time-Frequency Domain Equalizer for Single Carrier Broadband MIMO Systems," in *IEEE ICC*, June 2006.

[35] R. Kalbasi et al., "Hybrid time-frequency layered space-time receivers for severe time-dispersive channels," in *IEEE SPAWC Workshop*, July 2004.

[36] D. Hwang, A. Pandharipande, and H. Park, "An interleaved TCM scheme for single carrier multiple transmit antenna systems," *IEEE Comm. Letters*, vol. 10, no. 6, June 2006.

[37] L. Guo and Y.-F. Huang, "A Multi-user SC-FDE-MIMO System for Frequency-Selective Channels," in *IEEE ACSSC*, October-November 2005.

[38] J. Coon et al., "A Comparison of MIMO-OFDM and MIMO-SCFDE in WLAN Environments," in *IEEE Globecom*, vol. 1, December 2003, pp. 87 – 92.

[39] R. Heath and A. Paulraj, "Switching between diversity and multiplexing in MIMO systems," *IEEE Trans. Comm.*, vol. 53, no. 6, June 2005.

[40] H. Bolcskei et al., "Space-Frequency Coded MIMO-OFDM with Variable Multiplexing-Diversity Tradeoff," in *IEEE ICC*, May 2003, pp. 2837–2841.

[41] K.F. Lee, & D.B. Williams, "A Space-time Coded Transmitter Diversity Technique for Frequency Selective Fading Channels," in *IEEE Sensor Array and Multichannel Signal Processing Workshop*, Cambridge, USA, March 2000, pp. 149–152.

[42] H. Bolcskei, D. Gesbert et al., *Space-Time Wireless Systems: From Array Processing to MIMO Communications.* H. Bolcskei et al., Spring 2006.

[43] Y. Li et al., "MIMO-OFDM for Wireless Communications: Signal Detection with Enhanced Channel Estimation," *IEEE Trans. Comm.*, vol. 50, no. 9, September 2002.

[44] X. Zhuang et al., "Transmit Diversity and Spatial Multiplexing in Four-Transmit-Antenna OFDM," in *IEEE ICC*, vol. 4, May 2003, pp. 2316 – 2320.

[45] S. M. Alamouti, "A Simple Transmit Diversity Technique for Wireless Communications," *IEEE JSAC*, vol. 16, no. 8, October 1998.

[46] C.-B. Chae et al., "Adaptive Spatial Modulation for MIMO-OFDM," in *Proc. of WCNC*, vol. 1, March 2004, pp. 87 – 92.

[47] H. Skjevling, D. Gesbert, et al., "Combining Space-Time Codes and Multiplexing in Correlated MIMO Channels: An Antenna Assignment Strategy," in *Nordic Signal Processing Conference*, June 2003.

[48] M.H. Hairi et al., "Adaptive MIMO-OFDM Combining Space-Time Block Codes and Spatial Multiplexing," in *IEEE ISSSTA*, Sydney, Australia, August-September 2004.

[49] L. Zhao & V.K. Dubey, "Detection Schemes for Space-Time Block Code and Spatial Multiplexing Combined System," *IEEE Comm. Letters*, vol. 9, no. 1, January 2005.

[50] H. Bolcskei and A.J. Paulraj, "Space-Frequency Coded Broadband OFDM Systems," in *IEEE WCNC*, vol. 1, Chicago, USA, September 2000, pp. 1–6.

[51] A. Stamoulis, Z. Liu & G.B. Giannakis, "Space-Time Block-Coded OFDMA With Linear Precoding for Multirate Services," *IEEE Trans. on Signal Processing*, vol. 50, no. 1, pp. 19–129, January 2002.

[52] M.I. Rahman, N. Marchetti et al., "Combining Orthogonal Space-Frequency Block Coding and Spatial Multiplexing in MIMO-OFDM System," in *proc. International OFDM Workshop, InOWo'05*, Hamburg, Germany, 31Aug-01Sep 2005.

[53] ——, "Non-Linear Detection for Joint Orthogonal Space-Frequency Block Coding and Spatial Multiplexing in OFDM-MIMO Systems," in *proc. IEEE ISWCS*, Siena, Italy, 5-7 September 2005.

[54] D. Gesbert et al., "MIMO wireless channels: capacity and performance prediction," in *IEEE Globecom*, 2000.

[55] F.R. Farrokhi et al., "Spectral Efficiency of Wireless Systems with Multiple Transmit and Receive Antennas," in *IEEE PIMRC*, vol. 1, London, UK, September 2000, pp. 373–377.

[56] S. Reinhardt et al., "MIMO Extensions for SC/FDE Systems," in *IEEE European Conference on Wireless Technology*, 2005.

[57] D. Astèly, E. Dahlman, et al., "A Future Radio-Access Framework," *IEEE Journal on Selected Areas on Communications*, vol. 24, no. 3, pp. 693–706, March 2005.

[58] G.D. Golden, G.J. Foschini, R.A. Valenzuela, and P.W. Wolniansky, "Detection algorithm and initial laboratory results using V-BLAST space-time communication architecture," *Eletronics Letters*, vol. 35, pp. 14–16, January 1999.

[59] H. J. V. Tarokh and A. Calderbank, "Space-time block codes from orthogonal designs," *IEEE JSAC*, vol. 45, pp. 1456–1467, July 1999.

[60] G.V. Rangaraj, D. Jalihal, and K. Giridhar, "Exploting Multipath Diversity using Space-Frequency Linear Dispersion Codes in MIMO-OFDM Systems," in *IEEE ICC*, vol. 4, May 2005, pp. 2650–2654.

[61] J. Wu and S.D. Blostein, "Linear Dispersion Over Time and Frequency," in *IEEE ICC*, vol. 1, 2004, pp. 254–258.

[62] ——, "Linear dispersion for single-carrier communications in frequency selective channels," in *IEEE VTC-fall*, 2006.

[63] "Feasibility Stufy for Enhanced Uplink for ITRA FDD," 3GPP Technical Report 25.896, February 2004.

[64] H. Xu and J. Liu, "Joint beamforming and transmit diversity for wireless communications," in *IEEE ICCCAS*, vol. 1, 2004, pp. 195–199.

[65] J. G. Proakis, *Digital Communications*, 4th ed. McGraw-Hill, August 2000.

[66] W.C.Y. Lee, *Mobile Cellular Telecommunications Systems*. New York, USA: McGraw Hill Publications, December 1989.

[67] J. Heiskala and J. Terry, *OFDM Wireless LANs: A Theoretical and Practical Guide*, 2nd ed. Sams Publishing, July 2001.

Vita

Nicola Marchetti was born in Legnago, Italy, on October 2, 1978. On March 28, 2003 he received the MSc. in Electronic Engineering, from the Faculty of Engineering, University of Ferrara, Italy.

From July 2003 to April 2004 he was a research assistant in telecommunications at the Faculty of Engineering in Ferrara. In May 2004 he was a research assistant at the Department of Communication Technology, Aalborg University, Denmark.

From June 2004 to May 2007 he was a Ph.D. student at the Department of Communication Technology, Aalborg University. Since June 2007, he is an Assistant Research Professor at Aalborg University.

His research interests include: multiple antenna technologies, multi-carrier and single-carrier modulations, radio resource management, localization, cognitive radio technology, pure and applied mathematics.

Permanent Address: Aalborg University

Center for TeleInFrastruktur (CTIF)

Niels Jernes Vej 12

9220 Aalborg, Denmark

e-mail: *nm@es.aau.dk*